To the Graduate Council:

I am submitting herewith a thesis written by Mark L. Granger entitled "The Design and Prototyping of the Horizontal Positioning Mechanism Used in a Low-Cost, High-Speed, Cartesian-Motion Robot". I have examined the final copy of this thesis for form and content and recommend that it be accepted in partial fulfillment of the requirements for the degree of Master of Science, with a major in Mechanical Engineering.

Frank Speckhart

Frank Speckhart, Major Professor

We have read this thesis
and recommend its acceptance:

Clement C. Wilson

Robert W. Rochelle

Accepted for the Council:

C W Minkel

Vice Provost
and Dean of The Graduate School

THE DESIGN AND PROTOTYPING OF THE HORIZONTAL POSITIONING MECHANISM USED IN A LOW-COST, HIGH-SPEED, CARTESIAN-MOTION ROBOT

A Thesis

Presented for the

Master of Science

Degree

The University of Tennessee, Knoxville

Mark L. Granger

June 1988

ACKNOWLEDGMENTS

I thank the following individuals for their assistance with the development of the project.

Dr. Frank Speckhart, Major Professor

Dr. Robert Rochelle, Committee Member

Dr. Clement Wilson, Committee Member

Mr. Siak Yeo, Electrical Engineering Graduate Student

Mr. Gene Rohrer, International Business Machines

Mr. Paul Hakenewerth, International Business Machines

Mr. Victor Hair, International Business Machines

Mr. Jon Gordon, International Business Machines

ABSTRACT

International Business Machines, through the Technical Interchange Program, has sponsored the design and prototyping of a general-purpose, low-cost, high-speed, cartesian-motion robot. The parameters of the proposed robot are:

Cost to manufacture: $600,

Speed: 36 inches per second maximum velocity,

0.24 seconds acceleration and deceleration time,

26 inches per second average velocity for 12 inch move,

Resolution: 0.0157 inches,

Theoretical accuracy: 0.006 inches

Payload: 3 pounds,

Prototype work area: 38 by 38 inches,

Control: Open loop,

Drivers: four 2.1-amp step motors,

Bearings: recirculating ball bushings.

The robot uses a simple but effective mechanism that maximizes speed and accuracy, minimizes backlash and maintenance, and facilitates manufacturing and assembly. The design is modular so that the robot can be used in various work areas.

TABLE OF CONTENTS

LIST OF TABLES

LIST OF FIGURES

LIST OF PLATES

SECTION I: INTRODUCTION

LOW COST ROBOT PROJECT INITIALIZATION

The University of Tennessee is involved in the Technical Interchange Program (TIP) which is sponsored by International Business Machines Corporation (IBM). This program allows universities and IBM to interchange ideas and research on projects selected by IBM. One such project which is the subject of this thesis is the design and prototyping of a general-purpose, low-cost, high-speed, cartesian-motion robot. This project which was initialized in the summer of 1986, supported one mechanical and one electrical engineering graduate student for four quarters as well as three mechanical engineering senior design classes. IBM has assisted with the project by sharing technical material pertaining to the robot design and participating in design reviews twice a quarter.

The idea for the robot grew from the realization that the current robots available were too expensive and advanced for simple tasks such as pick and place. IBM believed that an alternative to the high cost cylindrical or spherical robots should exist. Their suggestion to the University of Tennessee was to design a robot with open-loop control, powered by step motors that used a simple cartesian-motion mechanism. Step motors provide an inexpensive method to drive and also control the positioning of the robot. A cartesian-motion mechanism is less complicated than spherical or cylindrical robot mechanisms and simplifies the kinematics and dynamics involved in the operation and positioning of the robot.

ROBOT DESIGN GOALS AND REQUIREMENTS

The overall goals of the design project are to design, analyze, built and test a prototype robot which has multiple purposes, similar performance characteristics and is less expensive than standard robots. The specific functional requirements and design goals that were developed by IBM are listed below.

FUNCTIONAL REQUIREMENTS

RECTILINEAR WORK SPACE
CARTESIAN MOTION
SIX DEGREES OF FREEDOM: 3 LINEAR, 3 ROTARY
39 INCHES PER SECOND AVERAGE VELOCITY OVER 12 INCHES
POSITIONAL ACCURACY OF WITHIN .118 INCHES
SETTLING TIME OF LESS THAN .1 SECOND
LIMITED NUMBER OF PREDEFINED MOVES

DESIGN GOALS

LOW COST: LESS THAN $500 FOR PARTS, LABOR AND OVERHEAD
HIGH SPEED
SIMPLE DESIGN
MODULAR DESIGN
STEP MOTOR OPEN LOOP CONTROL
ERROR DETECTION

Rectilinear work space means that the robot's end-of-arm tooling needs to reach anywhere inside a specific sized rectilinear volume. For the robot to have cartesian motion, each of the three positional axis must move linearly and orthogonal to each other. Both of the above characteristics are typical of gantry robots. Spherical robots do not have rectilinear work space or cartesian motion. The average velocity of the end effector from the start to the finish of the move has to be at least 39 inches per second if displaced over twelve inches. The actual positioning of the end effector must be within .118 inches (three millimeters) of the desired positioning. To simplify the control structure, the types of moves the robot can make will be limited. For example, the robot will be able to move point to point but not by controlled path moves. Also, the robot is to be driven by step motors in an open-loop rather than closed-loop control. With closed-loop control data is being feed from the robot to the controlling computer and back to the robot in real time. With open-loop control, no communication exist from the robot to controlling computer. Open-loop control reduces the computing power requirements and places the speed limits on the motor capabilities rather than the computational capabilities. The robot also needs to be modular so that it can be set up to fit various size work areas. The robot should also be modular so the robot components can be changed easily if they need to be replaced.

THESIS COVERAGE

The development of the robot project is divided into three parts: electrical control, vertical motion arm and horizontal positioning mechanism. The area of the project that will be covered in detail in this thesis is the design and prototyping of the horizontal positioning mechanism. This thesis will present a general robot overview, robot theoretical considerations, design and performance of the horizontal positioning mechanism, step motor performance evaluation, a cost analysis, a discussion on the integration of Computer Automated Design and Manufacturing (CATIA) graphic system into the design process and a conclusion.

SECTION II. ROBOT DESIGN OVERVIEW

In order to provide a general idea of how the robot operates before discussing detailed design aspects of the robot, this section describes the layout, operation, control, assembly and performance of the robot.

LAYOUT AND OPERATION

Figure 2.1 shows a conceptual design of the vertical motion arm assembly. This assembly positions the end effector vertically without allowing the slider beam to extend above the platform. This satisfies an IBM requirement that no part of the vertical motion arm can extend above the upper surface of the robot. The linear motion bearings attached to the slide beam allow the slide beam to slide vertically along two of the three support rods. The vertical positioning of the end effector is controlled by the step motor mounted on the platform and a timing belt mounting between a motor timing gear and an idler gear on the bottom platform. The belt is fixed to the slide beam. By rotating the motor, the timing belt, slider beam and end effector will move vertically.

Figure 2.2 shows the complete robot assembly. The platform of the vertical motion arm is aligned and supported by control tubes i and j which fit in the control tube holes of the vertical motion arm. To move the end effector in the x direction, control tube j moves perpendicular to stationary guide rods m and n. To move the end effector in the y direction, control tube i moves perpendicular to stationary guide rods k and l. By controlling the positions of control tubes i and j, the horizontal position of the platform and end effector is determined.

a. Platform

b. Step Motor

c. Control Tube Holes

d. Support Rods

e. Linear Motion Bearing

f. Bottom Platform

g. Slider Beam

h. End Effector

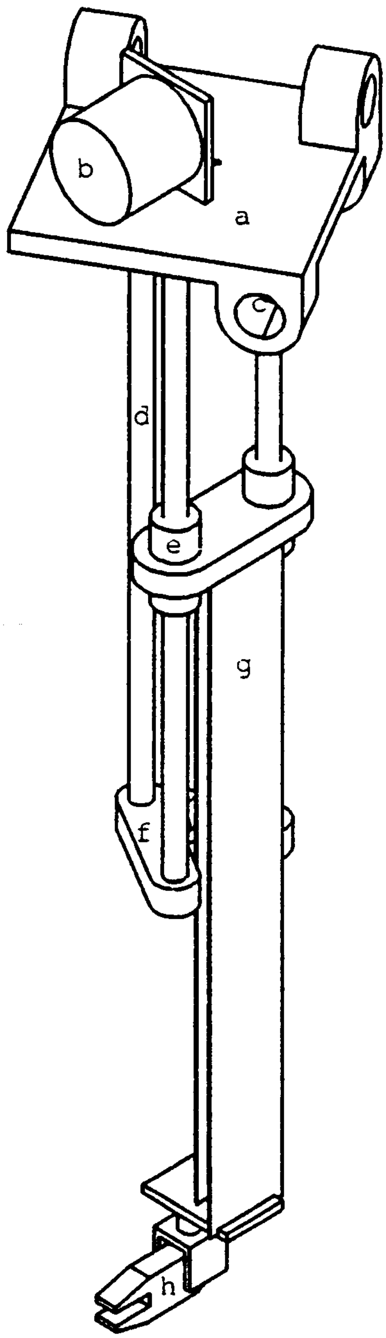

Figure 2.1: Vertical Motion Arm Conceptual Design

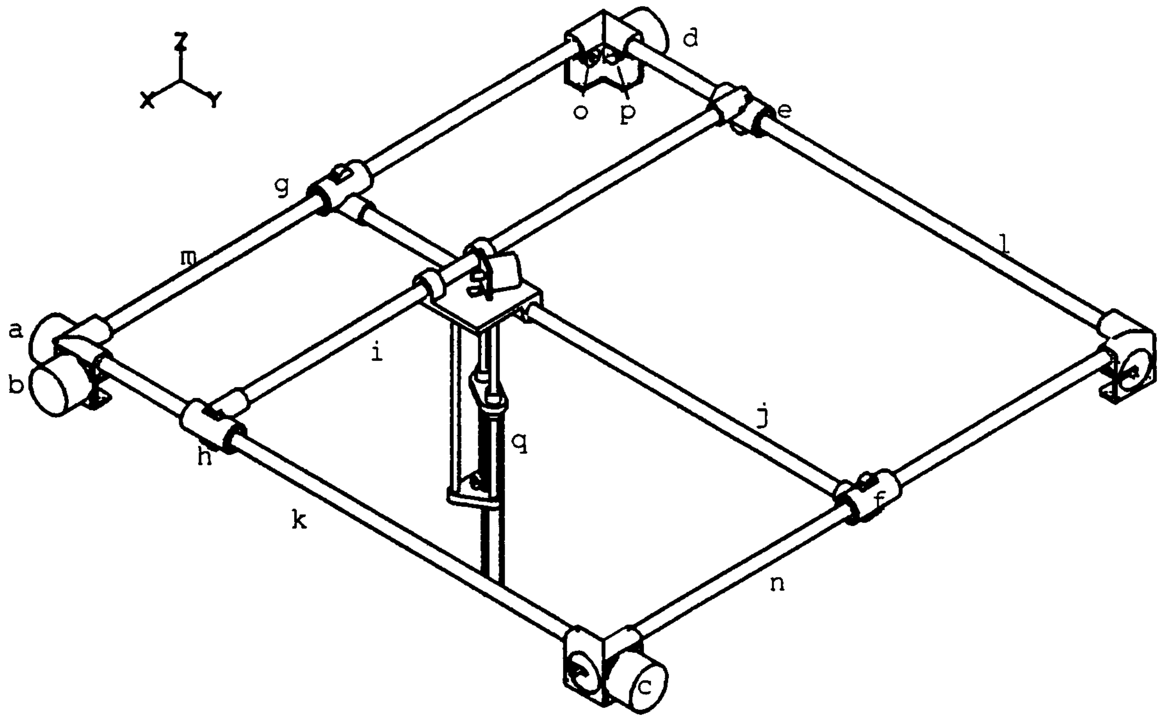

a.	Step Motor a for x axis positioning	i.	Control Tube i
b.	Step Motor b for y axis positioning	j.	Control Tube j
c.	Step Motor c for x axis positioning	k.	Guide Rod k
d.	Step Motor d for y axis positioning	l.	Guide Rod l
e.	Slider Bracket e	m.	Guide Rod m
f.	Slider Bracket f	n.	Guide Rod n
g.	Slider Bracket g	o.	Idler Gear
h.	Slider Bracket h	p.	Timing Gear
		q.	Vertical Motion Arm

Figure 2.2: Robot Assembly

The control tubes rest in the slider brackets. The four slider brackets are identical and house linear motion bearings which slide on the stationary guide rods. The positioning of the slider brackets and control tubes is controlled by the motors. Motor d controls the positioning of s'ider bracket e. Likewise, motor c controls the positioning of slider bracket f. Timing belts (not shown) are mounted on the timing gears on the motors and the idler gears attached to the corner brackets. The timing belts are fixed to slider brackets. By rotating the motors a and c simultaneously with the same speed and opposite direction, sliders brackets f and g move simultaneously and control the position of control tube j in the x direction. Details of the specific parts are discussed in section four.

A prototype of figure 2.2 minus the vertical motion arm has been built and tested. Photographs of the prototype are shown in appendix B. The distance between the corner brackets in 50 inches. The corner brackets and sliders brackets are machined from aluminum. The guide rods are one inch outer diameter Thomson shafting. One control tube is aluminum with a one-inch outer diameter and a quarter-inch wall thickness. The second control tube is stainless steel with a one-inch outer diameter and a 3/32 inch wall thickness. The vertical motion arm platform is represented by a four-inch cubed aluminum block. All the bearings in the prototype are slider bearings.

CONTROL

To drive the motors, three things are required: 1) ramps, 2) a controller and 3) motor drivers. The ramps contain information on how the step motor will accelerate and decelerate. Basically, a ramp is a table of delay times. A delay time is the time between motor steps. For an accelerating ramp, the delay times decrease which increases the angular velocity of the motor. The step motors used in the prototype have 200 steps per revolution. Two hundred delay times would be required to drive a motor for one revolution. The ramps are entered into a controller. The controller used for the prototype is an IBM developed Stepper Motor Simulation Generator (SMSG) program driven with an IBM PC AT. The production robots will be driven by a controller developed by Mr. Siak Yeo, the Electrical Engineering graduate student. SMSG converts the ramp data into motor phase signals which are sent to the motor drivers. The motor drivers contain the power supply and electronics that use the signals from SMSG to send current to the appropriate phases and actually drive the motor. The motor drivers used in the prototype are from IBM Proprinters. IBM Proprinters contain both the electronics and power supply to run the motors.

ASSEMBLY

Figure 2.3 shows a partial expanded assembly of the horizontal control section of the robot. The corner brackets support, align and hold together the robot. The corner brackets are the only parts that are mounted to a work area or framing. All four corner brackets are identical and are designed to be injection molded. They can be mounted either in the position shown or inverted. Mounted on the corner brackets are the motors and timing belt idlers. A timing belt idler for the prototype is composed of a idler shaft, roller bearing, idler timing

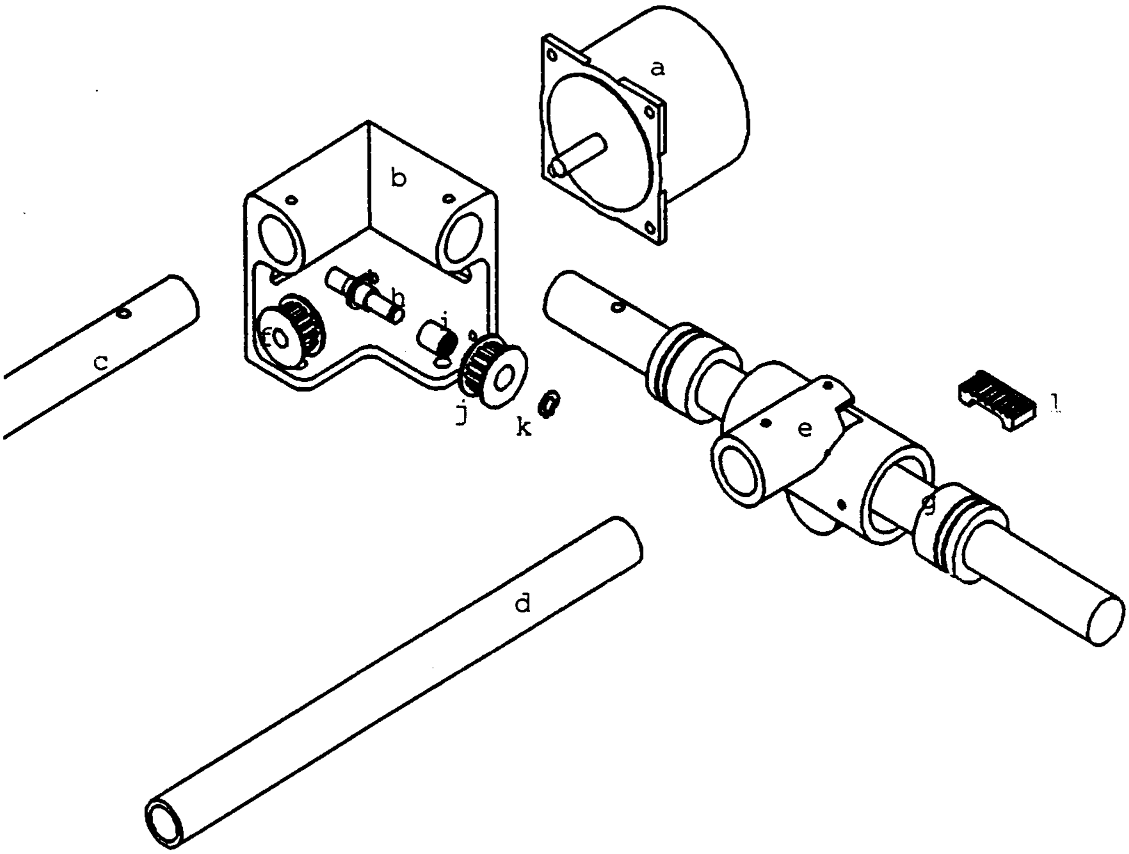

a.	Step Motor	g.	Linear Motion Bearing
b.	Corner Bracket	h.	Idler Shaft
c.	Stationary Guide Rod	i.	Roller Bearing
d.	Control Tube	j.	Idler Timing Gear
e.	Slider Bracket	k.	Snap Ring
f.	Motor Gear	l.	Belt Aligner

Figure 2.3: Partial Expanded Robot Assembly

gear, nut (not shown), washer (not shown), lockwasher (not shown) and a snap ring. The idler shaft is threaded on the end that fits in to the slider bracket so it can be attached to the corner bracket with the nut. The idler timing gear is pressed onto the roller bearing which rolls on idler shaft. The assembly can slide in the idler slot for belt tension adjustment. The stationary guide rods slide into and are restrained by the corner brackets at each end. Like the stationary guide rods, the control tubes slide into and are restrained by the sliders at each end. All four sliders are identical and are designed to be injection molded. The linear motion bearings are pressed into the sliders. The timing belt (not shown) loops between a motor timing gear and an idler timing gear on an opposite corner bracket. The timing belt is secured to the slider by positioning it on the belt aligner and then sliding the belt aligner into a fitted slot in the slider. The teeth on the belt aligner fit with the teeth on the belt. This prevents belt slippage and creates a place where the two ends of a discontinuous belt can be joined without having to splice the belt.

PERFORMANCE

Table 2.1 shows three sets of performance data for the robot. The data differs because of different types of bearings and motors used in each robot configuration. The choices for the bearings are slider bearings and recirculating ball bushing bearings. Slider bearings have more radial clearance, higher friction coefficients and cost less than the recirculating ball bushing bearings. The two choices for the motors are 2.1-amp step motors and 1.1-amp step motors. The 2.1-amp step motors are more powerful and expensive than the 1.1-amp motors. The performance is based on a 12-inch bi-directional move with a load (vertical motion arm and payload) of eight pounds attached five inches below the control tubes. With a bi-directional motion, the platform is moving at 45 degrees to the control tubes and guide rods.

TABLE 2.1: ROBOT PERFORMANCE DATA

PARAMETER	OPTION 1	OPTION 2	OPTION 3
BEARINGS	SLIDER	RECIRC. BALL	RECIRC. BALL
STEP MOTORS	2.1 AMP	2.1 AMP	1.1 AMP
MAX SPEED (IN/SEC)	36	36	18
ACCELERATION/DECELERATION TIME (SECONDS)	.43	.24	.12
AVERAGE VELOCITY (IN/SEC)[a]	21.1	26.1	16.0
RESOLUTION (IN)[b]	.0157	.0157	.0157
THEORETICAL ACCURACY[c]	047	.006	.006

[a]Average velocity is for a 12 inch move.
[b]Resolution is one motor step which for a 200 step motor and 0.5 inch raduis pulley is 0.0157 inches.
[c]Accuracy is based on the end effector being extended 20 inches below the control tubes.

The acceleration/deceleration time is the time for the robot to accelerate up to maximum speed and to return to zero speed.

Two factors in determining the data are percent of motor capability and delay time. IBM recommended that the motors be operated at no more than 70% of their torque capability. IBM also recommended that the minimum delay time be greater or equal to 0.00044 seconds. The minimum delay time determines the maximum angular velocity of the motors.

SECTION III. ROBOT DESIGN DETAIL

This section will discuss the robot layout, develop a dynamic model of the robot and analyze the robot forces, binding and accuracy.

LAYOUT SELECTION

Two requirements for the robot are cartesian motion and rectilinear work space. Two robot layout options which satisfy these requirements are the gantry layout as shown in figure 3.1 or designed system, which will be referred to as the plus system, shown in figure 3.2. Two technical reasons that the plus system was chosen over the gantry system are because of the plus system's stationary motor positioning and greater stiffness to weight ratio.

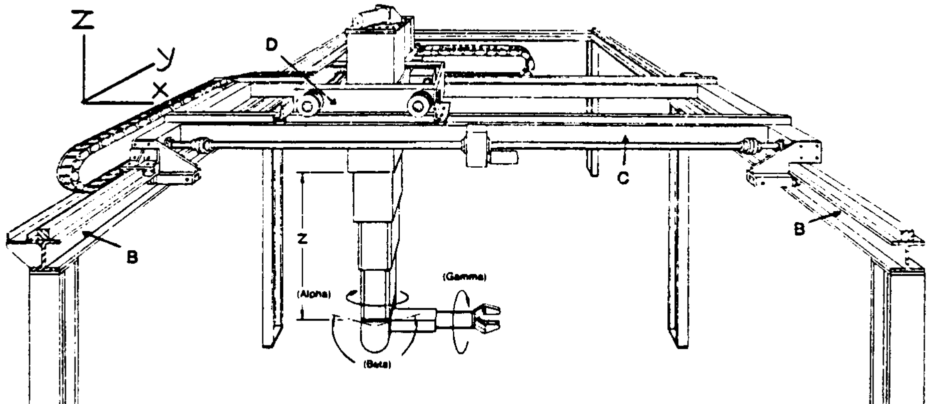

Figure 3.1: Gantry System

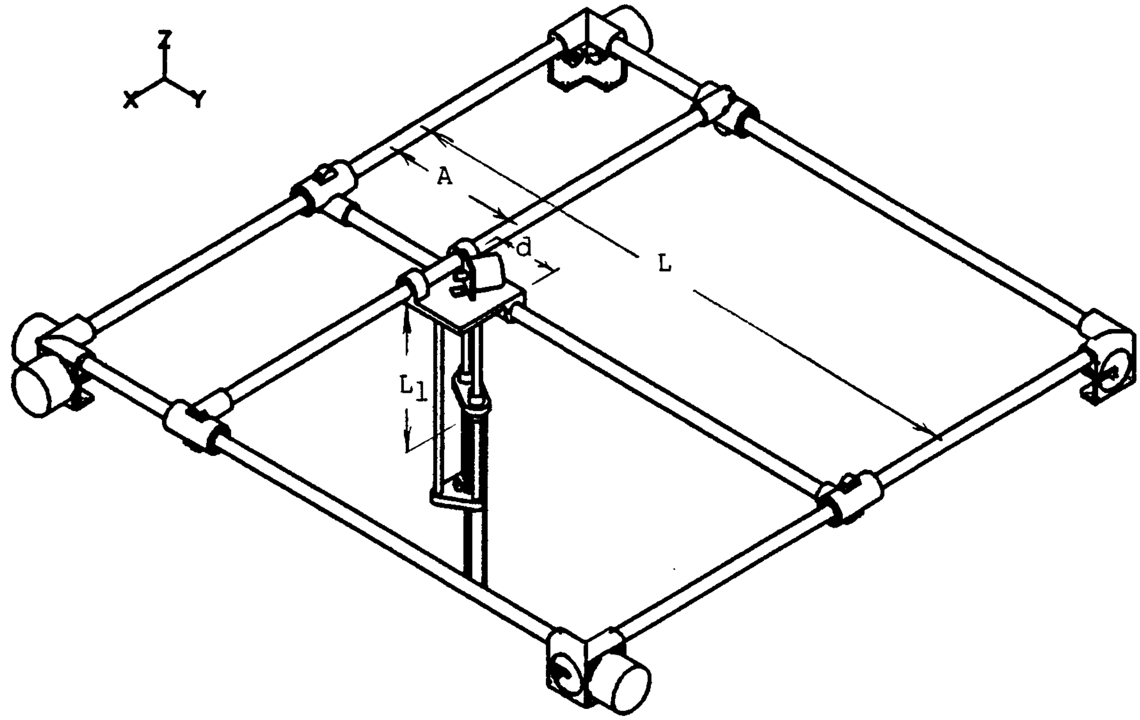

Figure 3.2: Plus System

MOTOR POSITIONING

As shown in figure 3.1, the gantry system positioning of the primary carriage C controls the end effector positioning in the y direction. The positioning of the secondary carriage D controls the end effector positioning in the x direction. Motors to control the position in the x direction must be either mounted on the secondary or primary carriage. These motors are not stationary to the frame. Their mass must be moved which increases the inertial and frictional forces the y direction motors must overcome. With the plus system all four motors are mounted stationary to the corner brackets.

The forces required to move a gantry system slider block are similar to the forces required to move a plus system slider bracket with the increased mass of a motor. To approximate the decrease in performance for the gantry system, a dynamic model of the plus system was be used to predict the performance of the a gantry system. This performance was compared to the performance of a typical plus system. The results are shown in figure 3.3. The performance measured was the average velocity for a six inch move of a robot with the dimensions and weight of the prototype. The load is represented as the weight of the platform and vertical motion arm. It is seen from figure 3.3 that the average velocity of the plus system is approximately 14% greater than the gantry system velocity.

SYSTEM STIFFNESS

Figure 3.4 compares the stiffness of the two systems in the y direction. The ratio of the platform width (d) to the distance to the center of gravity of the vertical motion arm (L_1) is represented by d/L_1. The ratio of the distance from the guide rod (A) to the distance between the guide rods (L) is represented as A/L (see figure 3.2). Figure 3.4 shows that the plus system is at least as twice as stiff as the gantry system. For the stiffness of the gantry system to equal the stiffness of the plus system, the control tubes would have to have a greater area moment of inertia which in order to keep the same control tube outer diameter would result in greater mass. The greater the mass, the slower the average velocity of the moves. The derivations of the equations to obtain figure 3.3 are shown in appendix A.

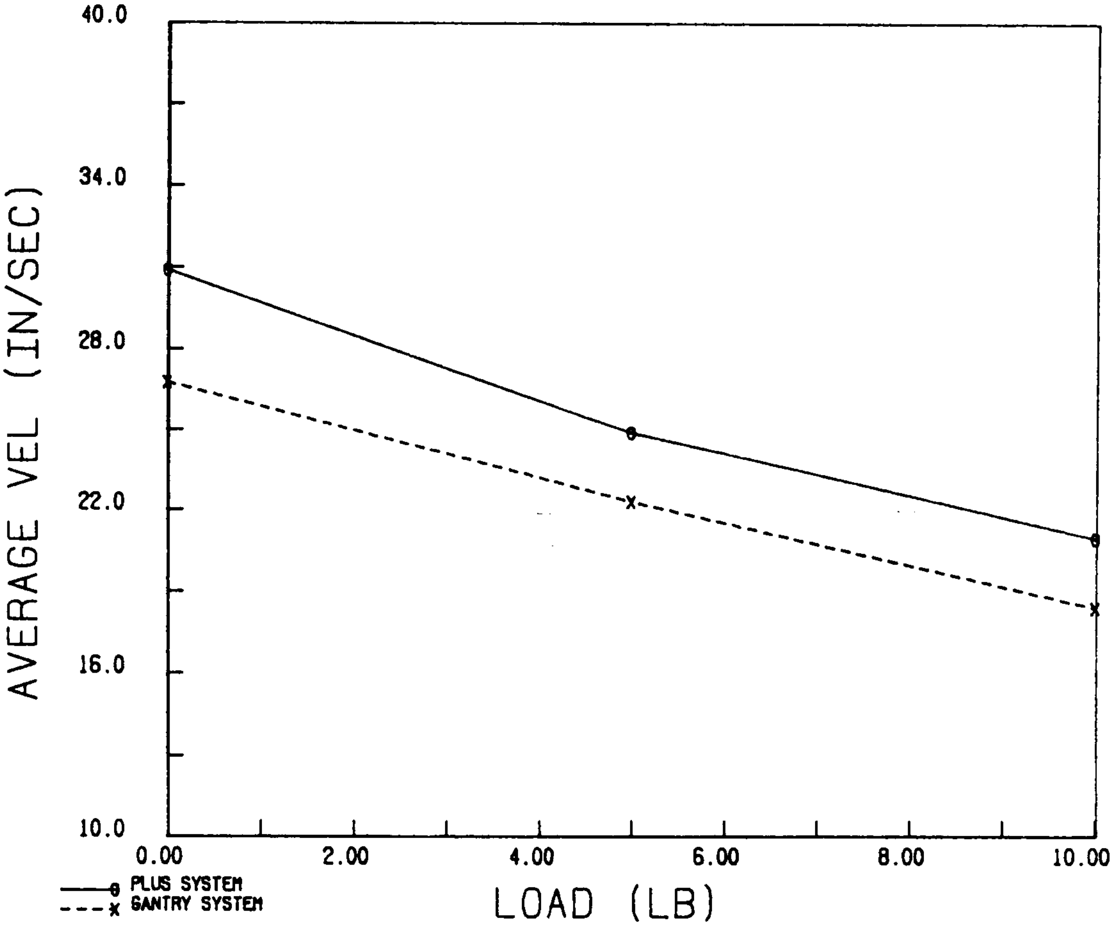

Figure 3.3: Average Velocity Comparison for Gantry and Plus System

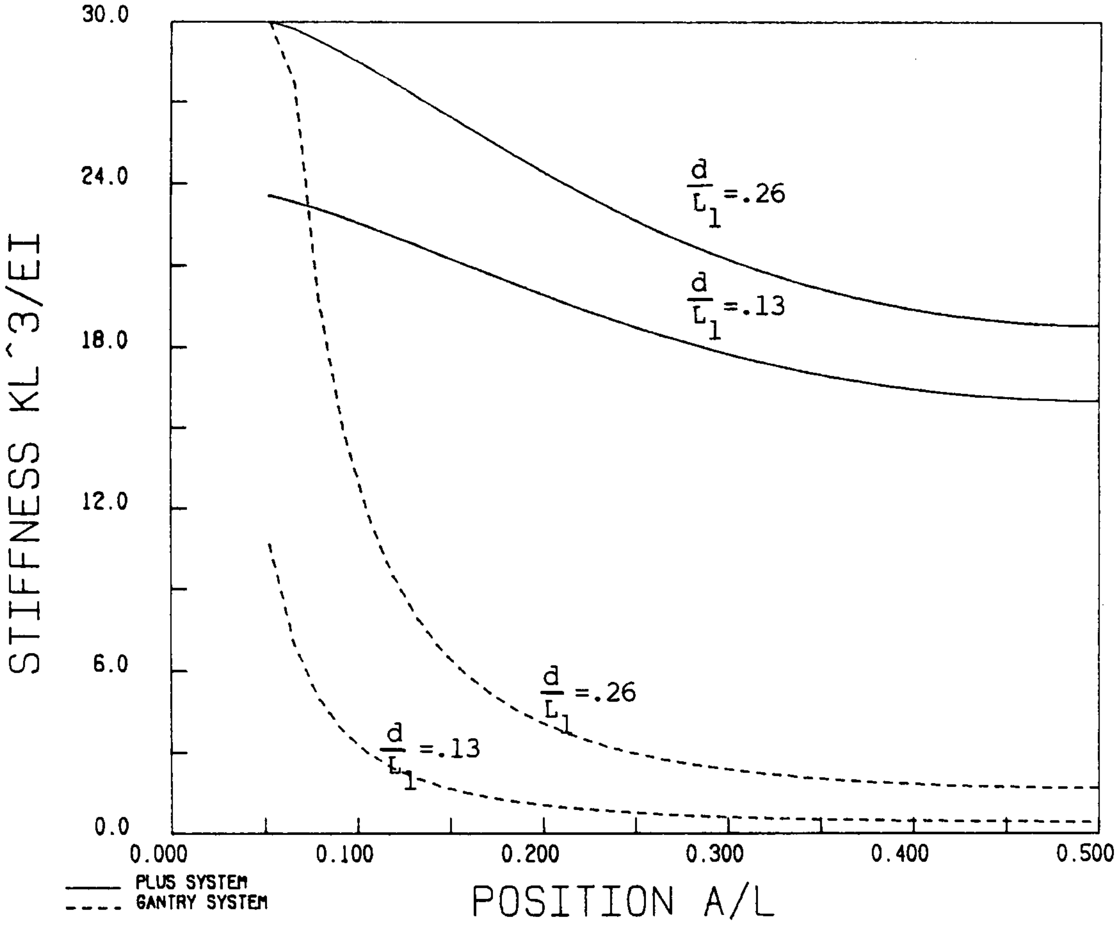

Figure 3.4: Stiffness Comparison for Gantry and Plus Systems

PLUS SYSTEM FORCE ANALYSIS

A force analysis of the plus system is required to develop a dynamic model of the system. This analysis is accomplished by analyzing each section of the robot.

PLATFORM AND VERTICAL MOTION ARM

The following schematic shows a force diagram of a plus system platform and vertical motion arm. Point 1 is the center of gravity of the platform and vertical motion arm assembly. The weight of the platform and arm, m_pg, is assumed to be equally distributed at four bearing contact points on the platform. An inertial force of m_pa_x exists at point 1 when the platform and arm are acceleration a_x in the x direction. The reactions caused by the inertial force are equally distributed at the y direction bearing mounts. The inertial force creates a moment M about the y axis. M equals $m_pa_xL_1$. L_1 is the vertical distance from the platform to the center of gravity. The width of the platform is d. Moment M creates force reactions of M/d at the two bearing contact points which are supported by the x direction control tube. Because of the friction between the platform bearings and the x direction control tube, a friction force F exists.

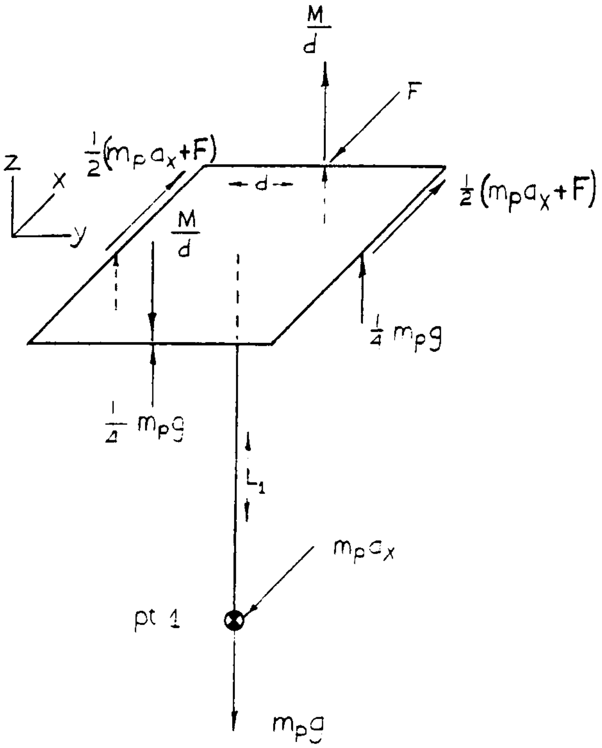

Forces Acting on Vertical Motion Arm Assembly

CONTROL TUBES

The following schematic shows the forces of the platform acting on the control tube caused by the acceleration in the x direction, a_x. R_6 and R_7 are the reactions at the contact point of the slider and control tube.

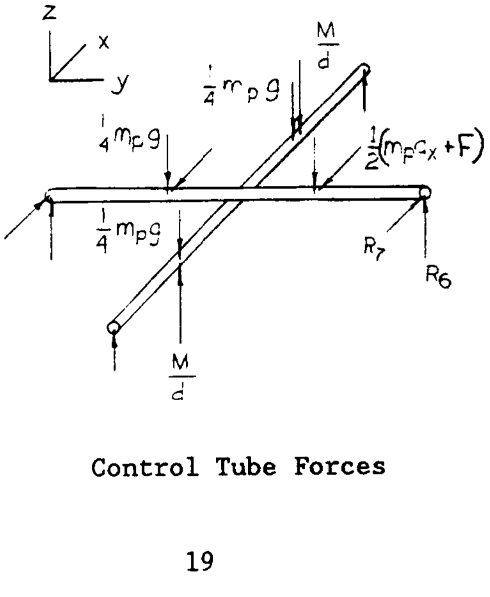

Control Tube Forces

By adding he normal forces on the control tube, the friction force F can be shown to be:

$$F = u|m_pg/4 - M/d| + u|m_pg/4 + M/d|,$$

where u is the friction coefficient between the platform bearings and the control tube. For $m_pg/4$ greater than or equal to M/d, F equals $um_pg/2$. For m_pg less than M/d, F equals 2uM/d. When a_x is greater than $gd/4L_1$ the platform will tilt on the x direction control tube, thus causing the friction to go from $um_pg/2$ to 2uM/d. The friction is schematically graphed below.

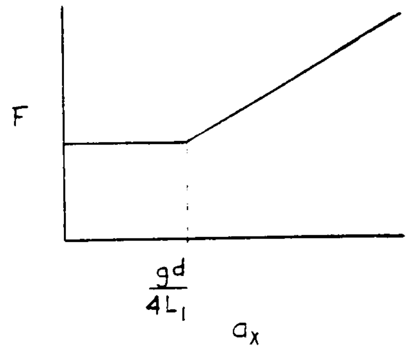

Friction Representation Graph

The following schematic shows a loaded y direction control tube. By summing moments at A about the x direction, the reaction R_6 is found:

$$R_6 = gC_1,$$

where:

$$C_1 = [m_{ct} + m_p(L-a)/L]/2.$$

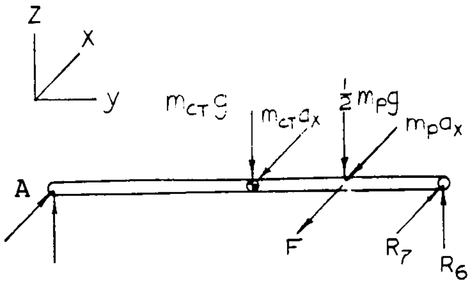

Loaded Y Direction Control Tube

By summing moments at A about the z axis, R_7 is found:

$$R_7 = a_x C_2 + f,$$

where:

$$C_2 = [m_{ct}/2 \; + m_p(L-a)/L],$$

and where:

$$f = F(L-a)/L.$$

If the platform is accelerating in both the x and y direction, F increases by um_pa_y. This is caused by an additional frictional force which results from the side loading m_pa_y on the x direction control tube. For $m_pg/4$ greater than or equal to M/d, F equals $um_p(g/2 + a_y)$. For m_pg less than M/d, F equals $u(2M/d + m_pa_y)$.

SLIDER BRACKET

The following schematic shows a loaded slider bracket.

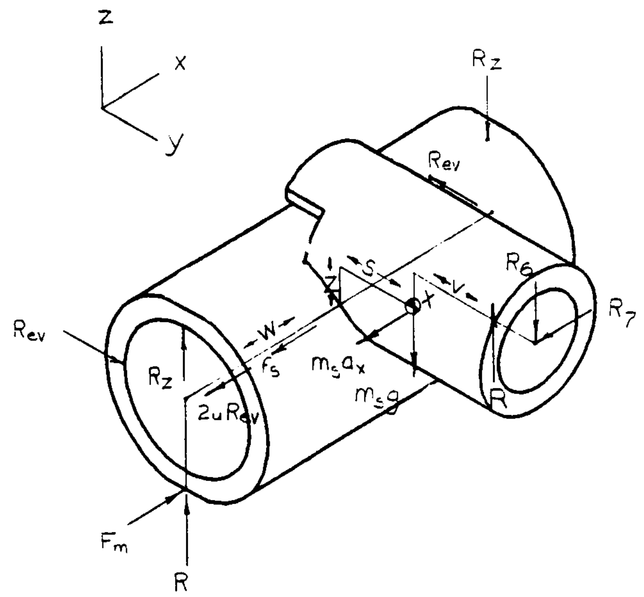

Loaded Slider Bracket

The reactions from the control tube, R_6 and R_7, are shown at the point where the control tube fits into the slider. The offset of the force of the motor F_m and R_7 in relation to the center of gravity of the slider causes a moment about the y axis which results with the couple R_z. R is the result of the weight of the control tube, platform and slider. R equals:

$$R = (m_s + C_1)g/2.$$

The offset of F_m and R_7 in relation to the center of gravity of the slider results in a moment about the z axis which results in the couple R_{ev}. R_{ev} cause a friction force $2uR_{ev}$. R or R_z cause a friction force f_s. Similar to the control tube analysis:

$$f_s = u|R - R_z| + u|R + R_z|.$$

For R_z greater than R, f_s equals $2uR_z$. For R_z less than or equal to R,

f_s equals 2uR. With the present slider design, R is approximately equal to R_z for the range of accelerations that the chosen motor is capable. Therefore, is will be assumed that:

$$f_s = 2uR.$$

By summing forces and moments the following equation is derived:

$$a_x = (K_1F_m - K_2)/m_{eq},$$

where:

$$m_{eq} = C_2 + m_s + u[s(C_2 + m_s) + C_2v]/w,$$

where:

$$K_2 = 2uR + f[u(s + v)/w + 1],$$

and where:

$$K_1 = 1.$$

The derivation of the equation of motion is shown in the appendix D.

DYNAMIC MODEL DEVELOPMENT

From above, the acceleration of the slider is given by:

$$a_x = (K_1F_m - K_2)/m_{eq},$$

where F_m is the force provided by the motor. By rearranging the above equation F_m is:

$$F_m = (a_xm_{eq} + K_2)/K_1. \qquad \text{eq 1}$$

The following schematic is a system schematic of the robot drive motor and its loading. T_m is the motor torque. r is the pulley radius. I is the gear and rotor inertia.

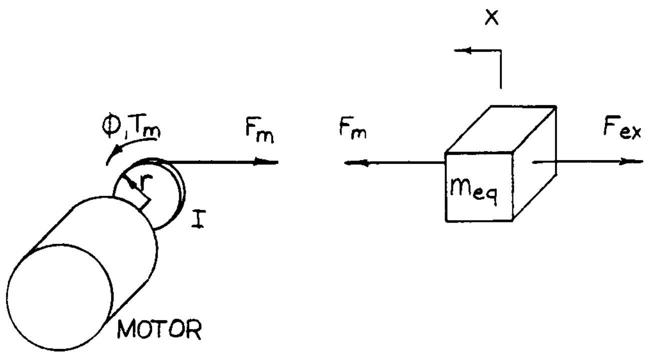

System Diagram of Drive Motor and Loading

The equation of motion for the motor and gear is:

$$T_m - F_m r = I\ddot{\phi}. \qquad \text{eq 2}$$

where 0 is the angular acceleration. The angular acceleration converts to linear acceleration by:

$$\ddot{\phi} = a_x/r. \qquad \text{eq 3}$$

The equation of motion for the system, found by substituting eq 1 and eq 3 into eq 2, is:

$$\ddot{\phi} = (-rK_2/K_1 + T_m)/(I + m_{eq}r^2/K_1).$$

Hence by knowing the motor torque and the robot parameters, the angular acceleration of the system can be found. By integrating the angular acceleration, the angular velocity is found. By integrating the angular velocity the angular position is found.

Step Motor Ramp Development Program, SMRDP, is a basic routine which uses the robot and motor torque parameters to model the dynamic performance of the robot. A fourth order Runge-Kutta integration method is used to integrate the ordinary differential equations of motion. The program output gives the time, robot position, velocity and acceleration and step delay time for each step starting from velocity equals zero at time zero to maximum velocity and back down to zero velocity. SMRDP will model one axis motion with the vertical motion arm moving parallel to the guide rods and bi-directional motion with the vertical motion arm moving at 45 degrees to the vertical motion arm. Figure 3.5 shows a flow diagram of SMRDP. Once the constant variables such as part specifications and motor torque parameters are read and the constant calculations are performed, the SMRDP starts simulating the acceleration of the robot. The simulated continues until speed of the robot reaches its maximum value. When the maximum speed is reached, the motor torque parameters change and the program starts simulating the deceleration of the robot. The robot decelerates until the minimum speed is reached. SMRDP is listed in appendix E.

To test how accurately SMRDP simulated the dynamic response, three ramps were developed for a linear one degree of freedom move. The first ramp was developed to utilize 70% of the motor's torque. The second ramp was developed to utilize 90% of the motor's torque. Both the first and second ramp when tested operated the robot continuously without failure. The third ramp was developed to utilize 100% of the motor torque. This ramp's performance was unreliable since the robot would typically complete several moves and then a motor would stall and the robot would fail. A second test involved modeling the system with a friction coefficient of 0.2 and a coefficient of 0.3. The actual coefficient of the system was 0.28. The ramps developed using the 0.2 friction coefficient were unreliable and would occasional fail. The

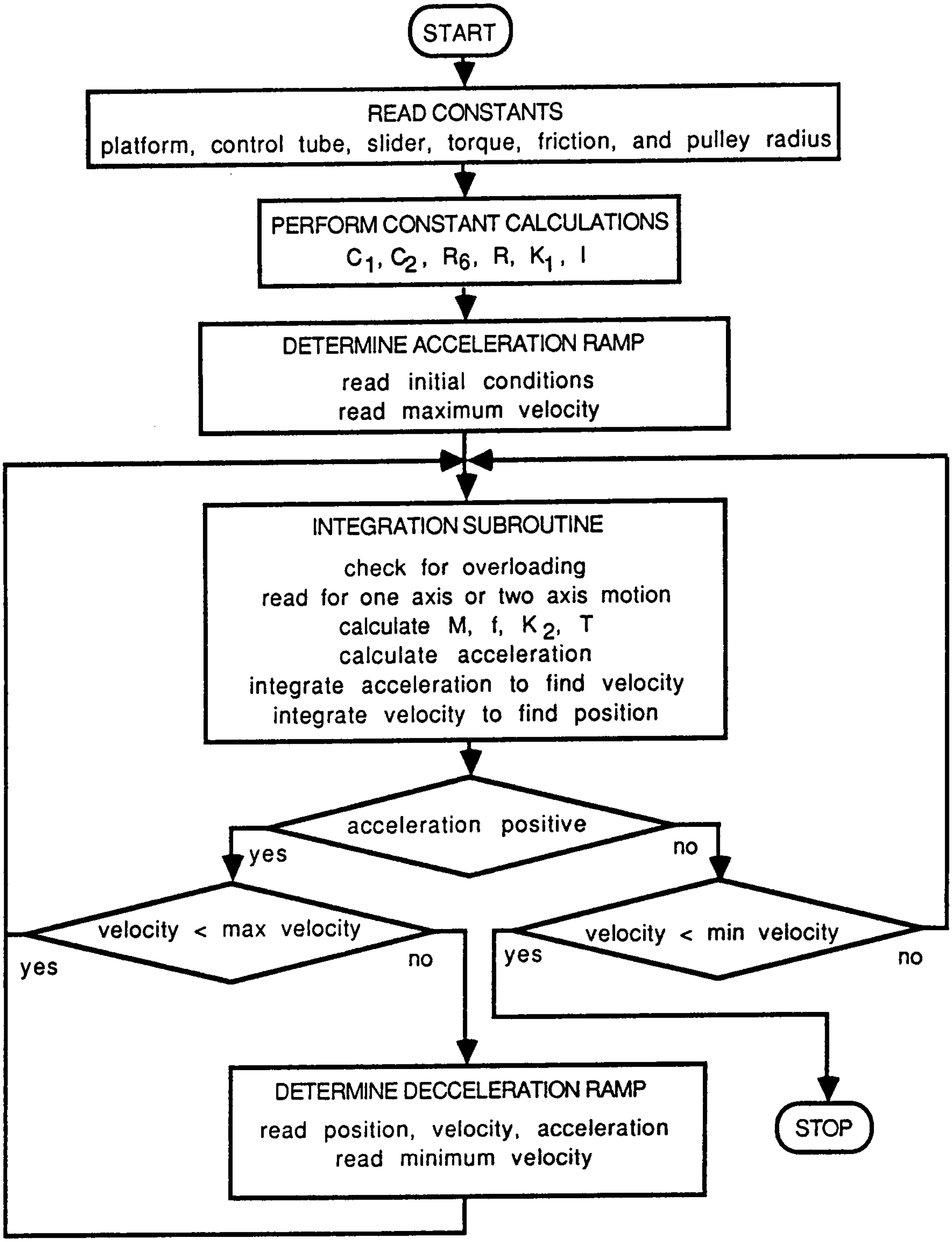

Figure 3.5: Step Motor Ramp Development Program Flow Diagram

ramps developed using the 0.3 friction coefficient provided smooth reliable operation. This response from the test ramps show that the SMRDP accurately models the performance the robot.

BINDING ANALYSIS

If the robot is moved by hand, it is easy to see that the robot will bind if one of the opposing sliders gets ahead of the other. This is shown schematically below with a control tube and sliders bound against the guide rods. By similar triangles the distance, X, that one slider can get ahead of the other is:

$$X = tL/L_3,$$

where t is the bearing tolerance, L is the distance between guide rods and L_3 is the length of the slider. If the above equation is applied to the prototype, X is approximately 0.05 inches or 3 motor steps.

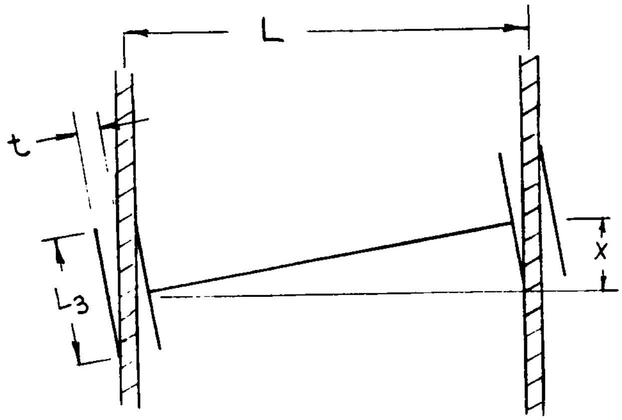

Plus System Binding

The following schematic is a free body diagram of the top view of the control tube and sliders.

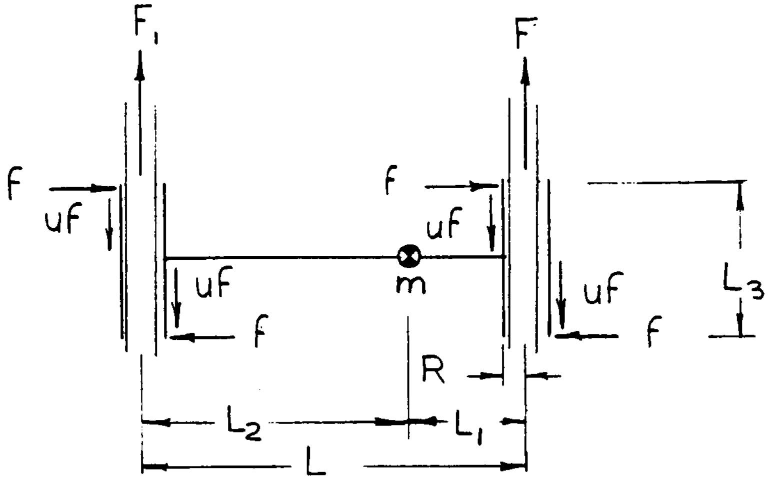

Force Diagram for Sliders and Control Tube When Binding

By summing forces in the y direction and summing moments about the center of gravity, for the system not to bind,

$$F + F_1 > 2u[(F_1L_2 - FL_1)/(uL_2 - uL_1 - L_3)].$$

Analyzing this equation when the mass is in the center or L_2 equals L_1 and F_1 equals F shows that binding will not exist. For any location of the center of mass when F_1 equals 0, the system will not bind when:

$$L_3 > uL.$$

When the mass is at the center and F does not equal F_1 ($d_f = F - F_1$) then for the system not to bind:

$$d_f/F < L_3/(L_3/2 + uL_1).$$

Derivation of these results are shown in appendix F.

ACCURACY ANALYSIS

The horizontal accuracy of the robot is determined by the robot's positional and tilt accuracies. The positional accuracy is the accuracy in the positioning of the platform. This accuracy is affected by the motor accuracy, the backlash in the drive system and the diametrical clearance in the platform bearings. The accuracy of the step motors is plus or minus 3% of a step. For the prototype with a half inch pulley radius, the linear accuracy of the step motor is 0.0005 inches. Since no gears are used in system and the timing belts act as tight springs which settle in at their neutral positions, the backlash for the system is modeled as zero. The diametrical clearance in the platform bearings for the prototype is 0.004 inches. The total positional accuracy for the prototype is 0.0005 plus 0.004 or 0.0045 inches.

The tilt accuracy is determined by the slider and platform bearing diametrical clearance. From a side view of the robot, the tilt accuracy, y, is shown schematically below.

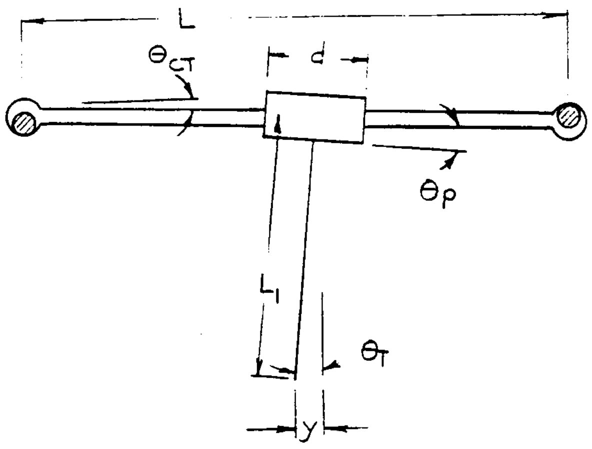

Robot Tilt Accuracy

From the above schematic,

$$y = L_1 \sin(\theta_{ct} + \theta_p),$$

where $\theta_{ct} = \sin^{-1}(2t/L)$ and $\theta_p = \sin^{-1}(2t/d)$. t is tolerance in-between the bearing inner diameter and outer diameter of the control tube or guide rods. For small angles:

$$y = 2L_1t(1/d + 1/L).$$

The total horizontal accuracy of the robot Y is,

$$Y = t[2_{L1}(1/d + 1/L) + 1] + .000942r,$$

where r is the timing gear radius. For the prototype with L_1 equal to 20 inches, the tilt accuracy is 0.043 inches. The total horizontal accuracy is +- 0.0478 inches.

SECTION IV. HORIZONTAL POSITIONING MECHANISM DESIGN AND PERFORMANCE

This section will discuss design features, part design and selection, testing, failure modes and recommended changes of the horizontal positioning mechanism.

ROBOT DESIGN FEATURES

The design features of the horizontal positioning mechanism are:

1. simple design,
2. modularity,
3. ease of manufacturing and assembly,
4. low maintenance.

The horizontal positioning mechanism is simple. Two pairs of synchronous driven step motors position the vertical motion arm horizontally using few, uncomplicated parts. The corner brackets align and support the robot and house the motors and idlers. The guide rods are standard shafting which provide support and provide bearing surfaces for the slider brackets. With the round bearing surface of the guide rods and control tubes, one standard linear motion bearing will provide accuracy in two directions. To achieve this with a track and roller design would require more parts which may have to be machined or are not standard. The motors drive the slider brackets directly: no gear trains exist. Only four parts have to be completely manufactured. All the other parts are common purchased items.

The horizontal positioning mechanism is modular since its configuration can be determined by the requirements of the task to be performed and environment where the tasks are performed. If a task requires a certain size work area or the environment limits the size of the work area, the robot can be assembled to fit that area. The work area is determined from the lengths of the control tubes, guide rods and belting. The prototype work area is 38 by 38 inches. To make the work area 28 by 38 inches, two guide rods and one control tube would have to be shortened ten inches. Also, two timing belts would have to be shortened 20 inches. The belting does not have to be continuous since it is easily spliced at the slider bracket.

The horizontal positioning mechanism is designed for ease of manufacturing and assembly. To manufacture the mechanism, four identical slider brackets, four identical belt aligners, and four identical identical corner brackets have to be injection molded. Four identical idler shafts have to be turned. The other parts are purchased parts. To assemble the horizontal positioning mechanism, the only tools required are tools to mount the motors, idlers, and corner brackets which would consist of two allen wrenches and an adjustable wrench.

The horizontal positioning mechanism is also designed for low maintenance. The roller bearings, linear motions bearings and motors do not require lubrication.

PART DESIGN AND SELECTION

CORNER BRACKET

Figure 4.1 shows a close up of a corner bracket. The corner bracket is the foundation of the robot. The four identical corner brackets align the guide rods and house and align the motors and idlers. The corner brackets can be mounted to the workspace as in figure 3.2 or

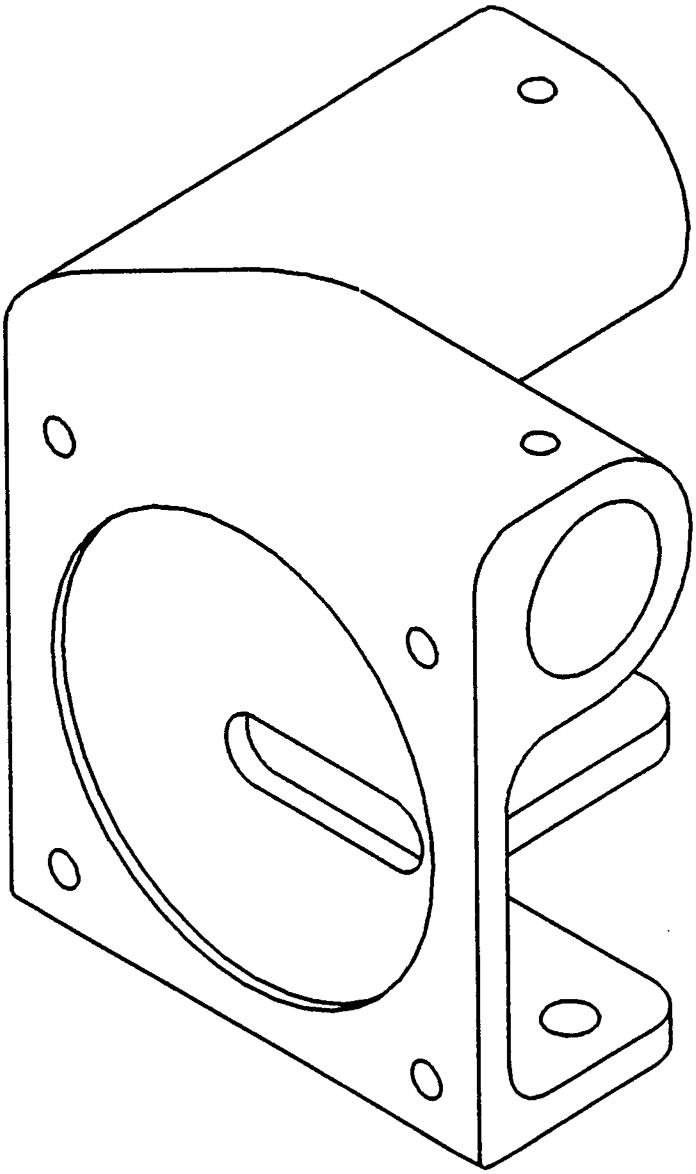

Figure 4.1: Corner Bracket

inverted to hang from the workspace. From a discussion with an IBM engineer, the corner brackets would be suitable to be injection molded. A disadvantage of the corner bracket design is that the space around the timing gears is limited. This makes it difficult to change or install belts. In developing a final design for the corner bracket, a stress analysis and a study of injection molding techniques and materials should be performed.

SLIDER BRACKET AND BELT ALIGNER

Figure 4.2 shows a close up of the slider bracket. Figure 4.3 shows a close up of the belt aligner. The slider bracket positions the control tube, houses the linear motion bearings and provides and attachment for the belting and belt aligner. The belt aligner fits into a slot in the slider. The belt-aligner teeth mate with teeth on the belt. This prevents slippage and creates a place where the two ends of a discontinuous belt can be joined. A screw in the slider is positioned to hold the belt aligner tight to the slider. Like the corner bracket, the slider bracket and belt aligner should be injection molded. Before the final slider bracket design, a stress analysis and material selection should be performed.

The slider bracket's width is a dimension which affects the robot performance. By maximizing the width, the binding for the system is minimized, the acceleration is maximized and the work space is minimized. Figure 4.4 show the effect of width of the slider bracket on average velocity and work area. The data in figure 4.4 is based on a 12-inch bi-directional move with an eight-pound load. Slider bearings with a friction coefficient of 0.167 and 2.1-amp step motors are used.

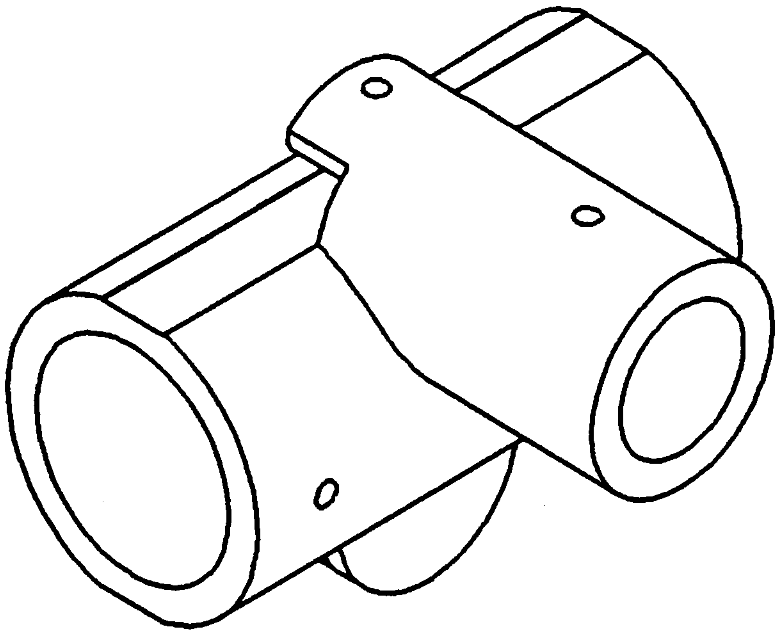

Figure 4.2: Slider Bracket

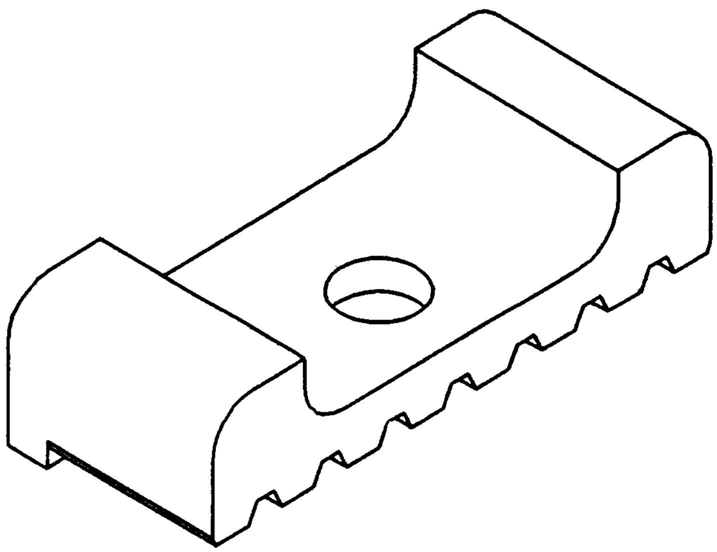

Figure 4.3: Belt Aligner

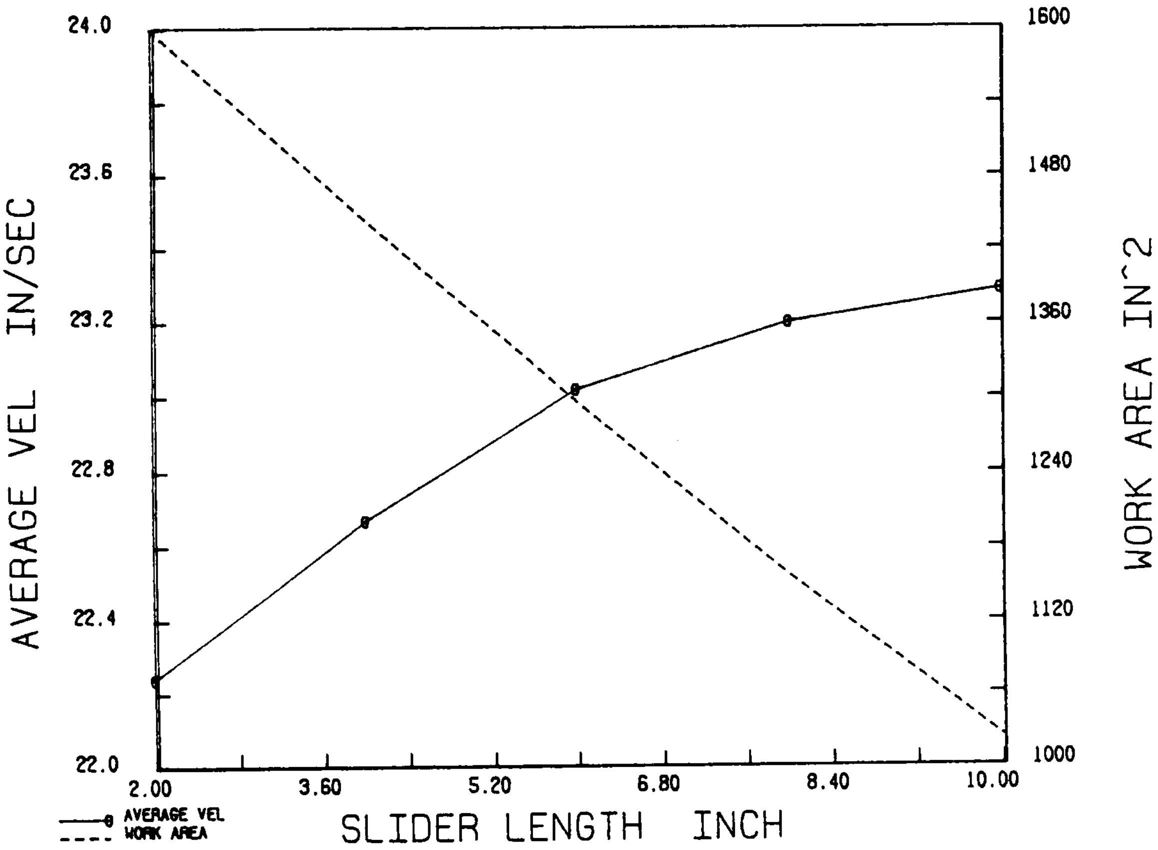

Figure 4.4: Effect of Slider Bracket Length on Performance for 12-Inch Bi-directional Move with an Eight-Pound Load

The effect of slider length will decrease with decreasing bearing coefficient. If recirculating ball bushing bearings with a friction coefficient of 0.002 are used, the effect of slider length is negligible. Because of this a slider bracket with the width of the bearing can be used. The width of the recirculating ball bushing bearings is two inches which is half the length of the prototype slider. This increases the work area and decreased the slider weight.

BELTING

Timing belts and power screws were the two methods considered for transmitting power from the motors to the slider. Drive screws were rejected since they would not be as modular, have greater backlash, have greater loses and cost more than a timing belt system. Concerns about the timing belts were the use of a belt over long unsupported distances and backlash in stopping and starting because of the belt stiffness. After the the prototype testing, the concerns about the belts disappeared. With the belts tightened so that there is no visible drop, the belts did not run off or vibrate excessively. The backlash is essentially zero since the belts act as a stiff spring and return to their neutral position.

GEARS AND IDLERS

The timing gears are 1/5 inch pitch, 3/8 inch wide and 1/2 inch radius. A problem existed with the timing gears. The set screws that secured the gears to the motors would loosen. This caused the revolutions of the two drive gears to change which caused the robot to bind and fail.

The idler assemblies have two problems. The first problem is that when the nut is tightened, it rotates in a direction that loosens the belt. To fix this problem, a tension screw could be inserted into the corner bracket perpendicular to the idler shaft so that is rests against the idler shaft. The second problem is that the roller bearings in the idler shaft require lubrication after an hour of operation so they will not squeak.

LINEAR MOTION BEARINGS

Three types of linear motion bearing were considered for use in the horizontal positioning mechanism. The characteristics of these bearings are shown in table 4.1.

TABLE 4.1: LINEAR MOTION BEARING CHARACTERISTICS

REFERENCE NAME	COMPANY	MATERIAL	TOLERANCE	COST[a]	FRICTION COEFFICIENT	SLIP-STICK
DURALON	REXNORD	TEFLON FABRIC	.003 - .004	$2.51	.17	NO
ROLLER	THOMSON	BALL BUSHING	.0000-.0005	$17.79	.002	NO
IGUS	IGUS	THERMOPLASTIC	.0007- .004	$0.49	.06-.17	YES

[a]wholesale cost

The Duralon and Igus bearings were tested on a steel shaft both lubricated and dry. The coefficient of friction of the Duralon bearing decreased slightly with increasing load. The Duralon was not effected by lubrication. The coefficient of friction of the Igus bearing decreased from about 0.17 to 0.06 when lubricated. When lubricated the coefficient of friction increased with load. Figure 4.5 shows the measured effect of load and lubrication on the bearings.

The performance of the robot is affected by the bearing friction coefficient. The greater the friction coefficient, the greater the drag seen by the motors. The greater the drag on the motor, the lower the average velocity of the robot. Figure 4.6 shows the effect that the coefficient of friction has on the average velocity for a 12-inch bi-directional move with an eight-pound load driven with 70% torque capability of the 2.1-amp step motors. For the various friction coefficients the motor pulley diameter remained one inch and the motor acceleration ramps were modified. The solid line represents the load being positioned at the level of the control tubes. The dashed line represents a load positioned ten inches below the control tubes. For low friction coefficients, the position of the load has little effect on the performance of the robot. With recirculating ball bushing bearings, the friction coefficient essentially goes to zero and factors such as slider bracket length or load positioning have little effect on robot the performance.

Figure 4.7 compares the costs of the bearings and the accuracy of an end effector which is twenty inches below the control tubes. The dimensions of the prototype were used to calculate the data. Along with the low friction coefficient and high accuracy, the recirculating ball bushing bearings are five times the cost of other bearings.

CONTROL TUBES

The weight of the control tubes is a factor in the performance of the robot since it is moving mass. Because of this, several materials

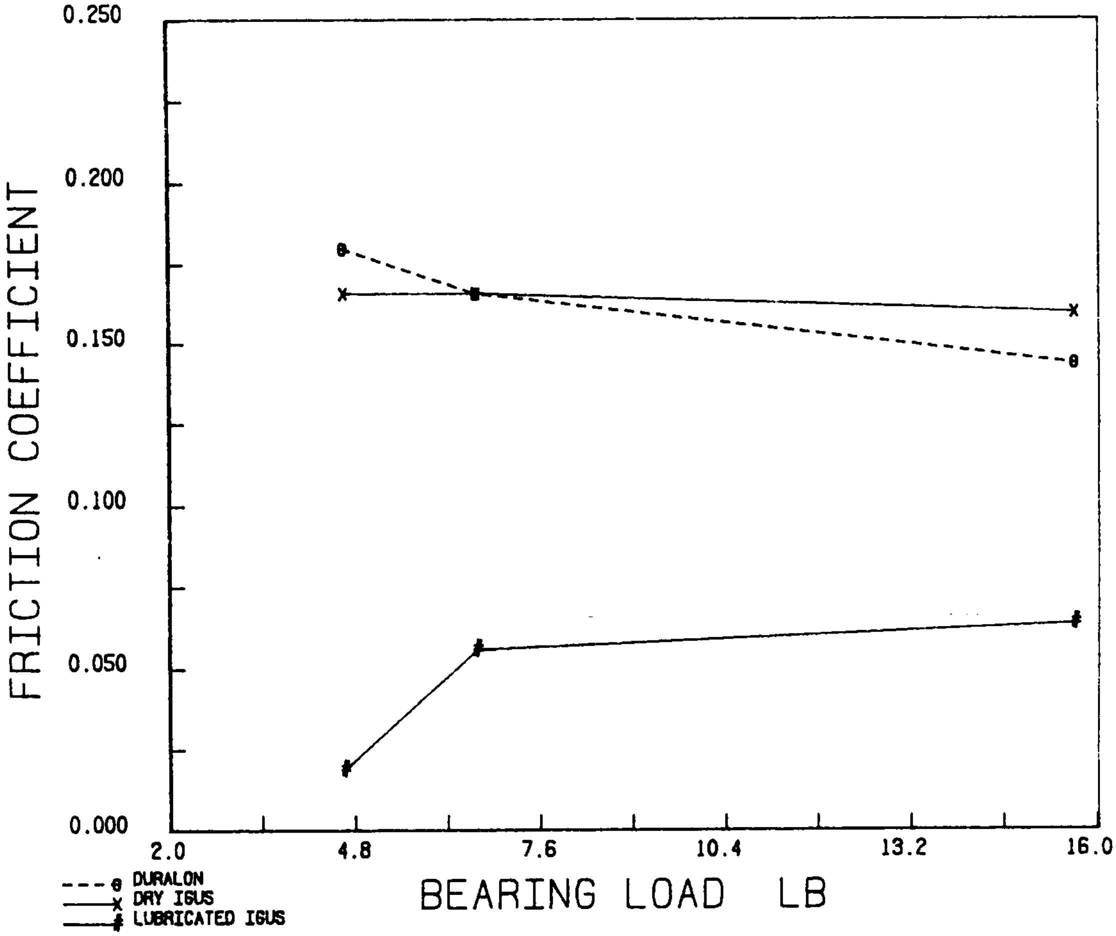

Figure 4.5: Effect of Load on Coefficient of Friction

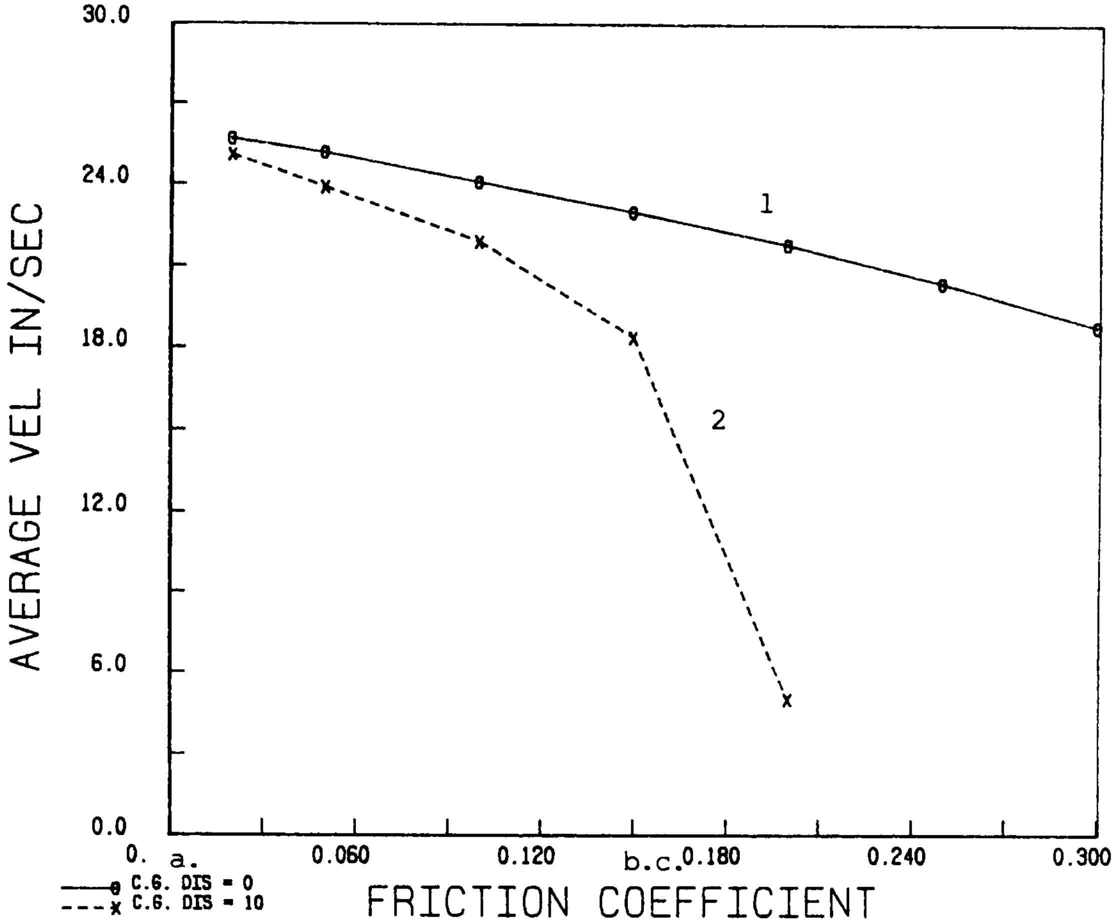

a. Recirculating Ball
b. Duralon
c. Igus

1. C.G. of Load at Control Tube Level
2. C.G. of Load Offset 10 Inches Below Control Tube Level

Figure 4.6: Effect of Bearings on Average Velocity For Bi-directional 12-Inch Move with Eight-Pound Load

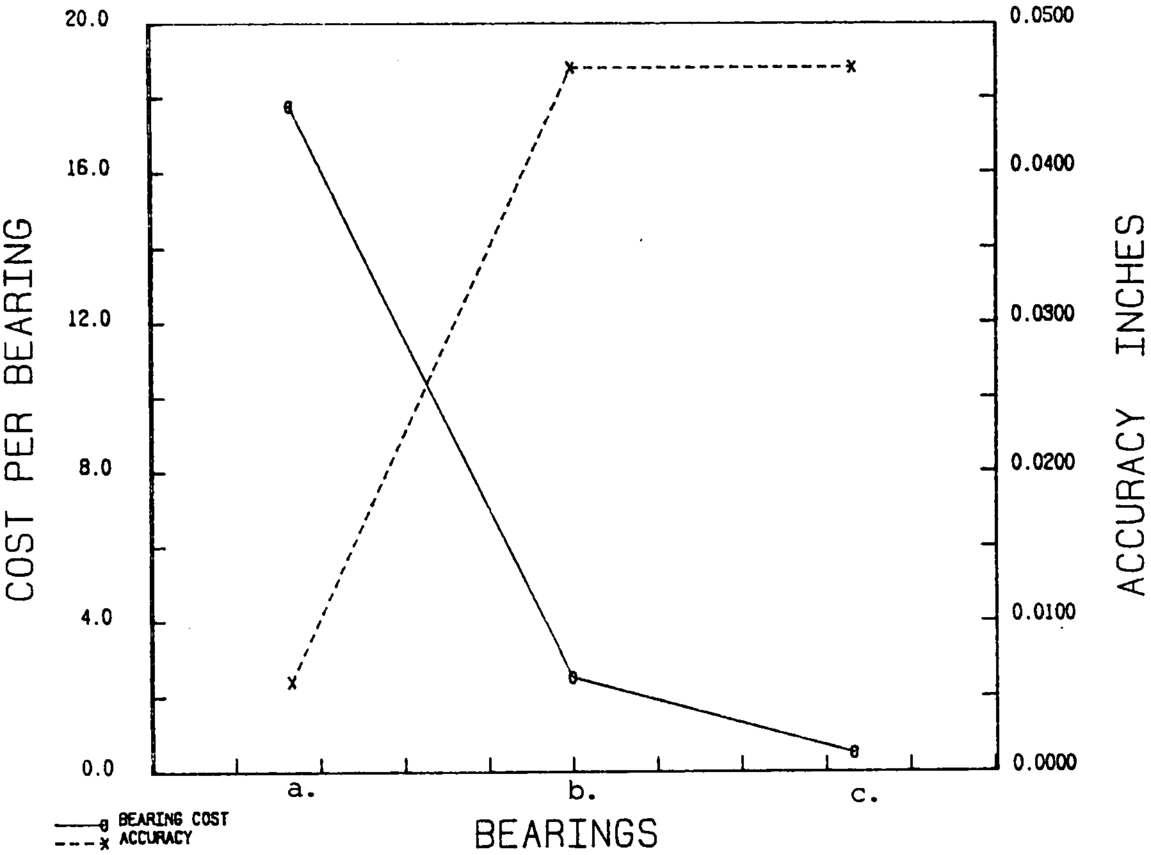

a. Recirculating Ball
b. Duralon
c. Igus
(Accuracy based on prototype dimensions with end effector 20 inches below level of control tubes)

Figure 4.7: Cost of Bearings and Effect on Accuracy For Robot with Dimensions of the Prototype

for the control tubes were studied. Table 4.2 shows the materials studied and their characteristics. The dimensions are based on the tubes having the same stiffness for each material. One inch outer diameter aluminum with the wall thickness of 1/8 inch is the reference size provided by an analysis done by one of the senior design classes that worked on the project. To obtain an equivalent stiffness with fiberglass, the outer diameter had to be increased to 1.25 inches. Aluminum makes a poor bearing surface because it is soft and has a coefficient of friction that is larger than the other materials.

TABLE 4.2: CONTROL TUBES CHARACTERISTICS FOR VARIOUS MATERIALS

MATERIAL	UNIT WEIGHT LB/IN^3	ELASTICITY 10^6 LB/IN^2	I.D IN	O.D IN	FRICTION COEF.	SECTIONAL WEIGHT LB/IN^2	COST/ FOOT[a]
GRAPHITE EPOXY	.058	18.5	.887	1.00	.17	.010	$4.75
STEEL	.28	27.5	.928	1.00	.17	.031	$1.75
ALUMINUM	.101	10.4	.750	1.00	.28	.035	$1.50
FIBERGLASS	.054	5.5	1.04	1.25	.20	.020	$1.00

[a]wholesale, large quantity cost

Figure 4.8 shows how the selection of materials effect the average velocity of a twelve-inch move with an eight-pound load. The figure also shows the relative costs of each of the materials. The average velocity of the aluminum is the lowest because of the increased friction coefficient of aluminum compared with the other materials. The velocity

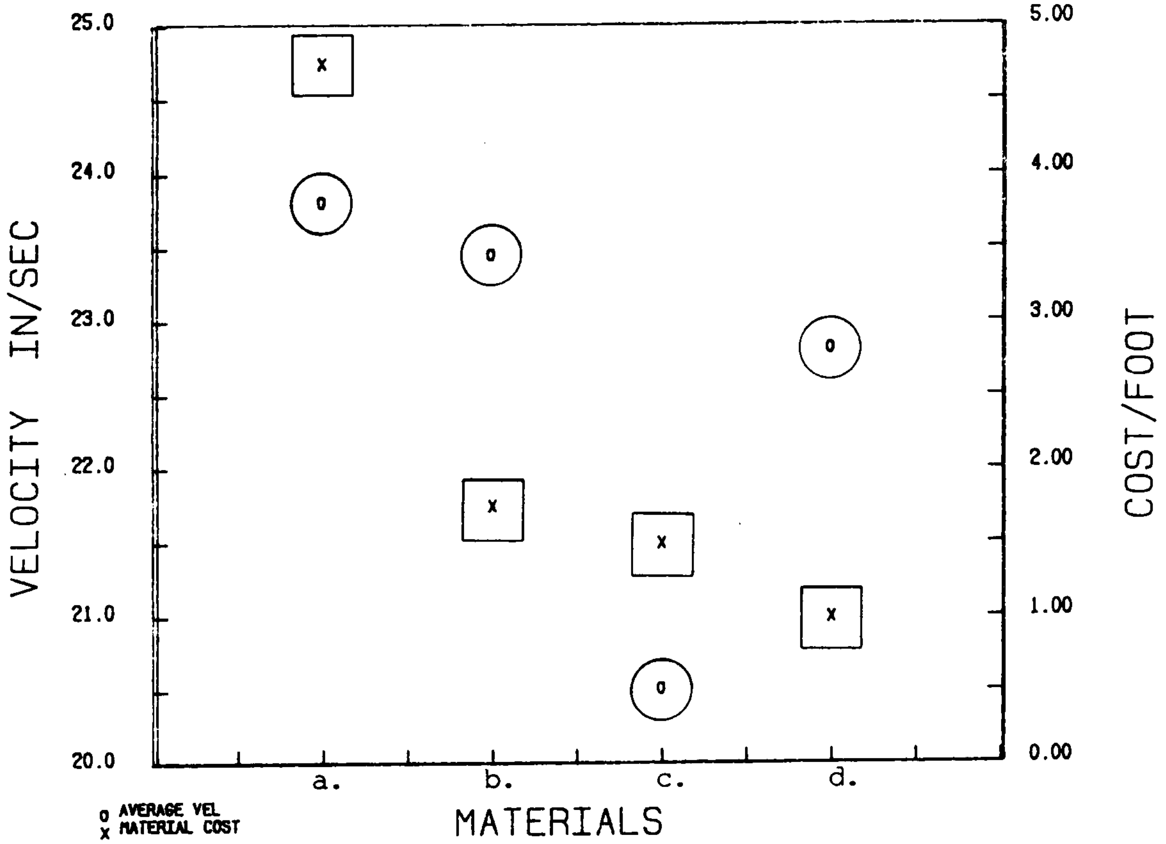

a. Graphite Epoxy
b. Steel
c. Aluminum
d. Fiberglass

Figure 4.8: Cost of Materials and Effect on Average Velocity for 12-Inch Bi-directional Move with an Eight-Pound Load

data was based on using sliding bearings with a friction coefficient of 0.167 and using 70% of the torque of 2.1-amp step motors. The pulley radius remained constant for the different materials while the acceleration ramps were modified.

PROTOTYPE TESTING

The testing of the horizontal positioning mechanism consisted of two formal reliability tests and many informal runs to check ramps or study the performance of the robot.

In the first reliability test, the horizontal positioning mechanism performed a move continuously 20,000 times. The move was a 23.2-inch, linear, one degree of freedom move. The move consisted of a ramp up, constant velocity and a ramp down period. The ramps were designed specifically for this move. The robot completed this test without missing any of the 29.6 million steps. The data for the test is shown below.

RUN TIME: 281 MINUTES
OF MOVES: 20,000
OF STEPS: 29.58 MILLION
TOTAL TRAVEL DISTANCE: 38,700 FEET
MOVEMENT: 1 AXIS / 23.2 INCH LINEAR MOVEMENT
MOTOR LOADING (% OF MAX CAPABILITY): 70
AVERAGE VELOCITY: 27.6 IN/SEC
SYSTEM FRICTION COEFFICIENT: .20
SYSTEM LOAD: 9.2 LB
RAMP UP: 0 - 35.7 IN/SEC IN 374 STEPS: ACC MAX = .38 G
CONSTANT VELOCITY: 35.7 IN/SEC FOR 1000 STEPS
RAMP DOWN: 35.7-0 IN/SEC IN 105 STEPS: ACC MAX = .98 G
MOTOR PULLEY RADIUS: .5 INCH

Using the same motor ramps, the robot was driven bi-directionally. The move distance per axis was 17.7 inches. All four motors were driven by the same signal so that the platform would travel at 45 degrees to the guide rods. The robot operated for several minutes and then failed due to a stalled motor because of improper ramps. The loading for two degree of freedom travel is greater than one degree of freedom travel because of increased frictional losses. The robot was retested with the bi-directional move using ramps designed for the move. Similar to the first test, the robot performed the move 20,000 times without failure. The data for the test is shown below.

RUN TIME: 257 MINUTES
OF MOVES: 20,000
OF STEPS/MOTOR: 22.5 MILLION
MOVEMENT: 2 AXIS / 17.66 INCH LINEAR MOVEMENT PER AXIS
MOTOR LOADING (% OF MAX CAPABILITY): 70
AVERAGE VELOCITY: 22.9 IN/SEC
SYSTEM FRICTION COEFFICIENT: .30
SYSTEM LOAD: 9.2 LB
RAMP UP: 0 - 35.7 IN/SEC IN 475 STEPS: ACC MAX = .29 G
CONSTANT VELOCITY: 35.7 IN/SEC FOR 500 STEPS
RAMP DOWN: 35.7-0 IN/SEC IN 125 STEPS: ACC MAX = .84 G
MOTOR PULLEY RADIUS: .5 INCH

The significance of these tests is that:

1. Ramps can be developed for mechanical loading that optimize the motor's performance and insure reliable performance,
2. Step motors can be used in open-loop control for robot positioning,
3. The plus system is appropriate for horizontal positioning.

FAILURE CONDITIONS

By running the horizontal positioning mechanism, two failure conditions were experienced. A failure condition occurs when a motor stalls or misses steps. This causes the mechanism to lose position or to stop completely and not be able to finish its task. A motor will stall when the torque from the mechanism is greater than the motor torque available. Assuming the motor is driven correctly with the proper ramps and the motor stalls, two failure conditions can exist with the mechanism. The first condition results from the distance between the guide rods changing because of the guide rods being bent or not parallel. This is shown schematically below.

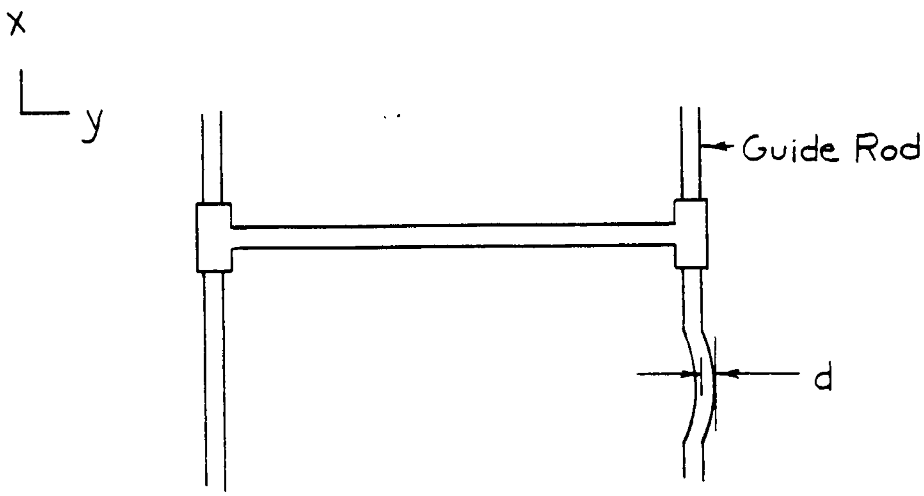

Top View of Plus System with Bent Guide Rod

The right guide rod is bent. For the slider and control tubes to pass over the bend, the guide rods will have to deflect the distance d in the y direction or the distance between the sliders will have to change. With the prototype mechanism, the control tubes have a minimum of 1/8-inch float in the slider sockets. This allow the distance between the sliders to change without having to deflect the guide rods if the guide rods are not parallel. If the sliders and control tube are rigid, a deflection force is required to deflect the guide rods. This force is equal to the equivalent stiffness of the guide rod times the deflection d. The force that the motors must overcome because of the deflection force is the deflection force times the friction coefficient of the system. If the deflection force is 100 pounds and the friction coefficient is 0.2, the motors would have provide an extra 20 pound of force. If the friction coefficient is 0.002, the motors would have to provide an extra 0.2 pounds of force. If the motors cannot provide the extra force required to deflect the rods, the the failure condition will exist and the system will fail. This condition occurred with the prototype when the float between the sliders and control tube was zero and the guide rods were not parallel. The lower the coefficient of friction, the less likely a failure conditions will occur.

The second failure condition results from the height between the the control tubes at the intersection point being different from height between the centerline of the bearings in the vertical motion arm platform. The schematic below shows that the x direction control tube is bent.

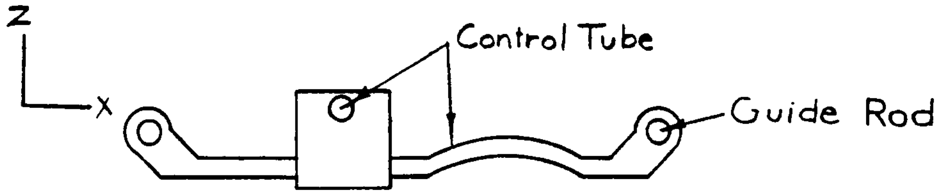

Side View of Plus System with Bend Control Tube

For the platform to pass over the bend, the system will have to deflect. Like above this will create extra loading for the motors. The extra force on the motors will be the amount of deflection times the equivalent stiffness of the deflected rods times the friction coefficient of the system. The failure condition will exist when this force overloads the motor. Figure 4.9 plots the motor force required to deflect a prototype control tube at its center for various friction coefficients. The motor force would be greater at all other points along the tube. Also plotted is the motor force required to move an eight-pound load at constant velocity. The motor modeled is the 2.1-amp step motor with a one-half inch pulley radius. These two forces are added to obtain the third line. The two constant lines represent the available force of the motor when the motor is operated at full recommended speed at 100% and 70% of its torque capability. From figure 4.9, the motor will stall when the friction coefficient is greater than 0.28 because the force required to move the load plus the force required to deflect the control tube is greater than the force that the motor can provide.

Both of the failure conditions are a function of guide rod and control tube straightness, parallelism, stiffness and friction coefficients. By controlling these variables, the failure conditions can be controlled.

An analysis should be developed to better understand the effect of the variables on system. From this analysis specifications can be developed for the straightness, parallelism and stiffness of the control tubes, guide rods. The analysis will consider the equivalent

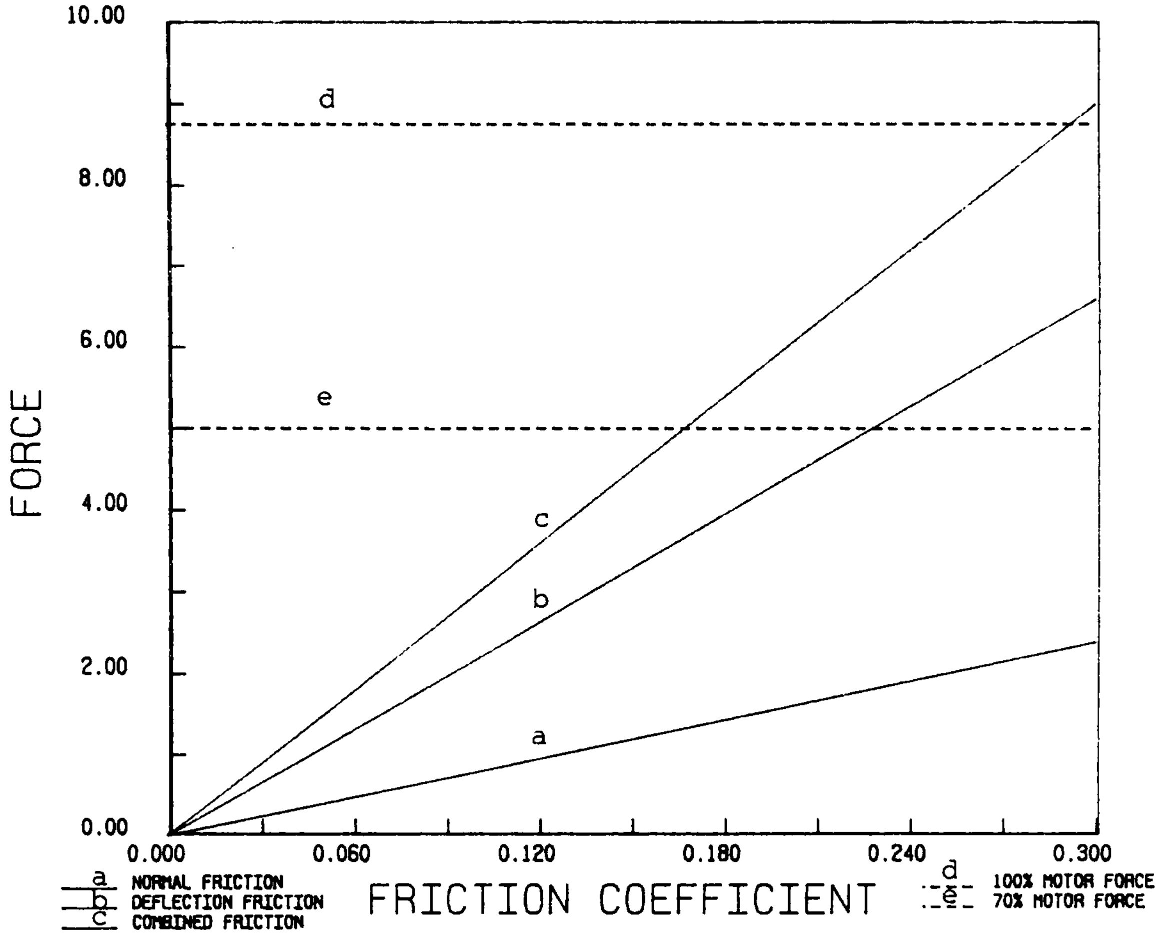

Figure 4.9: Friction Force Requirements and Motor Force Available

stiffness's of the parts of the robot that will deform. The stiffness's depends not only on materials and area moments of inertia, but also platform position. The analysis will have to consider the straightness and parallelism of the control tubes and guide rods. The parallelism will have an impact on the robot assembly procedures and or part tolerances. This could effect the cost of the robot. Also, the amount of extra torque that the motor can provide depends on if the torque is required during acceleration or constant speed. With the parallelism, straightness and stiffness specifications, the failure conditions can be controlled to insure the reliability of the robot.

SECTION V. STEP MOTOR PERFORMANCE

Step motors are essential for the operation of the robot. The steps of each pair of motors must be coordinated so that one slider will not get ahead of the other. The motors not only drive the robot but also control the positioning and timing of the robot in an open-loop manner. This section will discuss the performance characteristics of step motors and how to optimize their use in mechanical systems.

A step motor's torque varies with its speed. At zero speed the step motor has a holding torque. As the speed of the motor increases the torque decreases. Figure 5.1 shows a IBM-generated torque-speed curve for a 2.1-amp motor. The 2.1-amp motor is used on the prototype. The vertical axis shows the motor torque in inch-ounces. The horizontal axis shows the speed of the motor in steps per second. The top envelope of the data, made up of all the curves, represents the motor's maximum torque and will be referred to as the 100% curve. The curves that make up the maximum torque are constant lead angle curves. The lead angle is the angle in steps between the impulse of motor and equilibrium position of the rotor. For a given torque and speed, the lead angle can be determined. The dashed curve is the 70% curve of the motor. This curve is the same curve as the 100% except that it is lower by 30% of the maximum torque. The 70% curve is the torque speed curve that the motor is recommended to be operated at.

Figure 5.2 shows the torque-speed curve for the 2.1-amp motor for deceleration. The dashed curve or 70% curve is the torque speed curve where the motor should be operated. The torque-speed curves and curve

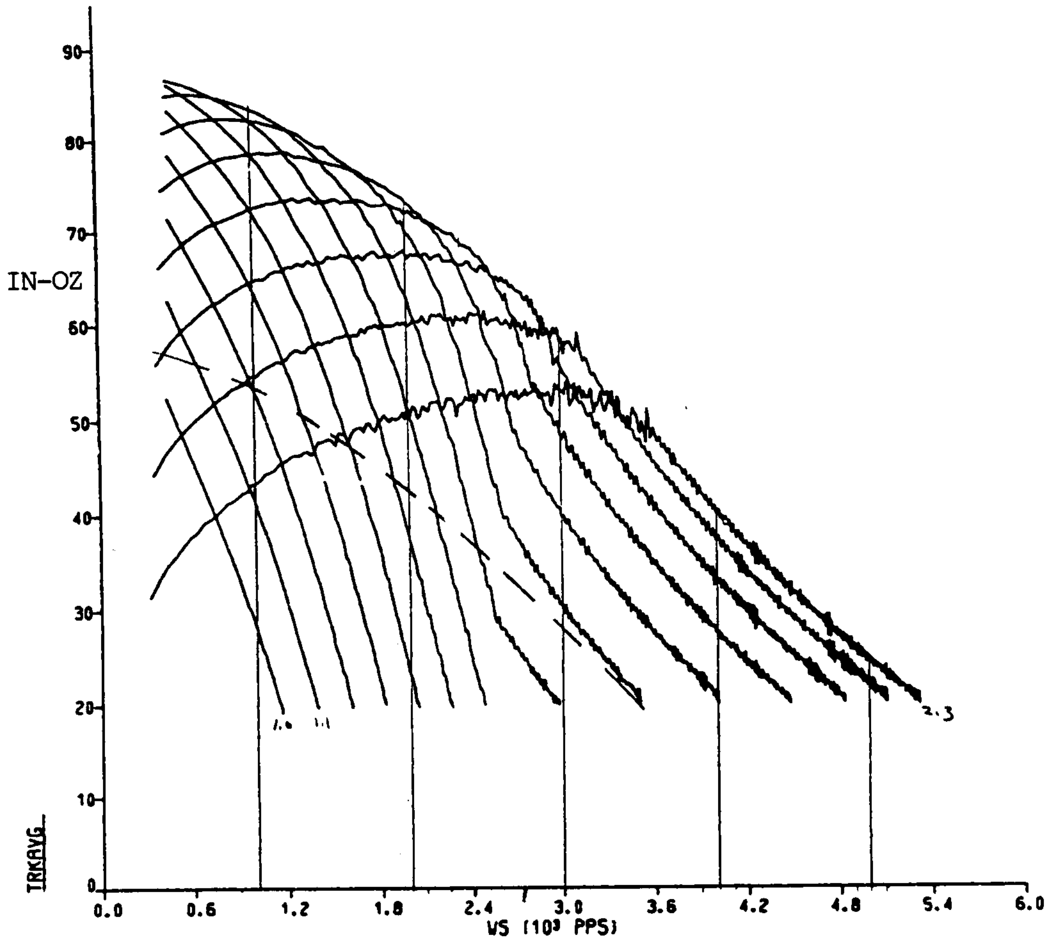

Figure 5.1: 2.1-Amp Motor Positive Acceleration Torque Speed Curve

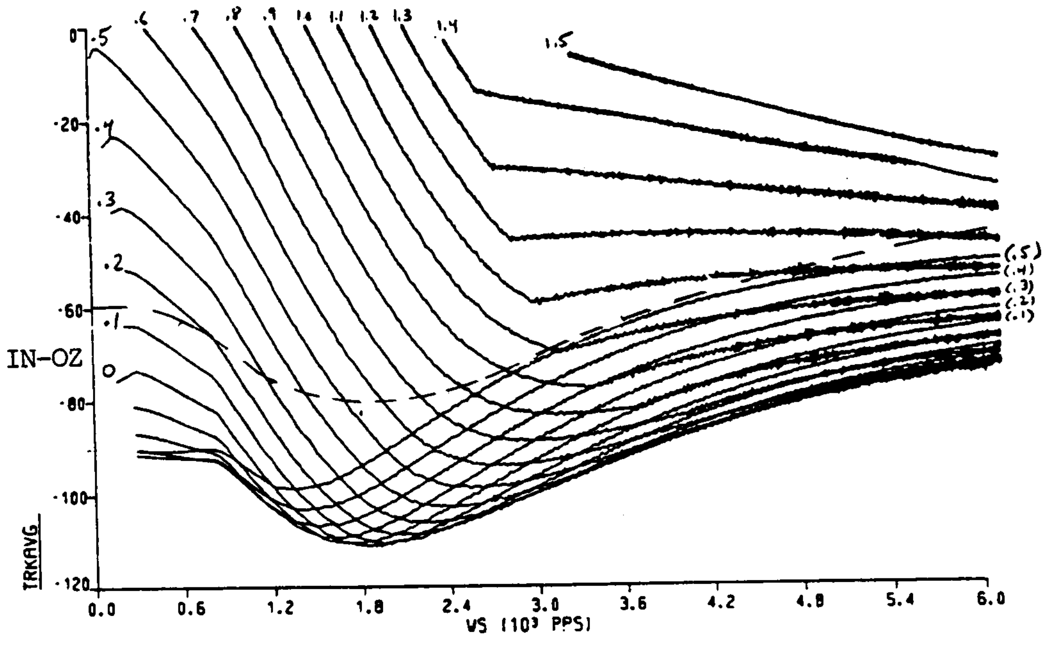

Figure 5.2: 2.1-Amp Motor Deceleration Torque Speed Curve

fit equations for the 2.1-amp motor and a 1.1-amp motor are shown in appendix G. The 2.1-amp and 1.1-amp motors are the two choices of step motors that can drive the robot.

The motor, gear or pulley radius, length of travel, and loading are variables that effect performance of a mechanical system driven by step motors. The loading includes the masses or inertias of the parts being driven and coulomb and viscous losses such as friction or aerodynamic drag. The pulley on the motor of the prototype converts the motor torque to a force that drives a load. At constant motor speed if the pulley radius increased, the speed of the load would increase and the force applied to the load would decrease. To obtain maximum acceleration of a load, a small radius would be used. To obtain maximum speed of a load, a large radius would be used. The force required to move the load must be less than the holding torque of the motor divided by the pulley radius or gear ratio. To obtain maximum performance given travel distances and loading parameters, the motor and gear radius selection have to be optimized.

The maximum performance for the robot is obtained by maximizing the average velocity for moves. The average velocity for a robot move is the move distance divided by the time for the robot to accelerate, move at constant velocity and decelerate. To study how the variables such as load conditions and pulley radius effect the performance of a mechanical system, a model was developed using the schematic shown below. The motor drives a gear or pulley of radius R which transfers the motor torque into a force to either lift or pull the attached mass. A similar model could be represented by a motor attached to a power screw with pitch P. With the power screw model, the equations would be the same except that R would equal P divided by two.

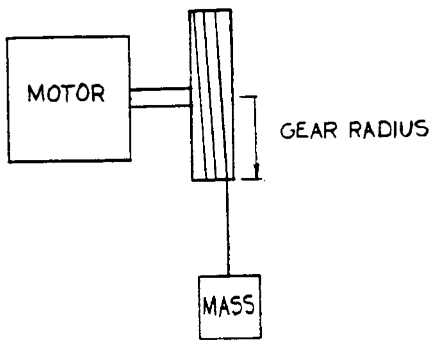

System Model

The equation of motions for the system are:

$$(I + mR^2)\ddot{\phi} = \text{motor torque} - mgR \quad \text{for upward motion}$$

$$(I + mR^2)\ddot{\phi} = \text{motor torque} - mguR \quad \text{for horizontal motion}$$

$\ddot{\phi}$ is the motor's angular acceleration. I is the mass moment of inertia of the motor rotor plus the inertia of th: pulley. A friction coefficient, u, of 0.02 is used for the horizontal motion analysis. Without the friction coefficient, the model would represent an ideal situation. The equation of motion for vertical motion is an ideal situation. The pulley is assumed to be a quarter inch thick aluminum disk. The motor torque is represented by a polynomial fit of the torque speed curves in the form of:

$$\text{motor torque} = a\dot{\phi}^2 + b\dot{\phi} + c.$$

Performance data for the motors was collected by solving the nonlinear equations of motions using a forth-order Runge-Kutta numerical integration for $\dot{\phi}$ and ϕ while varying the time, gear radii, masses and motors. The gear radii varied from 0.1 to 0.7 inches with 0.1 inch steps. The loads varied from two to 16 pound with 4 pound steps. Four motors were modeled. The performance data was then linearly interpolated into specific distances and sorted to find the maximum average velocities for specific loads, travel distances, motors and movements. Figures 5.3 and 5.4 show some of the results. The programs used to solve for the data and more performance plot are listed in appendix G. If the motor torque curve was linear, the equations of motion could be solved directly. Appendix I shows an analysis where the torque curves were assumed to be linear and the equations of motion were solved directly for $\dot{\phi}$ and ϕ.

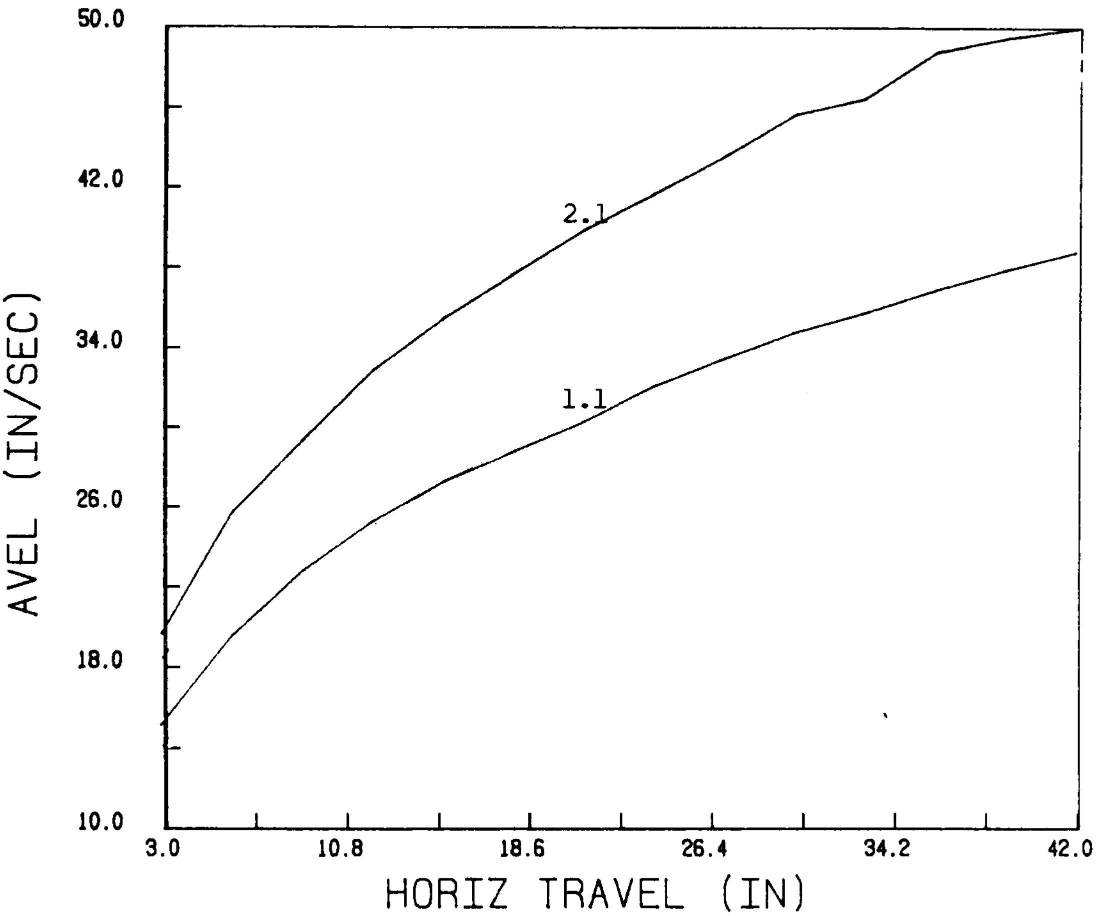

Figure 5.3: Maximum Average Velocity Versus Horizontal Travel For an Eight-Pound Load

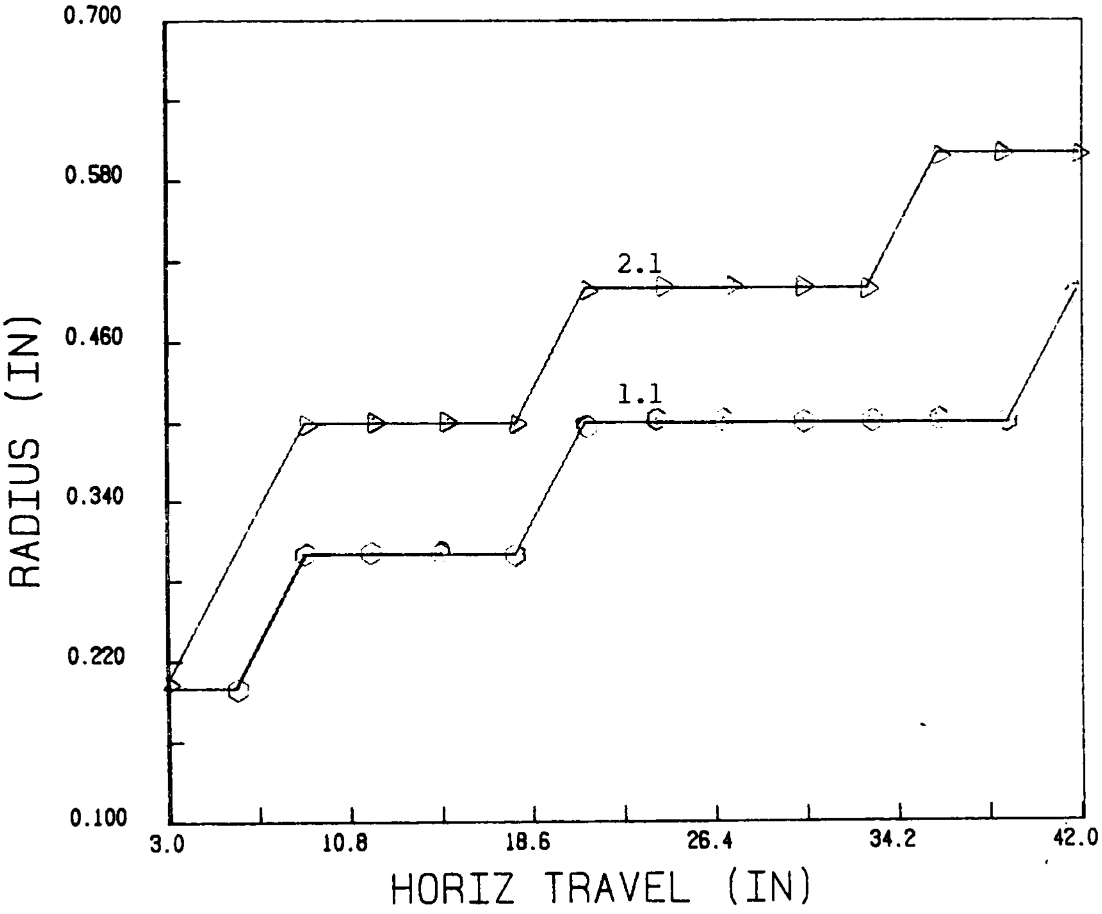

Figure 5.4: Optimum Radius Versus Horizontal Travel
For an Eight-Pound Load

Figure 5.3 shows maximum average velocity that can be obtained for moves of varying lengths caring an eight-pound load driven by either the 2.1-amp step motor or the 1.1-amp step motor. The gear radius for the curves is not constant. An example use of figure 5.3 would be if an eight pound load is moved 11 inches with the 1.1-amp motor, the maximum average velocity for that move would be around 24 inches per second. From the figure 5.3, the average velocities of the 2.1-amp motor are 30% to 50% greater than the average velocities of the 1.1-amp motor. The optimum gear or pulley radius to travel distance relationship is is plotted in figure 5.4. The program that developed the data in figure 5.4 varied the radii from 0.1 to 1 inch with 0.1-inch increments. Because of this, the data is based on the assumption that the only pulleys available are 0.1, 0.2, 0.3, . . . 0.9, and 1-inch radius pulleys. The program varied the travel distances from three to 42 inches with 3-inch increments. Between 9 and 18 inches of travel for the 2.1-amp motor, the optimum pulley radius is 0.4 inches. Between 21 and 30 inches for the 2.1 amp-motor, the optimum pulley radius is 0.5 inches. Figure 5.4 shows that the pulleys for the 2.1-amp motor can be attached directly to the motor which means that gear reductions or gear trains will not be required.

SECTION VI. COST ANALYSIS

A design requirement for the robot is that it must cost less than $500. The cost is based on 200,000 robots over 5 years. The $500 includes the horizontal positioning mechanism, the vertical motion arm and all the electrical control including power supplies and motors. Table 6.1 shows the costs of the horizontal positioning mechanism and electrical control parts. All parts except the roller bearings are based on high quantity orders. The cost of the corner bracket, slider bracket and belt aligner include the estimate cost of the molds. The items in parentheses are items that can be substituted for the part not in parentheses. A vendor and price reference list is in appendix H.

From the total at the bottom of table 6.1, the cost of horizontal positioning mechanism and electrical control parts using the 2.1-amp motors, steel control tube, and Duralon bearings is $396. This allows the cost of the vertical motion arm to be 20% of the total cost or about $100. If the average velocity requirements of the robot can be reduced about 50%, the 1.1-amp motors can be used. By using the 1.1-amp motors the cost of the horizontal motion parts would be reduced to $280. This allows the cost of the vertical motion arm to be 44% of the total cost or about $220. Replacing the the Duralon bearings with reciculating ball bearings results in the cost of the horizontal motion parts increasing to $490. This would not meet the cost requirements for the robot. If recirculation bearings and 1.1-amp motors were used the cost of the horizontal motion parts would be $374. This would allow the cost of the vertical motion arm to be 25% of the total cost or $126.

TABLE 6.1: HORIZONTAL MOTION COSTS

PART	INDIVIDUAL COST	COST PER ROBOT
CORNER BRACKET	1.00	4.00
SLIDER BRACKET	1.00	4.00
BELT ALIGNER	1.00	4.00
2.1 AMP STEP MOTOR/DRIVER	45.00	180.00
(1.1 AMP STEP MOTOR/DRIVER	16.00	64.00)
GUIDE ROD	2.00/FT.	32.00
CONTROL TUBE - STEEL	1.75/FT.	14.00
(ALUMINUM	1.50/FT.	12.00)
(GRAPHITE EPOXY	4.75/FT.	38.00)
(FIBERGLASS	1.00/FT.	8.00)
LINEAR MOTION BEARINGS - DURALON	2.51	30.12
(RECIRCULATING BALL	17.79	124.53[a])
(IGUS	.49	5.52)
TIMING GEARS	1.00	8.00
TIMING BELT	3.00	12.00
ROLLER BEARINGS	1.45	5.80
IDLER SHAFT	2.00	8.00
ELECTRICAL CONTROL	90.00	90.00
BOLTS,WASHERS, ETC.	4.00	4.00
TOTAL COST		**396.**
(USING 1.1 AMP MOTORS		**280.)**
(USING ROLLER BEARINGS		**490.)**
(USING 1.1 AMP & ROLLER BEARINGS		**374.)**

[a] Since the recirculating ball bushing bearings are two inches wide, one per slider will be required instead of two slider bearings per slider.

Items in parentheses can be substituted with the item not in parentheses.

SECTION VII. INTERFACE OF CATIA INTO DESIGN PROCESS

This section will describe the Computer Aided Three-Dimensional Interactive Application (CATIA) Computer Aided Design and Computer Aided Manufacturing (CAD/CAM) graphic system, discuss how it was applied to the robot design project and analyze its major attributes and shortcomings as they apply to the design process.

GENERAL DESCRIPTION OF CATIA

CATIA is a highly interactive three dimensional CAD/CAM graphic system written by Dassault System. CATIA was designed to facilitate the conceptualization, design and manufacturing of complex surfaces found in the aircraft industry. As a CAD system, CATIA is used for geometric modeling, defining complex surfaces and solids, analyzing shapes, simulating mechanisms and drafting. The geometry modeled appears as well defined colored two or three dimensional images that can be rotated about any axis or shaded in any light direction. As a CAM system, CATIA is used to design, simulate and program robot cells and generate tool paths to drive numerical control machines for part manufacturing. Both the CAD and the CAM use the same data base so that design changes can be quickly implemented into the whole system. Unlike typical CAD/CAM systems, CATIA recognizes the parts modeled as solids or surfaces instead of lines and curves which represent orthographic projections. Like a machinist, the CATIA designer could start with a block and remove cylinders or make cuts about a plane to create a final part. CATIA is run on a IBM 308x, 303x, or 43xx type computer. The workstation consists of a color IBM 5080 graphic terminal and a local IBM 5085 processor which performs graphic tasks.

INCORPORATION OF CATIA INTO THE ROBOT DESIGN

CATIA was used extensively in the design and prototyping of the robot during the author's three month work session at IBM in Charlotte, North Carolina. Before CATIA could be applied to the robot project, forty hours were required to learn the basic CATIA operations using an IBM written tutorial manual. This forty hours covered enough material to start modeling the conceptual ideas of the robot parts on CATIA. The initial modeling developed the basic CATIA skills. When the parts were being modeled and assembled together they could be visualized almost as well as if they were actually built and assembled. Because of vision capabilities, several manufacturing and part interference problems were discovered immediately which may have not been discovered until the prototype was built. The increased visualization and spatial representation greatly increased the effectiveness of the initial design review. The problem of not knowing exactly what parts or assemblies look like until they are built was eliminated. Because of inexperience with the system, the time required to model the first conceptual design took approximately 90 hours. With CATIA experience, the same modeling would take approximately 40 hours.

After the initial design review, the parts were redesigned and put into one model or file instead of an individual file for each part. The model is made up of one master section and one detail section for each part. The master section contains the assembled images of the parts. Each detail section contains a solid model of the a robot part. The images of the parts in the master section are called dittos of the solids located in the detail sections. With this method of organization, the geometry of a part is stored only once so when a part is modified in its detail section, the modifications occur automatically in the master section. For example, instead of having to store four sets of equal geometry data for the four corner brackets, only one set is stored in a detail file and then dittoed four times in the master section to represent the four corner brackets. When the corner bracket is modified, the modification automatically occurs on the four corner brackets in the master section. This method of project organization also allows for layers to be created. A layer shows only selected parts or sections in the master section. A layer containing just the corner brackets and guide rod was formed to represent the frame system of the robot. Figure 7.1 shows the robot without corner bracket and the drive system. Layering increases the ability to communicate concepts and ideas to others.

After the redesign and reorganization of the parts, CATIA was used to develop detailed prints of the robot for prototyping. To do this, the screen for the detail sections was divided into the standard three dimensional space mode and a drafting mode. Complete orthographic projections were projected from the solids in the space mode to the drafting mode. Also two isometric views of each part were projected into the draft mode for added clarification of the part geometry. The orthographic projections were dimensioned using techniques similar to CADAM or other CAD/CAM systems. Assemblies from the master section were

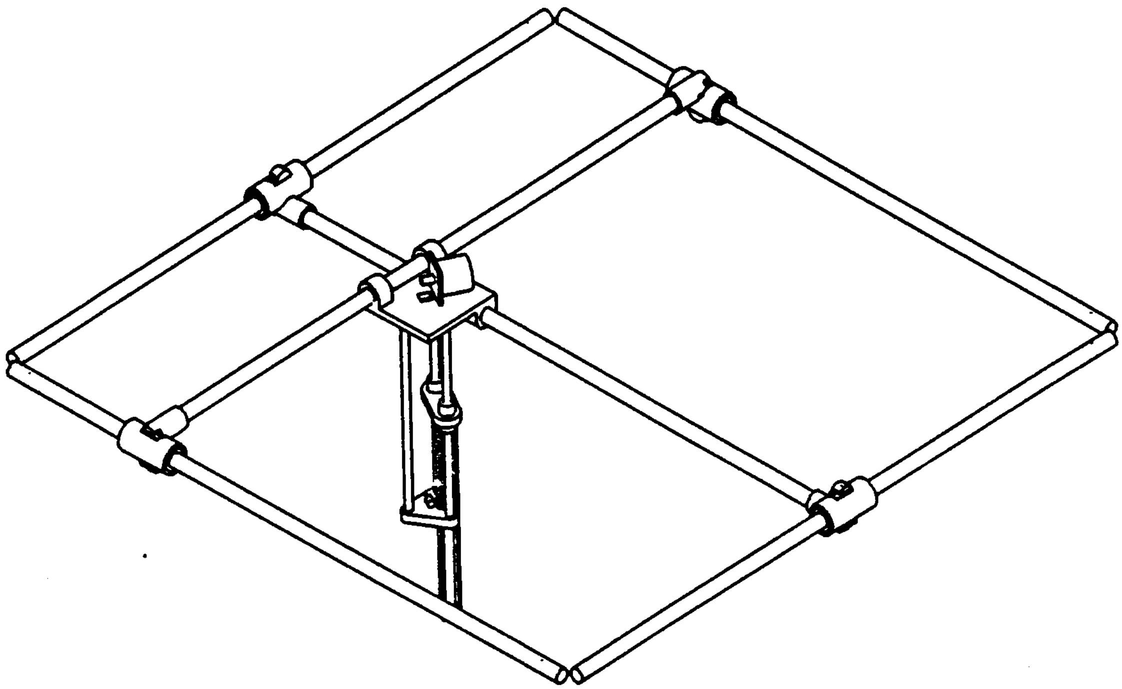

Figure 7.1: Robot Without Corner Brackets and Drive System

also projected into draw modes. All the draw modes were merged with a standard drawing boarder and then printed. These drawings are located in the pocket as plates. If a part is modified in the space mode, it is universally modified in the draw modes. Dimensioning the parts using CATIA was approximately twice as fast a it would be to dimension them by hand.

CATIA's analysis capabilities were also utilized for the robot design. Mass and center of gravity data for the slider and control tube were required for the dynamic model. The mechanical properties including principle axis and mass moment of inertias about the principle axis of a part are analyzed and displayed almost instantly. The analysis was also used to get an approximation of the mass and inertias of the vertical motion arm by conceptually modeling and analyzing it. An example of the results of the analysis are shown in figure 7.2 as they are displayed by CATIA.

INFLUENCE ON DESIGN PROCEDURE

CATIA strongly influences the design process by its;

1. Technical Benefits,
2. Consolidation,
3. Visualization.

Figure 7.3 shows various groups that could be involved in the design process. Each of these groups can use CATIA to facility their jobs because of its technical functions. With CATIA it is easy to develop fast conceptual designs that provide an accurate spatial representation. The vertical motion arm assembly shown in figure 2.1 is

VOLUME	=	0.135E+06				
WEIGHT	=	0.135E+06				
WETTED AREA	=	0.042E+06				
CENTER OF GRAVITY	: X =	50.000	Y =	9.077	Z =	5.450
1ST AXIS	: X =	0.000000	Y =	0.827243	Z =	0.561845
2ND AXIS	: X =	-1.000000	Y =	0.000000	Z =	0.000000
3RD AXIS	: X =	0.000000	Y =	-0.561845	Z =	0.827243
MAIN INERTIA I1	=	0.112E+09				
MAIN INERTIA I2	=	0.115E+09				
MAIN INERTIA I3	=	0.154E+09				

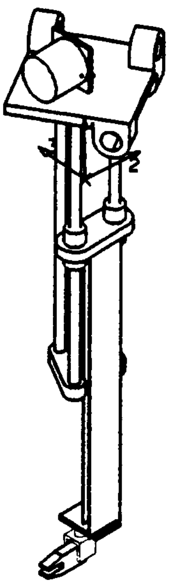

Figure 7.2: Sample Inertial Analysis Results

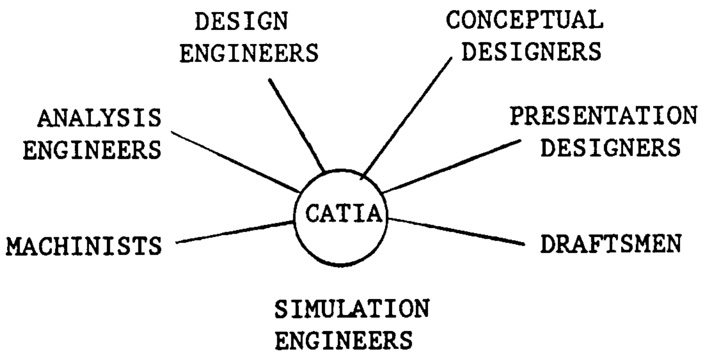

Figure 7.3: CATIA Organization

a result of the mental images transformed into graphic images. The time required to represent this conceptual design on CATIA was between 4 and 8 hours. From the conceptual design, the designer engineer can develop the parts with CATIA in the same manner and organization that the robot parts were developed and assembled. The draftsmen can take the developed parts and project image to create the prints. Analysis engineers use the developed parts to find the mechanical properties such and center of gravities and inertias about the principle axis of the parts. For the machinists CATIA will generate tool paths of the developed parts for the computer numerical control machines. The simulation engineer use the assemblies to simulate the kinematic motion of the parts. The simulation engineers can also develop a work cell were the parts will be made and assembled. The work cell can be simulated and controlled by CATIA. For the graphic developers, the three dimensional color images exist from the developed parts to develop graphics for presentations, manuals, advertisements. CATIA can be incorporated in many steps of the design process.

In figure 7.3 each group utilizes the same system and same project file to perform the work that can be facilitated by using a computer system. CATIA consolidates what could be several system into one system and one data file. The problem of having to manage multiple sets of data and not knowing which one is up to date is eliminated. With one system and one data file, the data only has to installed once and when it is changed the changes are universal for all users. With several systems, the data has to be installed more than once and when it is modified it has to be modified at all systems. An example of a non-consolidated system would be where the drafting is done using a CAD system like CADAM, the analysis is done using a package like CAEDS and the presentation material is prepared by hand or a separate graphic system. To expand on this example, a series of robot links were modeled for inertial analysis. Detailed CADAM prints were used to model the parts or install the data on CATIA. The time required to accomplish this was well over 200 hours, which is probably close to the time required to create the CADAM prints. The time required for the analysis of all the individual parts and assembled links was 40 hours. Also before the CATIA analysis, an analysis of all the approximate center of gravities of the parts and assemblies were performed by hand. The results were 160 pages of calculations. If the data had originally been modeled with CATIA, the 200 hours and 160 pages of calculations would have been eliminated. CATIA consolidates computer services and data into one system and one set of data. This consolidation increases project development efficiency.

Some have said that all CATIA is good for is making "pretty pictures". Making pretty pictures cannot be taken lightly when one's success can depend on being able to communicate ideas efficiently and professionally to other engineer's, managers and customers. A part shown using a three dimensional visualization is visualized much easier than a part visualized with three orthographic projections. A three dimensional visualization that is accurate, colorful and shaded is better than a three dimensional image that is not accurate or colorful or shaded. Even if all CATIA did was make pretty pictures, the illustrations increase ones ability to visualize the concept of the picture in an impressive and professional manner. Figure 7.4 shows a shaded color image of the corner bracket.

CATIA SHORTCOMINGS

CATIA's shortcomings concerns data storage space. The first of these has to do with the linking of models. This problem will be explained using a car's drive train as an example. To model a complete car drive train with CATIA, several models dividing the drive train into sections would have to be developed. The model size for the total drive train would not be large enough to contain all the data in one model. The models developed could represent the short block, the transmission, the differential and other equipment like the drive shafts and U-joints. The models, being similar the the robot model, would consist of assemblies and detailed parts. Linking the models into a total drive train assembly, which could be visualized and analyzed as one assembly, is not possible because the combined data of the models would be too large for one model. CATIA needs a function that could transform an

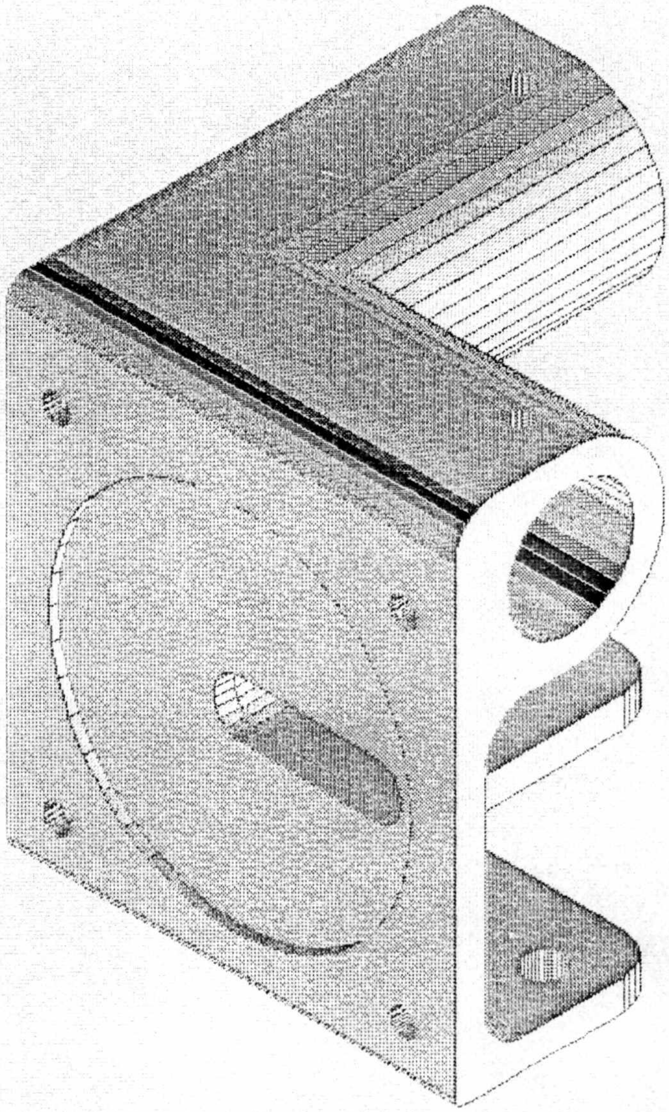

Figure 7.4: Shaded Color Image of the Corner Bracket

assembly of parts like a transmission into an solid with equivalent mechanical properties and outward appearance.

The second of the data storage problems with CATIA is that it cannot shade complex assemblies or parts. Figure 2.2 contains too much data to be shaded. The reason is shading requires much more data space than the object or objects being shaded.

The third data storage frustration is that when a model is close to being full, the system response time is slow. To change from a detail to the total robot assembly would take about at least a minute for the buffer to refresh itself.

CATIA's frustrations are outweighed by its positive attributes which greatly benefit the design process.

SECTION VIII. CONCLUSION

This section will compare the plus system robot to commercial robots, evaluate the completion of the design requirements and recommend design improvements.

ROBOT COMPARISON

Table 8.1 compares the plus system robot with commercial machine loading or part transferring robots. The plus system robot shown uses the 2.1-amp motors and recirculating ball bushing bearings.

TABLE 8.1: ROBOT COMPARISON

ROBOT MAKE	ACCURACY (INCH)	MAX VELOCITY (INCH/SECOND)	PAYLOAD (POUND)	COST[a]
RECOMMENDED PLUS SYSTEM	.006	36	3	\$600[b]
PUMA 550	.004	39	6.6	\$47,000
TASKHANDLER 25	.126	30	26	\$39,500
SEIKO M-100	.0004	39	4.4	\$5,700
MICROBO MR-02	.0007	106	2.2	\$50,000

[a]Typical U.S. cost
[b]Cost to manufacture

The major advantages of the recommended plus system robot are cost, programming ease and modularity. Table 8.1 shows that the cost of the plus system robot could be much less than typical robots. The low cost allows large companies and small companies to start automating the tasks that could be performed with the plus system robot without enormous costs. The plus-system robot provides high technology without high technology prices. The programming of the robot, developed by Mr. Yeo, is performed on a IBM PC using menu driven screens. No special language is required. The only knowledge required is the end effector locations, desired speeds, and delay times for the robot moves. The modularity of the robot gives the users freedom to configure the robot for particular applications and work spaces.

COMPLETION OF DESIGN GOALS

IBM provided a goal at the start of the robot project that was to designed a low-cost, high-speed robot that is modular, uses a simple control and has an accuracy of .118 inch. These goals where possible are satisfied. With a rigid vertical motion arm extended 20 inches below the control tubes, the accuracy of the prototype would be .05 inches which exceeds the required accuracy. A major emphasis of the robot development has been its cost. The prototype design satisfies the cost requirements. A robot using the designed horizontal positioning mechanism would cost around $500 to manufacture for high production. The requirement that is not satisfied is the average velocity. The average velocity for a 12-inch move of the prototype varies between 20 and 26 inches per second for a typical load of eight pounds. This is considerably less than the functional requirement 39 inches per second. Only with ideal conditions, the largest motors and loads of less than four pounds would the robot be able to meet the functional requirement. The robot design in modular. By shortening the control tubes, guide rods and belt length, the robot's work area is changed. The robot design also facilitates manufacturing and assembly: two unspecified goals.

DESIGN CHANGES

Table 8.2 shows the performance data that was displayed in Table 2.1 with the cost shown for each option.

TABLE 8.2: PERFORMANCE DATA FOR ROBOT OPTIONS

PARAMETER	PROTOTYPE	OPTION 2	OPTION 3
BEARINGS	SLIDER	ROLLER	ROLLER
STEP MOTORS	2.1 AMP	2.1 AMP	1.1 AMP
MAX SPEED (IN/SEC)	36	36	18
ACCELERATION/DECELERATION TIME (SECONDS)	.43	.24	.12
AVERAGE VELOCITY (IN/SEC)	21.1	26.1	16.0
RESOLUTION (INCHES)	.0157	.0157	.0157
ACCURACY	.047	.006	.006
COST	$496	$590	$474

As shown above, by spending an additional $100, the robot's accuracy and speed would be increase substantially. More important than increasing the robot's performance, would be an increase in the robot's reliability. From the section on failure conditions, the potential for a failure condition would be reduced if recirculating ball bushing bearings were used. This would make the robot essentially friction independent.

Besides using recirculating ball bushing bearings in place of sliding bearings, other design changes to the prototype exist. A list of recommended design changes to the prototype design is shown below.

ROBOT CHANGE RECOMMENDATIONS

Use low friction bearings

Determine parallelism, straightness, and stiffness specifications

Eliminate set screws in timing gears.

Install rubber boots on ends of guide rods and control tubes.

Provide positive adjustment mechanism for idlers.

Use quality roller bearings in idlers.

A potential failure condition can be eliminated if the control tubes and guide rods have a surface suitable for recirculating ball bearings, are straight and are assembled either parallel or perpendicular to each other. The surface finish and hardness will be specified by the bearing vendor. The exact specifications for guide rod and control tube parallelism, straightness, and also stiffness will have to be determined by the type of analysis discussed in the failure condition section. The timing gears need to be attached securely to the motor shafts. The set screws in the shafts are unsatisfactory since they often come loose. Rubber boots that fit over the ends of the control tubes and guide rods would isolate the tubes or rods from the slider or corner brackets. This will eliminate chatter and add compliance to the system. An idler tension mechanism needs to be installed to insure and facilitate the proper tensioning of the timing belts. Quality roller bearings should be used in the idlers to provide long life and no maintenance. The above changes will produce a robot that is faster, more accurate and more reliable.

LIST OF REFERENCES

LIST OF REFERENCES

Asada, Haruhiko, and Jean-Jacques E. Slotine. Robot Analysis and Control. New York: John Wiley and Sons, 1986.

Hair, Victor D. "A Systematic Approach To Step Motor Algorithm Design." 1987.

Korein, J. U., and J. Ish-Shalom. "Robotics." IBM Systems Journal, 26, No. 1, 1987, pp. 55 - 95.

Nof, Shimon Y. Handbook of Industrial Robotics. New York: John Wiley and Sons, 1985.

Robotic Equipment Survey. San Jose: Robotics Technology, Advanced Manufacturing Engineering Department, 1983.

APPENDIXES

APPENDIX A: SYSTEM STIFFNESS DERIVATIONS AND CALCULATION PROGRAM

GANTRY SYSTEM STIFFNESS

The below schematic shows the gantry system with a force F applied to center of gravity of the end effector.

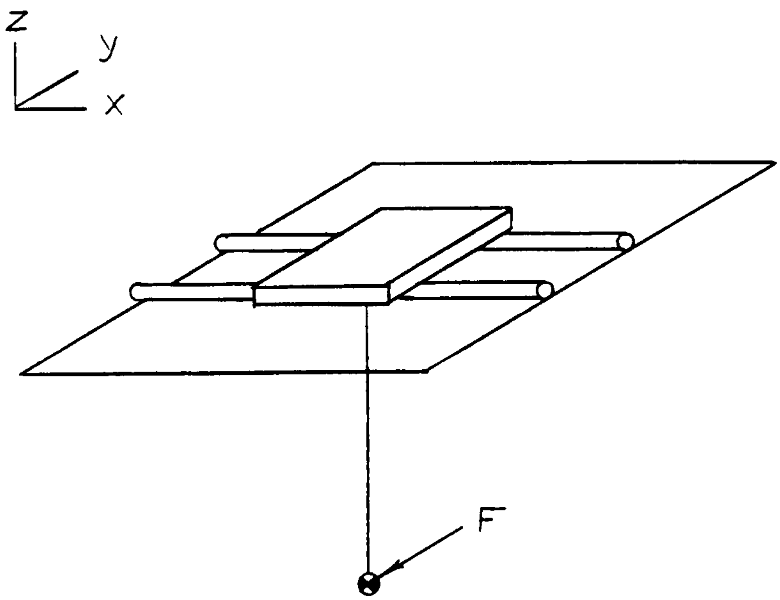

Gantry System Schematic

The next schematic shows a side view of the system.

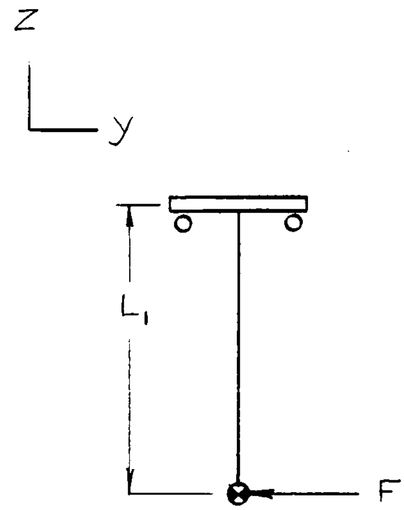

Side View Gantry System

An equivalent force and moment are shown acting on the system below. The following schematic shows the reaction of the force and moment on the control tubes.

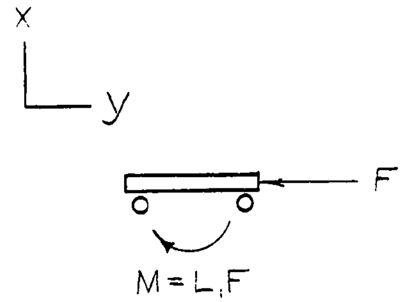

Equivalent Force and Moment

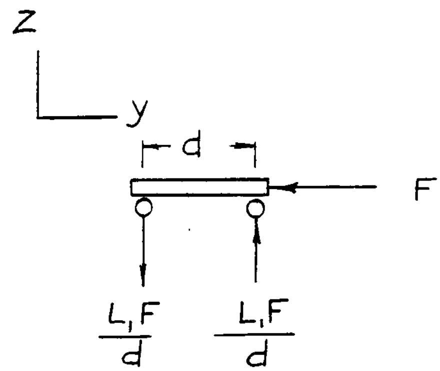

Reactions on Guide Tubes

A control tube deflects in the y direction because of F and L_1F/d or:

$$delt(y) = delt(F) + delt(L_1F/d).$$

For delt(F), the control rods are assumed to be simply supported with point loading of F/2 as shown below. The deflection at 'a' for this system is:

$$\text{delt}(F) = Fba(L^2 - a^2 - b^2)/6LEI \qquad \text{eq1}$$

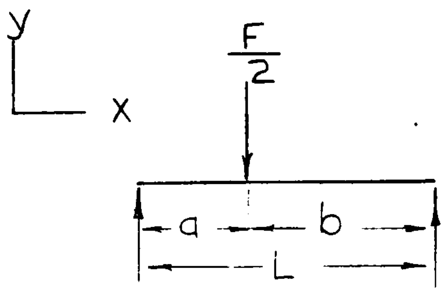

Guide Tube Loading

For vertical deflection, delt(vert), the control tubes are assumed to be simply supported with point loading of L_1F/d as shown in the below schematic. The vertical deflection at a for this system is:

$$\text{delt(vert)} = L_1Fba(L^2 - a^2 - b^2)/6dLEI$$

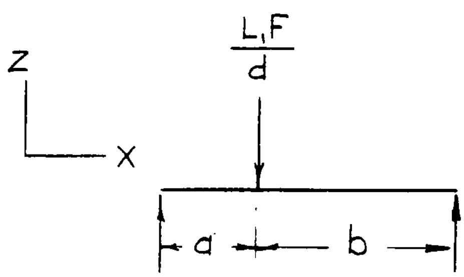

Guide Tube Vertical Loading

From the below schematic it is seen that:

$$\text{delt}(L_1F/d) = 2\text{delt(vert)}L1/d \qquad \text{eq2}$$

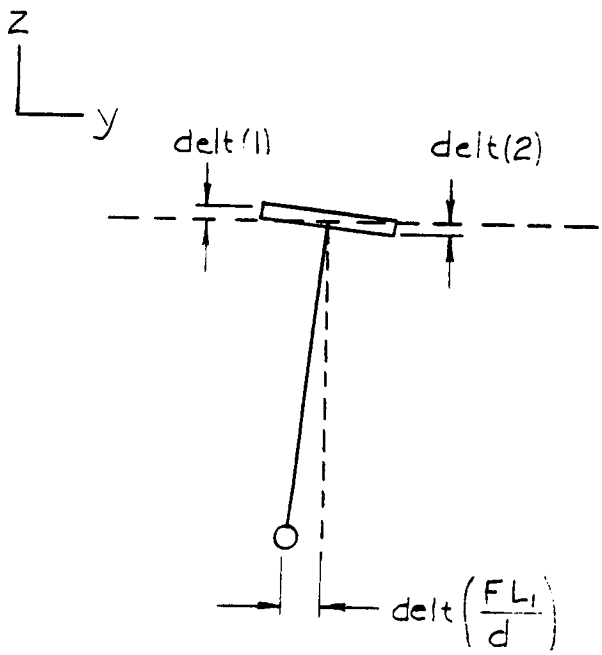

Y Direction End Effector Deflection

Combining eq1 and eq2, the total deflection in the y direction is:

$$\text{delt}(y) = Fab(L^2 - a^2 - b^2)[1/12 + L_1{}^2/(3d^2)]/(EIL)$$

Rearranging this equation for non-dimensional stiffness results in:

$$\text{delt}(y)EI/FL^3 = ba(L^2 - a^2 - b^2)[1/12 + L_1{}^2/3d^2]/L^4.$$

PLUS SYSTEM STIFFNESS

The below schematic shows the plus system with a force acting at the center of gravity of the vertical motion arm.

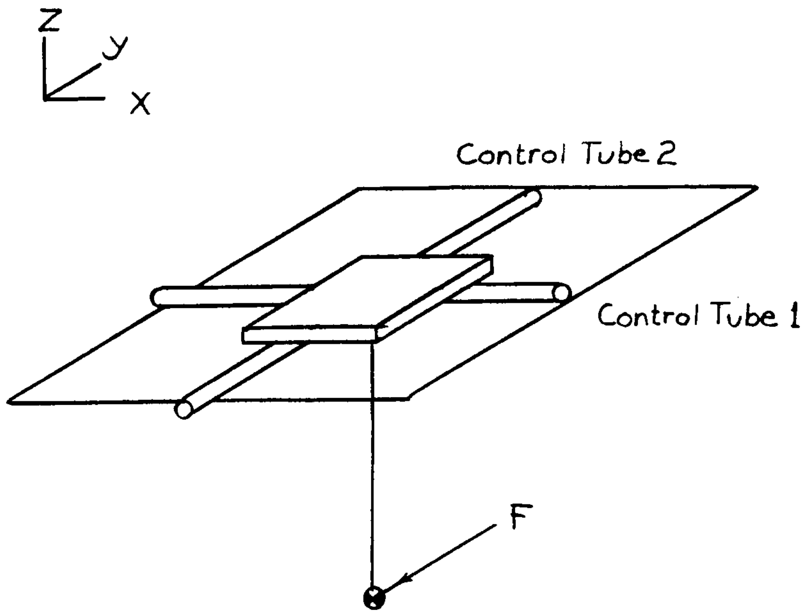

Plus System Schematic

The next schematic shows the side view of the system.

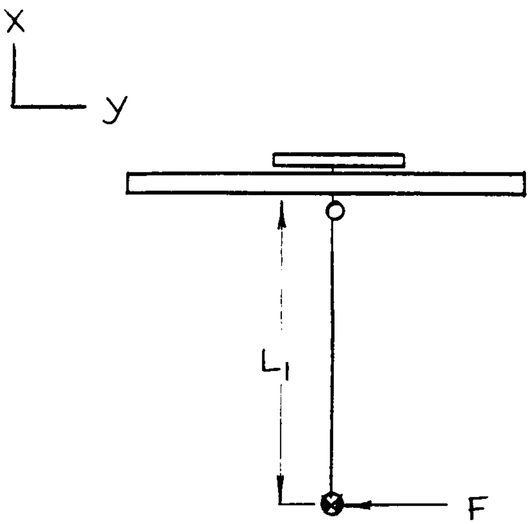

Side View of Plus System

An equivalent system is shown below. The following schematic shows the forces acting on the control tubes.

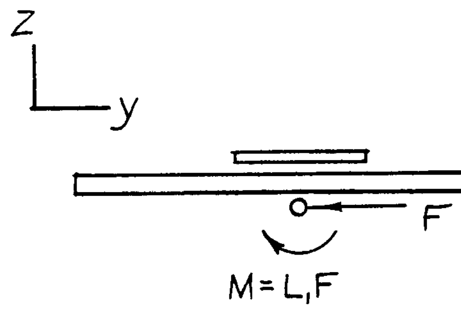

Equivalent System

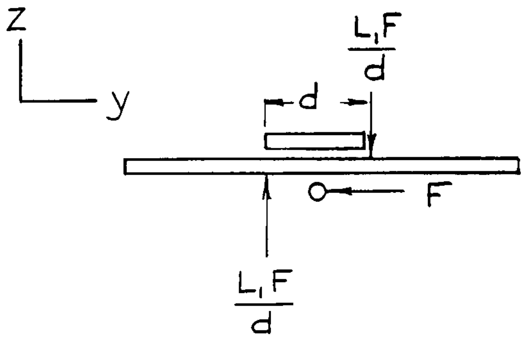

Control Tube Forces

The deflection in the y direction is caused by F and L_1F/d:

$$delt(y) = delt(F) + delt(FL_1/d)$$

Delt(F) effects control tube 1. To determine delt(F), control tube 1 will be assumed as simply supported beam with a point load F as below. The deflection will be:

$$delt(F) = Fba(L^2 - a^2 - b^2)/6LEI$$

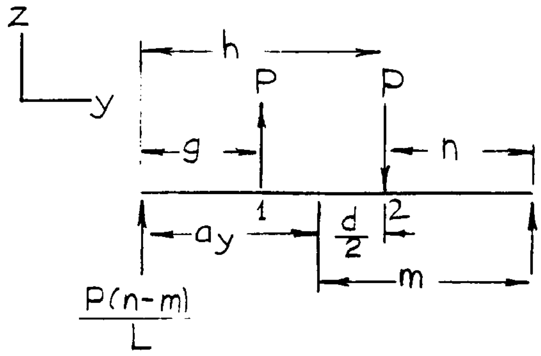

Horizontal Control Tube Loading

Delt(FL_1/d) effects control tube 2. To determine delt(FL_1/d), control tube 2 will be assumed as a simply supported beam with loads at 1 and 2 as shown in below.

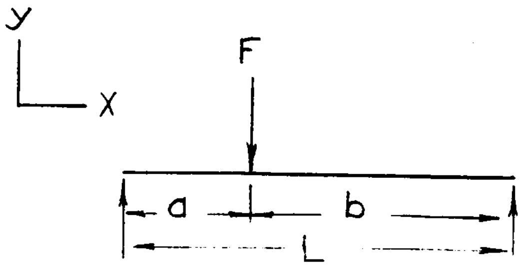

Vertical Control Tube Loading

The force P equals FL_1/d. By summing moments about a point x, the deflection for this system is:

$$y = P[(n - m)x^3/L + \langle x - g\rangle^3 - \langle x - h\rangle^3 + x(n^3 - m^3 + dL^2)/L]/6EI.$$

The expression $\langle a - b\rangle$ equals either zero if b is greater than a, or (a - b) if a is greater than b.

The deflection at 1 is:

$$delt(1) = L_1F[-dg^3/L + g(n^3 - m^3 + dL^2)/L]/6EId.$$

The deflection at 2 is:

$$delt(2) = L_1P[-dh^3/L + d^3 + h(n^3 - m^3 + dL^2)/L]/6EId.$$

From the below schematic for small delt(1) and small delt(2):

$$delt(FL_1/d) = L_1[delt(1) - delt(2)]/d.$$

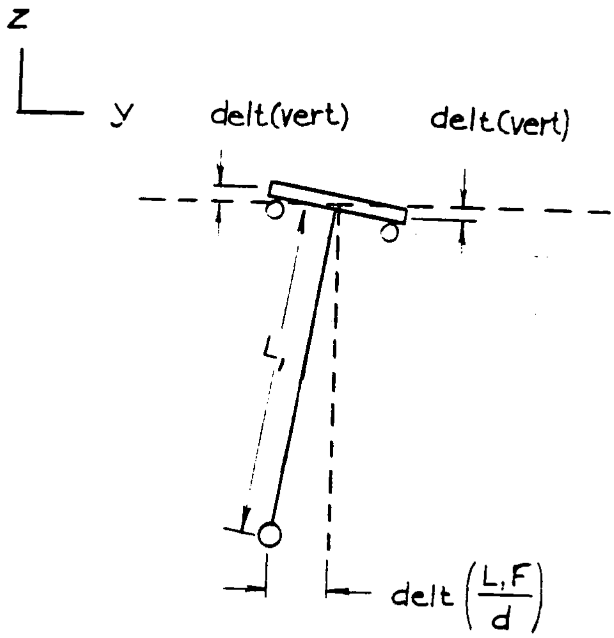

Y Direction End Effector Deflection

The equation for stiffness of the system is:

$$delt(y)EI/FL^3 = [L_1EI[delt(1) - delt(2)]/Fd + ba(L^2 - a^2 - b^2)/6L]$$

Using the derived stiffness equation for the plus and gantry system robots, the below program calculates the data shown in figure 3.4.

STIFFNESS CALCULATION PROGRAM

```
10 '*****************************************************************
20 '** PROGRAM TO CALCULATE THE STIFFNESS OF GANTRY AND PLUS SYSTEMS **
30 '*****************************************************************
40 '
50 '----output data files------
60 OPEN "A:PLUSD4.DAT" FOR OUTPUT AS #1
70 OPEN "A:GANTD4.DAT" FOR OUTPUT AS #2
80 '----constants-------------
90 L = 38: LI = 30 'L = control tube length: LI = vert arm c.g. dist'
100 D = 4                  'D = platform width
110 '----vary A, platform positioning on control tube-----
120 FOR A = D/2 TO 20  STEP .5
130  '------constants---------
140 B = L - A
150 AY = 19
160 H = AY + D/2
170 G = AY - D/2
180 M = L - G
190 N = L - H
200 '------stiffness equation for gantry system
210 KI = B*A*(L^2-A^2-B^2)*(1/12 + LI^2/(3*D^2))/L^4
220 '------nondimensional deflections for plus system------
230 YG= (LI/(6*D*L^3))*(-D*(G^3)/L + (G/L)*(N^3 - M^3 + D*L^2))
240 YH= (LI/(6*D*L^3))*(-D*(H^3)/L + D^3 + (H/L)*(N^3 - M^3 + D*L^2))
250 DELTA = (YG - YH)*LI/D
260 YY = B*A*(L^2-A^2-B^2)/(6*L*L^3)
270 DELTT = DELTA + YY
275 '-----print statements--------
280 PRINT USING "####.#### ####.#### ####.####";A/L,1/KI,1/DELTT
290 PRINT #1, USING "####.#### ####.####";A/L,1/DELTT
300 PRINT #2, USING "####.#### ####.####";A/L,1/KI
310 NEXT A
320 CLOSE #1
330 CLOSE #2
```

APPENDIX B: PROTOTYPE PHOTOGRAPHS

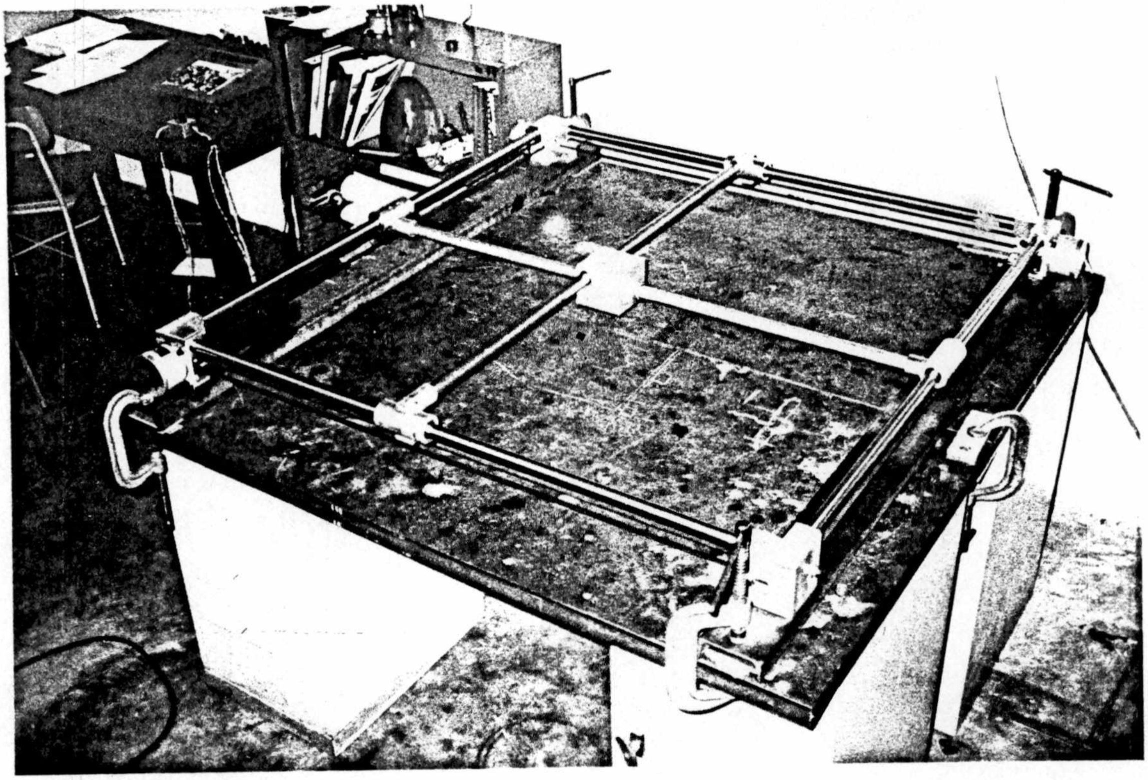

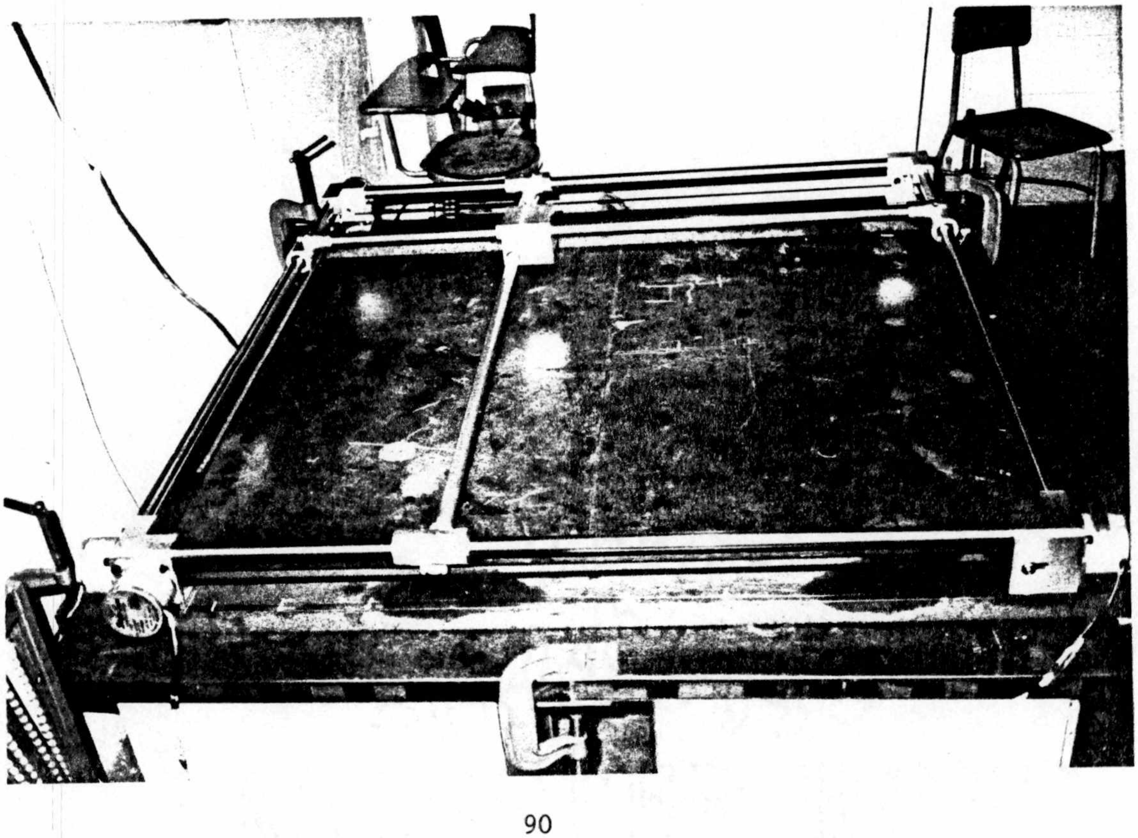

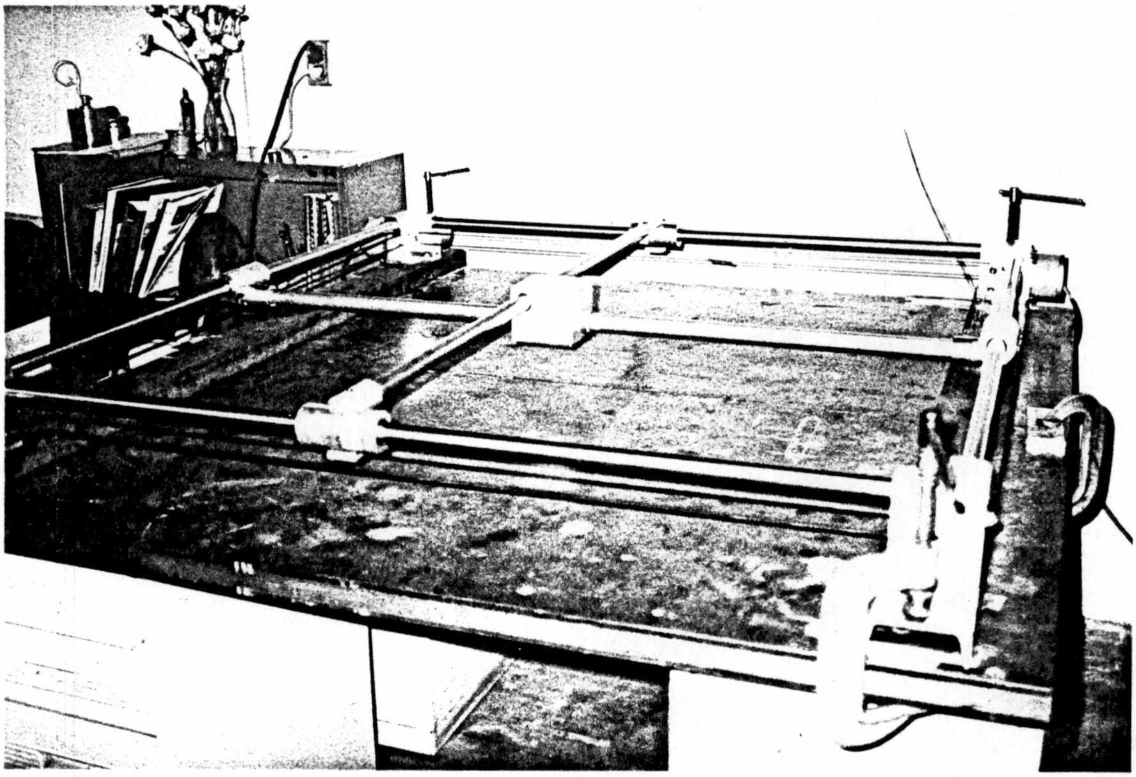

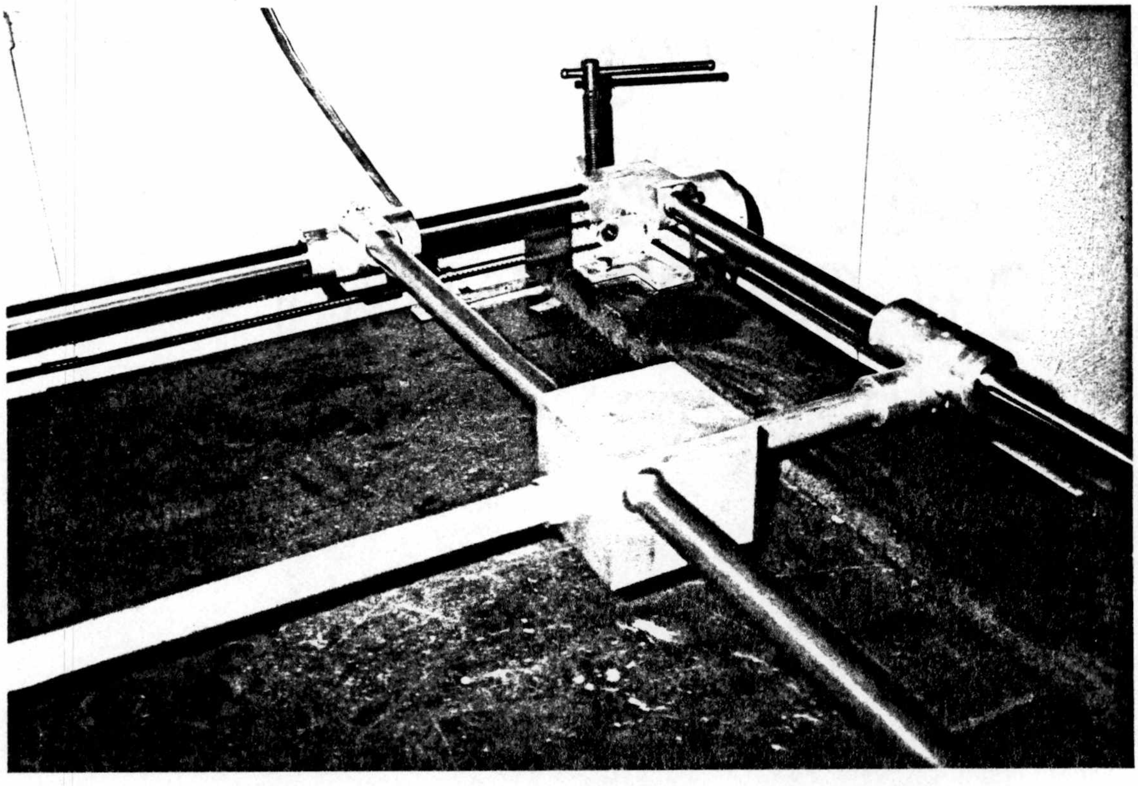

APPENDIX C: STEP MOTOR SPECIFICATIONS

The following information shows the dimensions of the three step motors that were considered for use in the prototype. The information was provided by IBM.

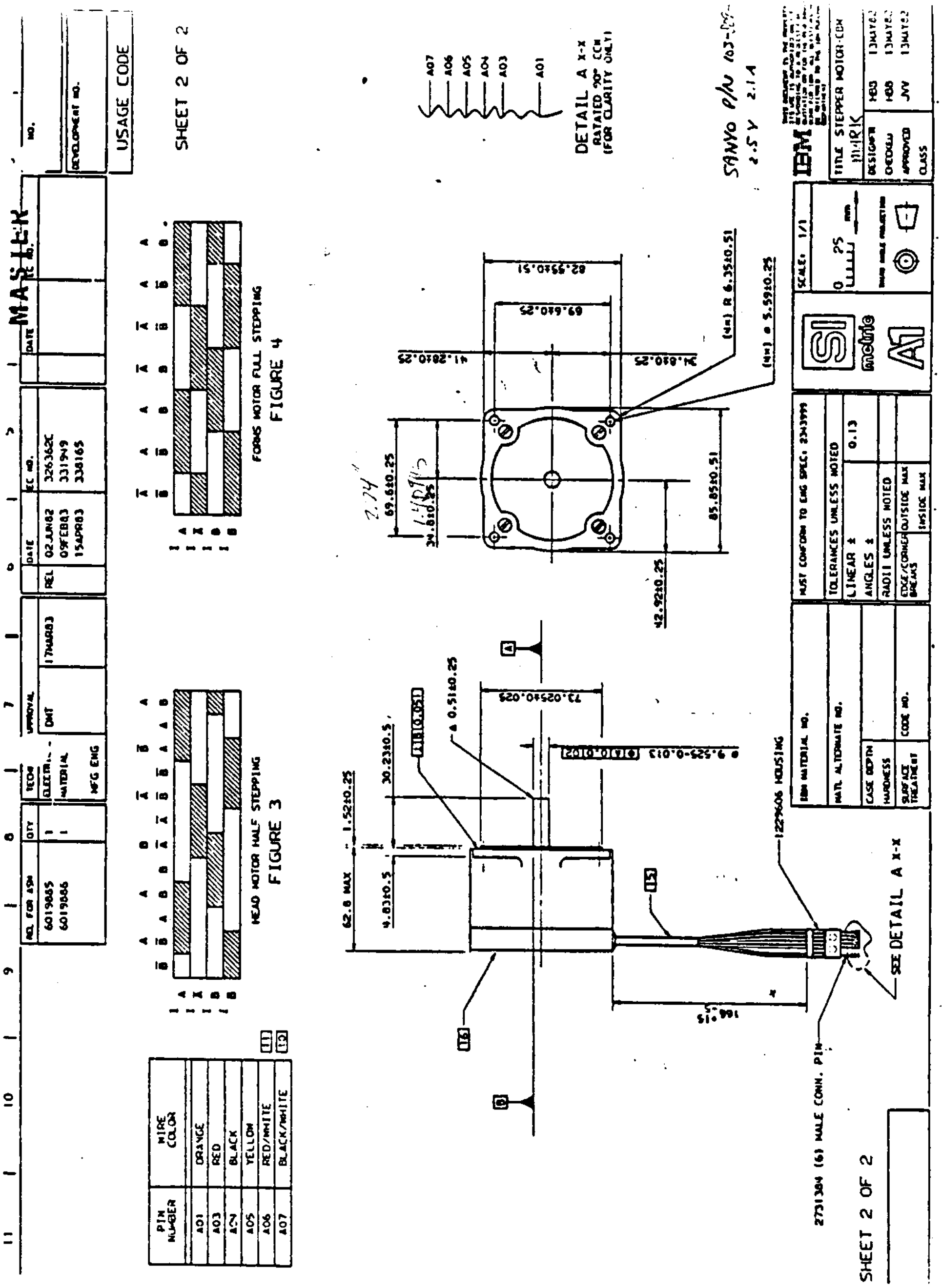

2.1 Amp Step Motor Information

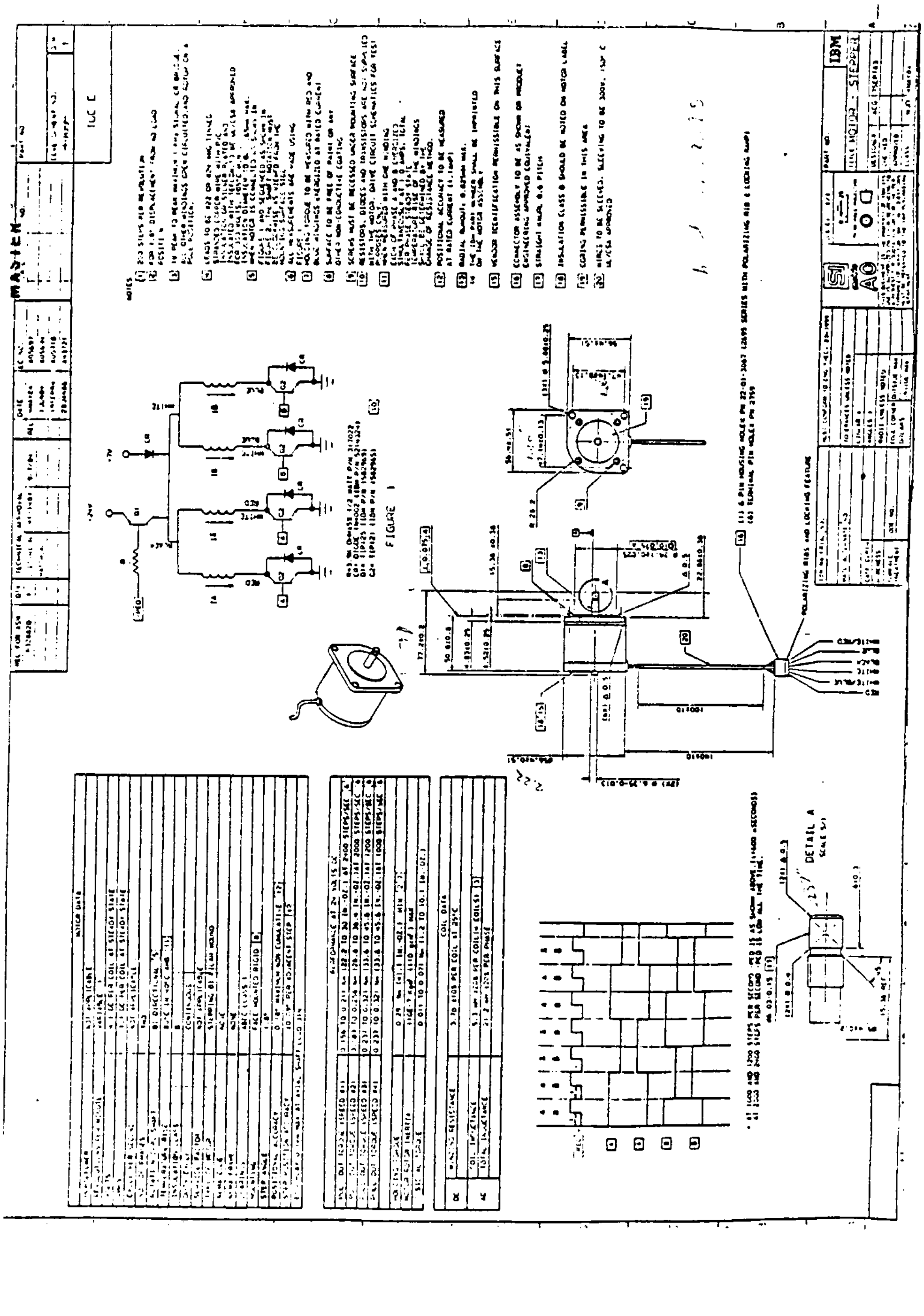

1.1 Amp Step Motor Information

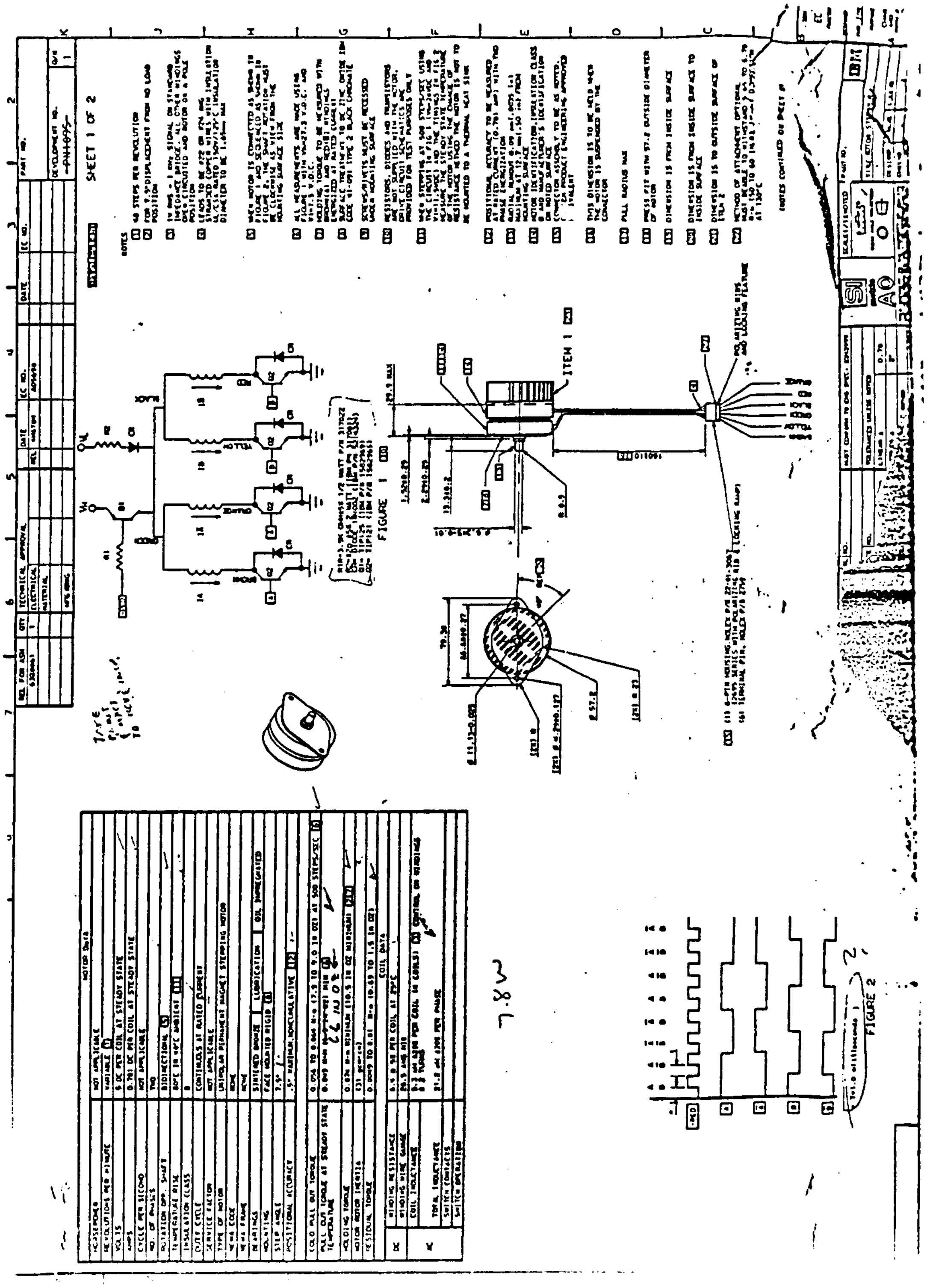

0.8 Amp Step Motor Information

APPENDIX D: DERIVATION OF SYSTEM EQUATION OF MOTION

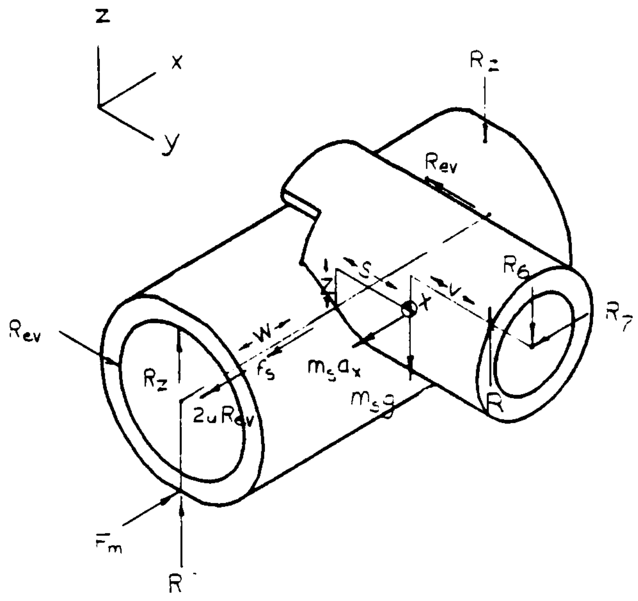

Slider Bracket Schematic

By summing forces in the x direction:

$$F_m - (C_2 + m_s)a_x - f_s - 2uR_{ev} = f \qquad \text{eq 1}$$

By summing moments at the center of gravity about the z axis:

$$-F_m s - a_x C_2 v + f_s s + 2R_{ev}(us+w) = fv \qquad \text{eq 2}$$

By summing moments at the center of gravity about the y axis:

$$F_m y + C_2 a_x x - 2R_z w - 2uR_{ev} z - f_s z = -fx \qquad \text{eq 3}$$

The vertical distance form the motor force to the center of gravity is y. By manipulating equations 1 and 2 the equation of motion for the slider is derived:

$$a_x = (K_1 F_m - K_2)/m_{eq}$$

where:

$$m_{eq} = C_2 + m_s + u[s(C_2 + m_s) + C_2 v]/w$$

where:

$$K_2 = 2uR + f[u(s + v)/w + 1]$$

and where:

$$K_1 = 1.$$

APPENDIX E: STEP MOTOR RAMP DEVELOPMENT PROGRAM

The below program dynamically models the horizontal positioning mechanism. Referring to figure 2.4, the constants of the mechanism are shown on lines 170 through 510. The constant calculations are performed on lines 510 through 590. The positive acceleration ramp is determined on line 620 through 670. The negative acceleration ramp is determined on lines 690 through 720. The integration subroutine starts at line 830 and ends on line 1580. For single axis motion of the robot, line 1450 should be changed to "ACCY = 0."

```
10  ' ******************************************************
20  ' ** PROGRAM TO DETERMINE POSITION, SPEED, ACCELERATION**
30  ' ** AND DELAY TIME IN-BETWEEN STEPS FOR HORIZONTAL     **
40  ' ** MOTION OF THE PLUS SYSTEM ROBOT                   **
50  ' ** BY: MARK GRANGER                                  **
60  ' **     UNIVERSITY OF TENNESSEE MECHANICAL ENGINEERING**
70  ' **                                                   **
80  ' ** LAST EDITED FEBRUARY 27, 1988                     **
90  ' ******************************************************
100 '
110 DIM K(4,80),Y(80),Z(80),YD(80)
120 'OPEN "c:DISP1.DAT" FOR OUTPUT AS #1        '--DISPL OUTPUT--'
125 '--------DATA FILES FOR GRAPHING-------
130 'OPEN "c:accl.dat" FOR OUTPUT AS #2         '--BEARING LOSS OUTPUT'
140 'OPEN "c:VEL1.dat" FOR OUTPUT AS #3    '--vel file output--'
150 PI = 3.14159: G = 386
160 '---------PLATFORM AND CONTROL TUBE CONSTANTS -----------

170 LENG = 36        'length of control tube (inches)'
180 DD= 4            'width of platform (inches)'
190 LI = 2           'vertical distance from platform to c.g. (inches)'
200 AI = 3           'horizontal dist from end of tube to c.g. (inches)'
220 MLOAD = 8/386    'mass of platform and vert arm (lb-s^2/in)'
230 MCT = .00719     'mass of control tube'
240 MS = .00306      'mass of slider'
250 '---------SLIDER CONSTANTS -----------------
260 V = .75         'refer to diagram'
270 XS = .627
280 SS = .36
290 ZS = .214
300 YS = 1.19
310 WS = 1.97
```

```
320 '--------- STEP MOTOR CONSTANTS ----
330 '    TORQUE ACC=A*OMEG^2+B*OMEG+C  TORQUE DEACC=D*OMEG^2+E*OMEG+C---
340 '    MOTOR ROTOR INERTIA = IMOT (OZ-IN-S-S) -- TORQUE = IN-OZ ------
350 '-----1.1- amp motor 6185917 ---------
360 'A=-1.017E-06:B=-.002043:C=28.08:IMOT=.00156
370 'D=1.38E-06:E=-.00711:F=-27.25:GOTO 390
380 '-----2.2-amp motor 6019919 ---------
390 G2=1.6927E-16: H2=-2.6651E-12: I2=1.4019E-08: J2=-2.4312E-05
400 L2=-62.57: A=-1.1229E-16: B=1.015E-12: C=-3.4792E-09: D=3.296E-06
410 E=-.007244: F=62.21: K2=.0020146
420 IMOT=.00165
460 '
470 ' ------- OTHER CONSTANTS ---------
480 NUM = 1
490 MU = .3                                    'friction coefficient'
500 R = .5                                     'motor gear radius (inches)'
510 C1 = (MCT + MLOAD*(LENG-AI)/LENG)/2
520 C2 = (MCT/2 + MLOAD*(LENG-AI)/LENG)
530 R6 = G*C1
540 RR = (MS + C1)*G/2                         'R'
550 KK1 = 1                                    'K1'
560 FS = 2*MU*RR                               'fs'
570 ME = C2 + MS + MU*(SS*(C2+MS) + C2*V)/WS
580 IGEAR = 1.6*PI*R^4/(8*386)                 'gear inertia (OZ-IN-S-S)'
590 IEQ = (IGEAR + IMOT)/16      'equivalent system inertia (LB-IN-S^2)'
600 IF MU*G*MLOAD>F/16 THEN
    PRINT "CHECK MOTOR LOAD" 'CHECK FOR MAXIMUM LOAD'
610 '--------POSITIVE ACCELERATION RAMP -----------
620 Y1 = 0: Y2 = 0: TT = 0                     'initial conditions'
630 TYPE = 1
640 MAXVEL = 70                 'max velocity obtained by motor (RAD/SEC)'
650 PRINT "  TIME    DISPL    VEL    ACC    STEP #   DELAY  "
660 PRINT "   (S)     (IN)   (IN/S)  (IN/S^2)          (S)"
670 GOSUB 830
680 '-------- NEGATIVE ACCELERATION RAMP -----------
690 Y1 = Y(1): Y2 = Y(2): TT = T
700 TYPE = 2
710 MINVEL = 0
720 GOSUB 830
730 '
740 CLOSE #1
750 CLOSE #3
760 CLOSE #2
770 END
780 '
790 '**** SUBROUTINE USING 4TH ORDER RUNGE-KUTTA INTEG METHOD TO SOLVE**
800 '**** SYSTEMS OF FIRST-ORDER ORDINARY DIFFERENTIAL EQS WRITTEN BY **
810 '**** F.H. SPECKHART  UNIVERSITY OF TENNESSEE MECH ENGINEERING *****
820 '
830 Y(1)=Y1: Y(2)=Y2: T=TT
840 T9 = 4                 '----T9 = MAXIMUM RUN TIME ----'
```

```
850 T8 = .005                '----T8 IS EQUAL TO THE PRINT INTERVAL ----'
860 D1 = .0005               '----D1 = INCREMENT OF INTEGRATION STEP SIZE--'
870 T8 = T8/D1
880 N = 2                         '----N = NUMBER OF FIRST ORDER D.E.s----'
890 SS= 1
900 '
910 ' ********* START OF SUBROUTINE **********
920 FOR I = 1 TO 10
930 Z(I)= Y(I)
940 NEXT I
950 T7 = 9.000001E+09
960 GOTO 1190
970 FOR J = 1 TO 4
980 ON J GOTO 1120,990,1040,1080
990 T = T+D1*.5
1000 FOR I = 1 TO N
1010 Y(I) = K(1,I)*D1*.5 + Z(I)
1020 NEXT I
1030 GOTO 1120
1040 FOR I = 1 TO N
1050 Y(I)= K(2,I)*D1* .5 + Z(I)
1060 NEXT I
1070 GOTO 1120
1080 T = T + .5*D1
1090 FOR I = 1 TO N
1100 Y(I) = K(3,I)*D1 + Z(I)
1110 NEXT I
1120 GOSUB 1410
1130 FOR JK = 1 TO N
1140 K(J,JK) = YD(JK):    NEXT JK
1150 NEXT J
1160 FOR I = 1 TO N
1170 Z(I) = Z(I) + D1*(K(1,I) + K(4,I) + 2*(K(3,I)+K(2,I)))/6
1180 NEXT I
1190 FOR I = 1 TO N
1200 Y(I)= Z(I)
1210 NEXT I
1220 IF Y(2)>MAXVEL AND TYPE =1 THEN RETURN    '-RAMP UP CHECK   ---'
1230 IF Y(2)<MINVEL AND TYPE = 2 THEN RETURN   '-RAMP DOWN CHECK ---'
1240 STEPS = Y(1)*31.831:IF Y(2)=0 THEN DELAY=0
     ELSE DELAY=1/(Y(2)*31.831)
1245 '-------linearly interpolate steps to intergers-------
1250 IF STEPS > NUM THEN 1260 ELSE 1290
1260 DELAYS=DELOLD + (NUM-STPOLD)*(DELAY-DELOLD)/(STEPS-STPOLD)
1270 PRINT USING " ##.### ##.### ##.### ####.### ###.#   .#####";
     T,Y(1)*R,Y(2)*R,YD(2)*R,NUM,DELAYS
1280 NUM = NUM + 1 : GOTO 1250
1290 STPOLD = STEPS : DELOLD = DELAY
1300 T7=T7+1
1310 IF T7<= T8-.0002 THEN 1390
1320 T7=0
```

```
1330 '
1340 ' **** PRINT STATEMENTS ****
1350 'PRINT #1, USING ".###  ###.##"; T,Y(1)*R
1360 'PRINT #3, USING ".### ###.###"; T, Y(2)*R
1370 'PRINT #2, USING ".### ####.#"; T, YD(2)*R
1380 'PRINT USING "##.###  ###.##  ####.####  ####.##  ####.#  .######";
     T, Y(1)*R,Y(2)*R,YD(2)*R, STEPS, DELAY
1390 IF T= < T9 THEN 970
1400 RETURN
1410 '
1420 '***** DIFFERENTIAL EQUATIONS OF MOTION AND MOTOR TORQUE *****
1430 '-Y(1)=ANGULAR POSITION (RADIANS) --Y(2)=ANGULAR VELOCITY (RAD/SEC)
1440  '-YD(2)=DERIVATIVE OF Y(2) OR ANGULAR ACCELERATION (RAD/SEC/SEC)-
1450 ACCY = YD(2)                                'acceleration normal'
1460 MOM = MLOAD*YD(2)*LI                        'M or moment (in-lb)'

1470 FR1 = MU*(2*MOM/DD + MLOAD*ACCY)            '2 possibilities of F'
1480 FR2 = MU*MLOAD*(G/2 + ACCY)
1490 IF MLOAD*G/4 > MOM/DD THEN FR = FR2 ELSE FR = FR1
1500 FRIC = FR*(LENG - AI)/LENG                  'f (lb)'
1510 KK2 = 2*MU*RR + FRIC*(MU*(SS+V)/WS + 1)     'K2'
1520 YD(1) = Y(2)
1530 SPS = Y(2)*100/PI                       'convert rad/sec to step/sec'
1540 POSTQ = (A*SPS^5+B*SPS^4+C*SPS^3+D*SPS^2+E*SPS+F)/16
1550 NEGTQ = (G2*SPS^5+H2*SPS^4+I2*SPS^3+J2*SPS^2+K2*SPS+L2)/16
1560 IF TYPE=1 THEN TMOT= POSTQ ELSE TMOT= NEGTQ
1570 YD(2) = (-R*KK2/KK1 + TMOT)/(IEQ + ME*R^2/KK1) 'equation of motion'
1580 RETURN
```

APPENDIX F: BINDING DERIVATIONS

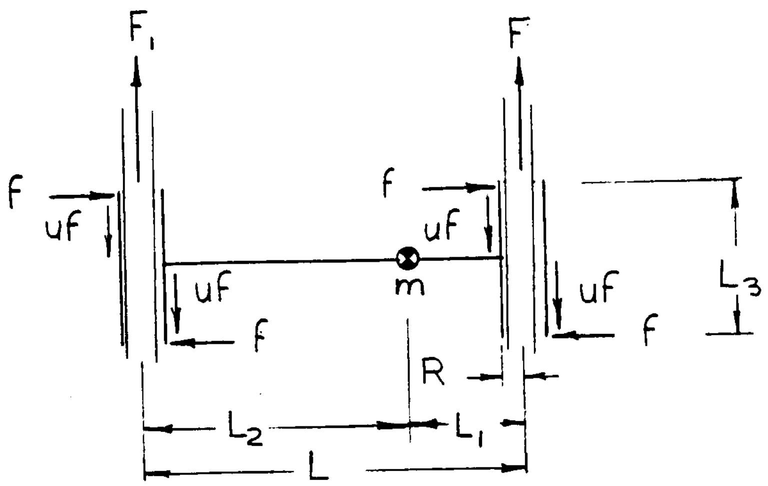

Force Diagram For Binding Slider and Control Tube

F and F_1 are external forces acting on the sliders brackets. u is the friction coefficient between the slider bearing and guide rod. f is normal force caused by binding acting at the slider bearings at the ends of the control tubes. All normal forces are assumed to be equal. The friction coefficient for the system is assumed to constant for the system.

By summing forces in the Y direction:

$$F + F_1 - 4uf = ma \qquad \text{eq1}$$

By summing comment about the center of gravity:

$$FL_1 - F_1L_2 + 2ufL_2 - 2ufL_1 - 2fL_3 = 0 \qquad \text{eq2}$$

Combining eq2 and eq1:

$$ma = F + F_1 - 2u[(F_1L_2 - FL_1)/(uL_2 - uL_1 - L_3)] \qquad \text{eq3}$$

For binding not to exist:

$$F + F_1 > 2u[(F_1L_2 - FL_1)/(uL_2 - uL_1 - L_3)] \qquad \text{eq4}$$

Case 1: $L_2 = L_1$ and $F_1 = F$.

From eq2, $-2fL_3 = 0$ or $f = 0$. Therefore, no binding.

Case 2: $F_1 = 0$.

From eq4:

$$F > -2uFL_1/(uL_2 - uL_1 - L_3)]$$

which reduces to:

$$L_3 > 2uL_1 - u(L_1 - L_2) \qquad \text{eq5}$$

Substituting $(L - L_2)$ for L_1 into eq5:

$$L_3 > uL.$$

Case 3: $F_1 = F - d_f$

From eq1:

$$2F - d_f - 4uf = ma \qquad \text{eq6}$$

From eq2:

$$L_1d_f - 2fL_3 = 0 \qquad \text{eq7}$$

Combining eq6 and eq7:

$$2F - d_f(1 + 2uL_1/L_3) = ma$$

For nonbinding:

$$2F - d_f(1 + 2uL_1/L_3) > 0$$

Rearranging:

$$d_f/F < L_3/(L_3/2 + uL_1).$$

APPENDIX G: STEP MOTOR PERFORMANCE DATA

STEP MOTOR DATA

Three step motors were considered for use in the robot. They are differentiated by their required amperage. A step motor's output torque is a function of its speed and its acceleration. The equation for the torque is:

$$T = aw^2 + bw + c$$

where w is the angular velocity in steps/second. The below table is a performance table for the available step motors.

STEP MOTOR PERFORMANCE TABLE

AMP	HOLDING TORQUE inch/oz	a	b	c	STEPS/ REV	ROTOR INERTIA inch-oz-sec^2	ACC	COST RELAT[a]	WEIGHT (LB)
2.1	70.0	-2.14E-6	-4.16E-3	59.08	200	.0075	+	1.5	2.93
		1.86E-6	-6.21E-3	-69.91			-		
1.1	28.7	-1.02E-6	-2.04E-3	28.08	200	.0016	+	1.0	
		1.38E-6	-7.11E-3	-27.25			-		
0.8	9.8	-2.00E-7	-2.80E-3	7.6	48	.0003	+	0.6	NA
		0.0	0.0	-9.8			-		

[a]Provided by IBM

PLOT DESCRIPTION

The plots are divided into upward motion or horizontal motion plots. In each division three types of plots exist. The first type are "AVEL VS TRAVEL" plots. These plots show maximum average velocities for a specific length robot moves. The second type are "RADIUS VS TRAVEL" plots. These show the gear radii versus travel distances that obtained the maximum average velocities. The first two plot types are for a specific load with the motors varing. The third type show the radii versus travel for a specific motor and varying loads. For the upward travel moves, specific travel distances were calculated from 3 to 24 inches stepping 3 inches. The radii were varied from .01 to .51 inches stepping .05 inches. For the horizontal travel moves, the travel distances were calculated from 3 to 42 inches stepping 3 inches. The radii were varied from .1 to 1 inches stepping .1 inch.

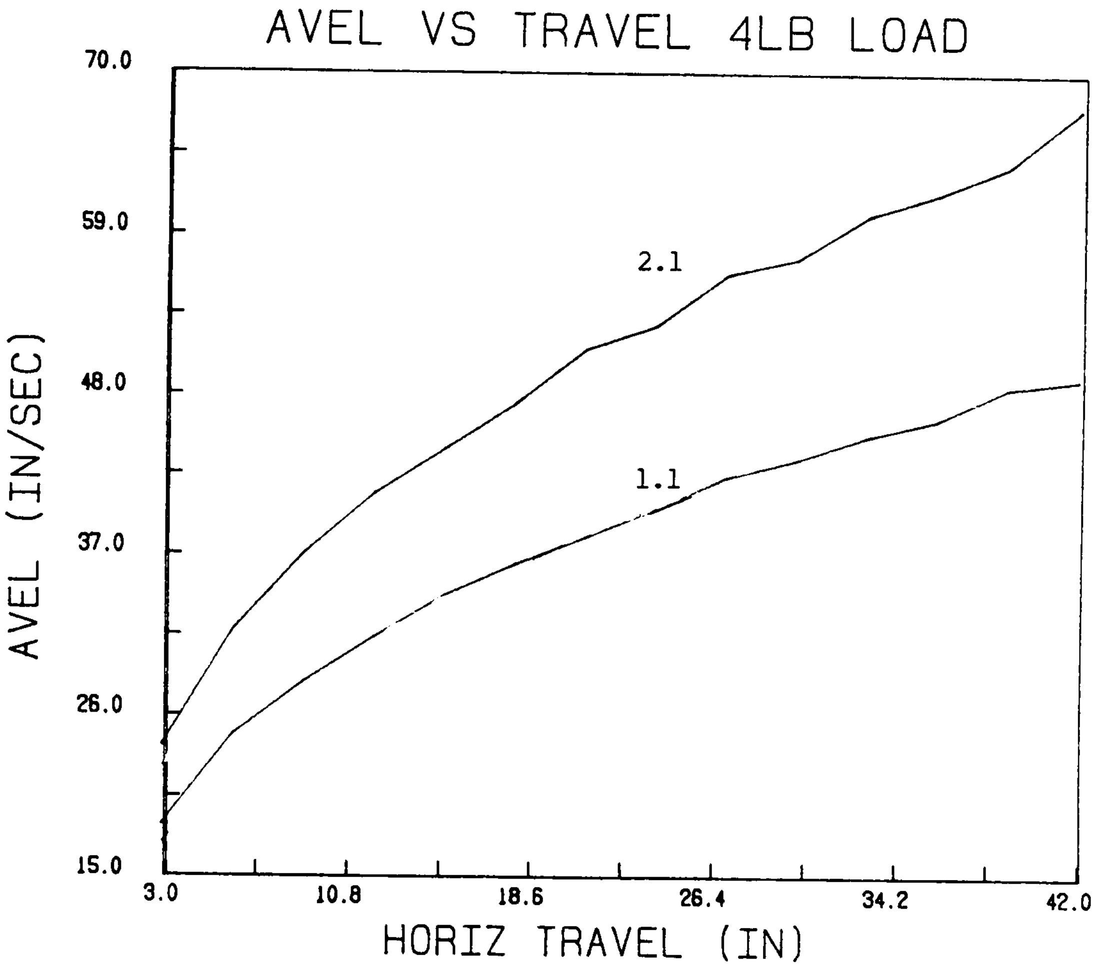
AVEL VS TRAVEL 4LB LOAD
70.0
59.0
48.0
37.0
26.0
15.0
AVEL (IN/SEC)
2.1
1.1
3.0
10.8
18.6
26.4
34.2
42.0
HORIZ TRAVEL (IN)

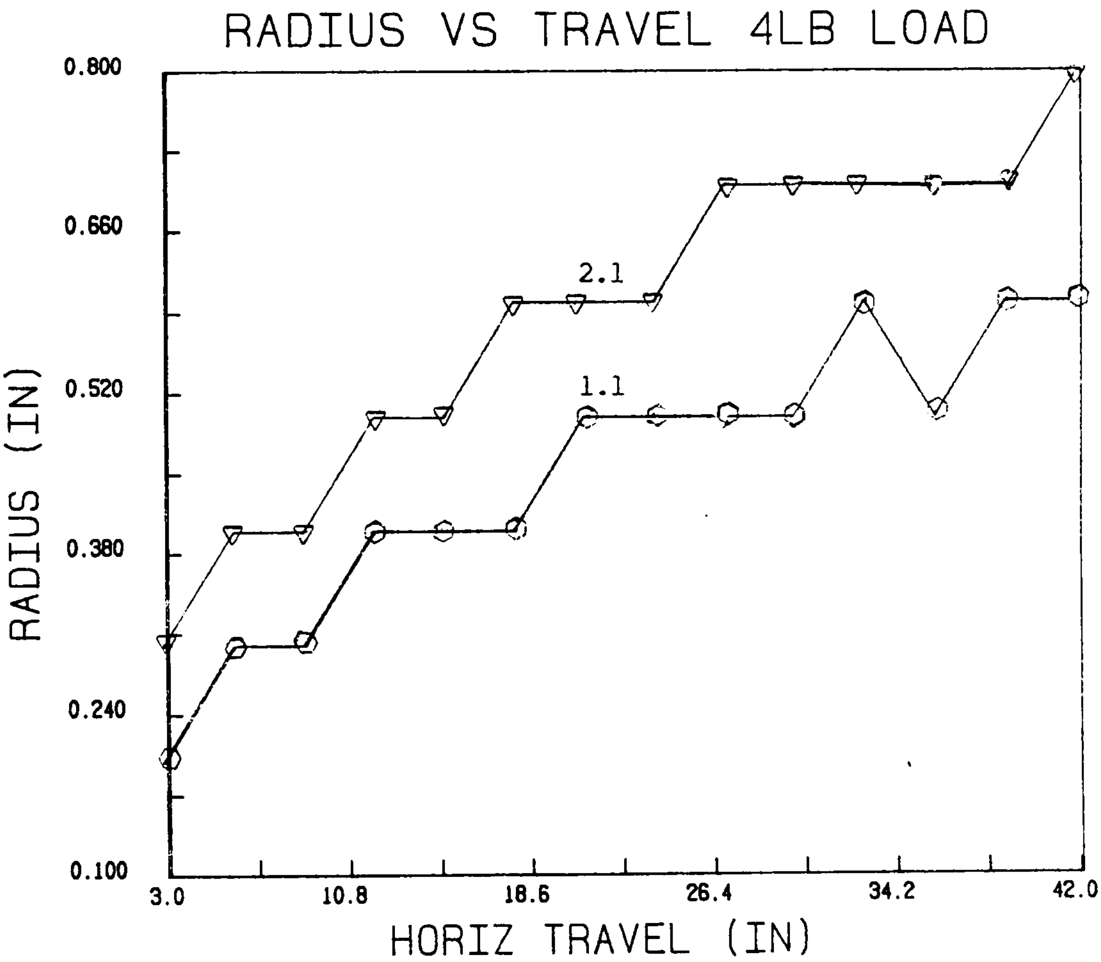
RADIUS VS TRAVEL 4LB LOAD
0.800
0.660
0.520
0.380
0.240
0.100
RADIUS (IN)
2.1
1.1
3.0
10.8
18.6
26.4
34.2
42.0
HORIZ TRAVEL (IN)

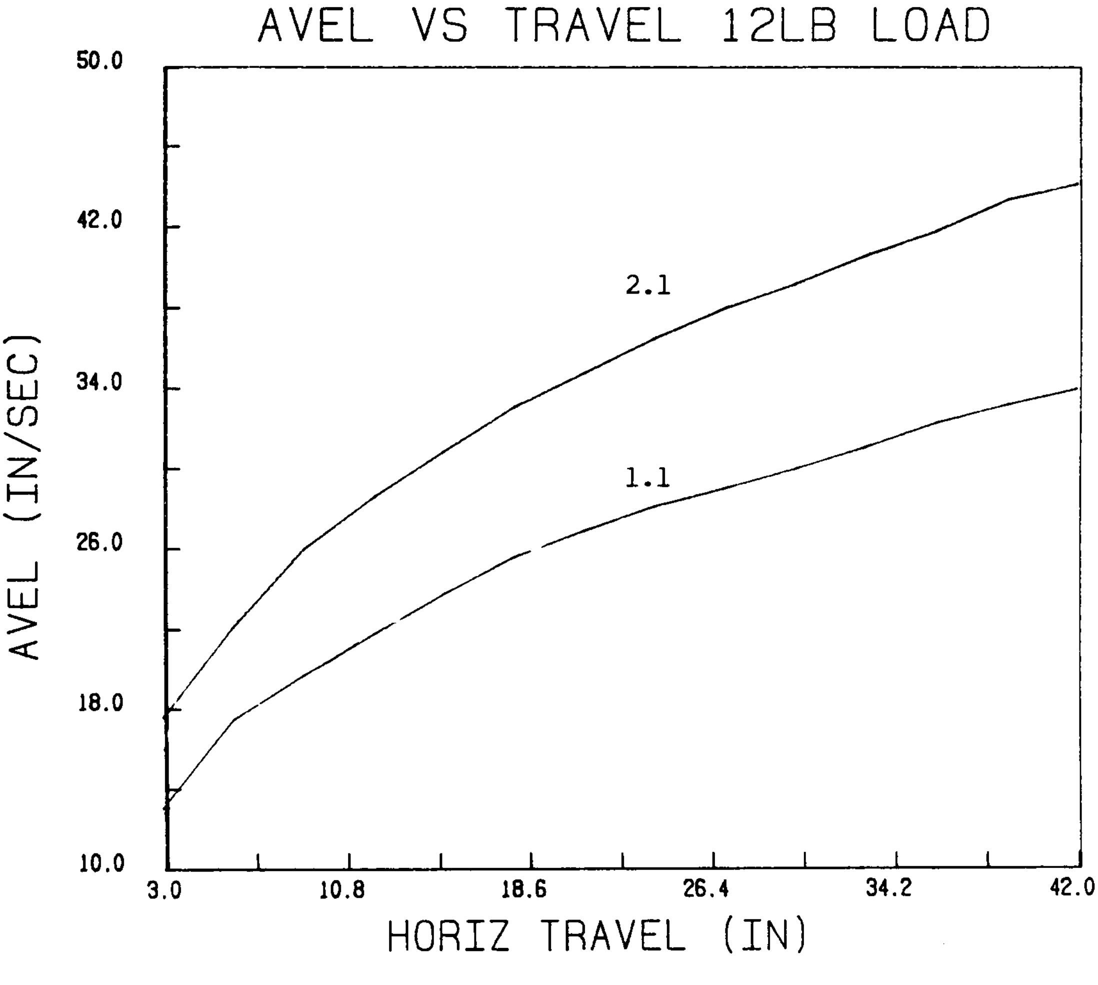

AVEL VS TRAVEL 12LB LOAD
50.0
42.0
34.0
26.0
18.0
10.0
AVEL (IN/SEC)
2.1
1.1
3.0
10.8
18.6
26.4
34.2
42.0
HORIZ TRAVEL (IN)

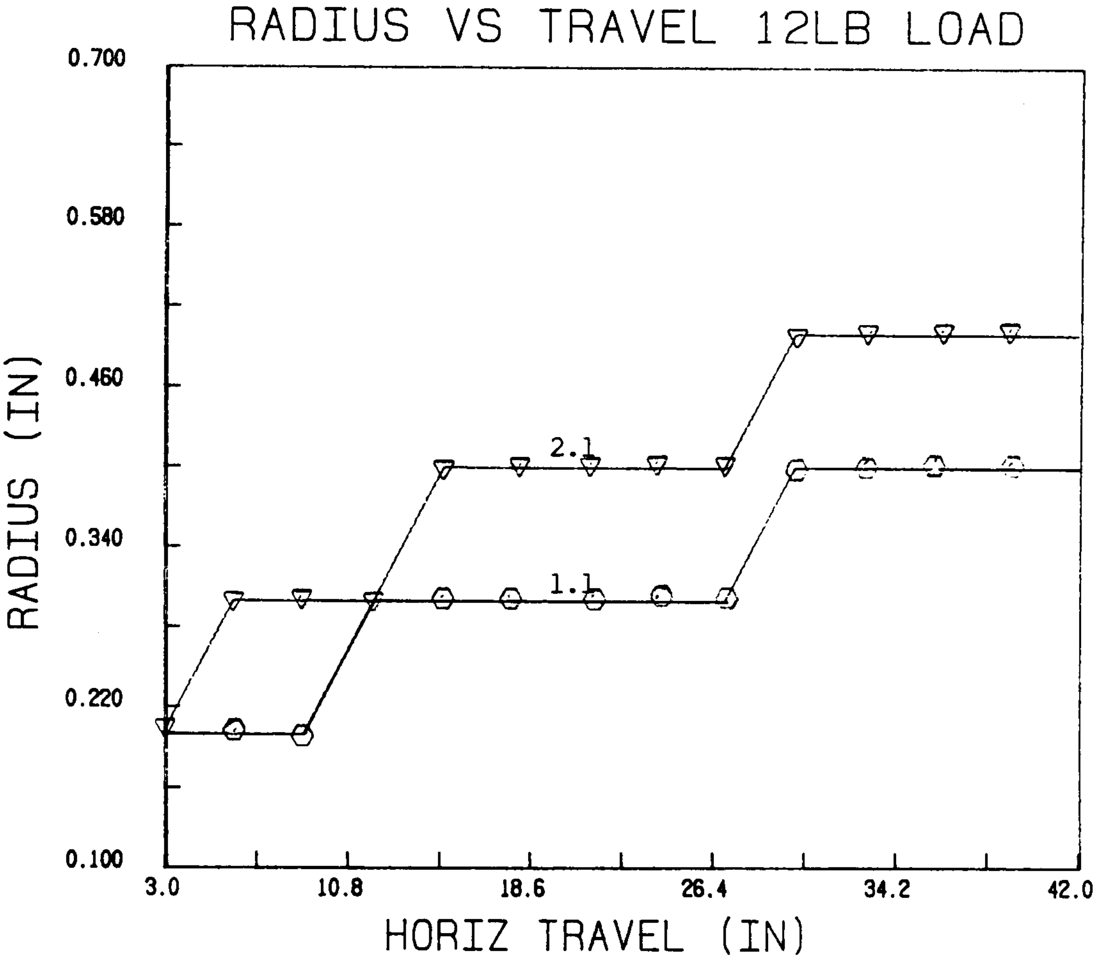

RADIUS VS TRAVEL 12LB LOAD
0.700
0.580
0.460
0.340
0.220
0.100
RADIUS (IN)
2.1
1.1
3.0
10.8
18.6
26.4
34.2
42.0
HORIZ TRAVEL (IN)

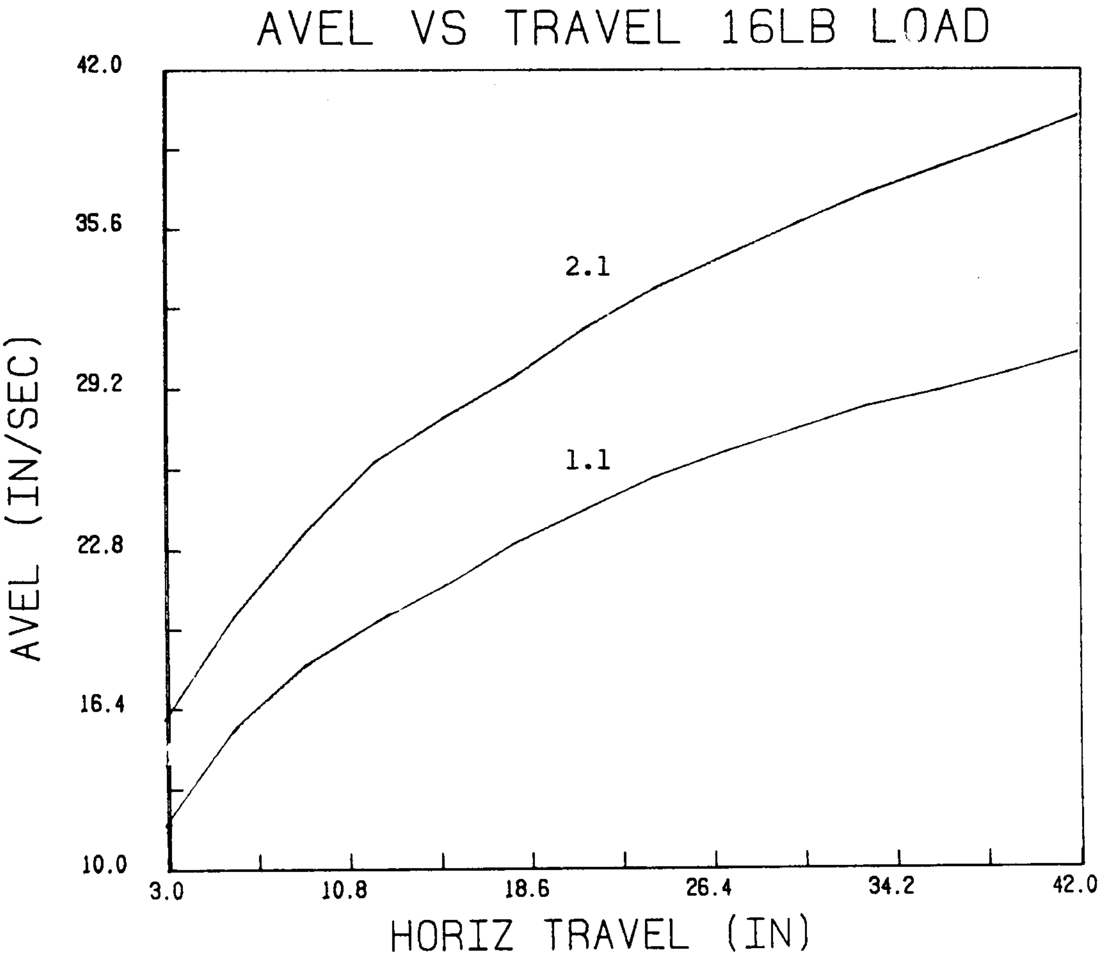
AVEL VS TRAVEL 16LB LOAD
42.0
35.6
29.2
22.8
16.4
10.0
AVEL (IN/SEC)
2.1
1.1
3.0
10.8
18.6
26.4
34.2
42.0
HORIZ TRAVEL (IN)

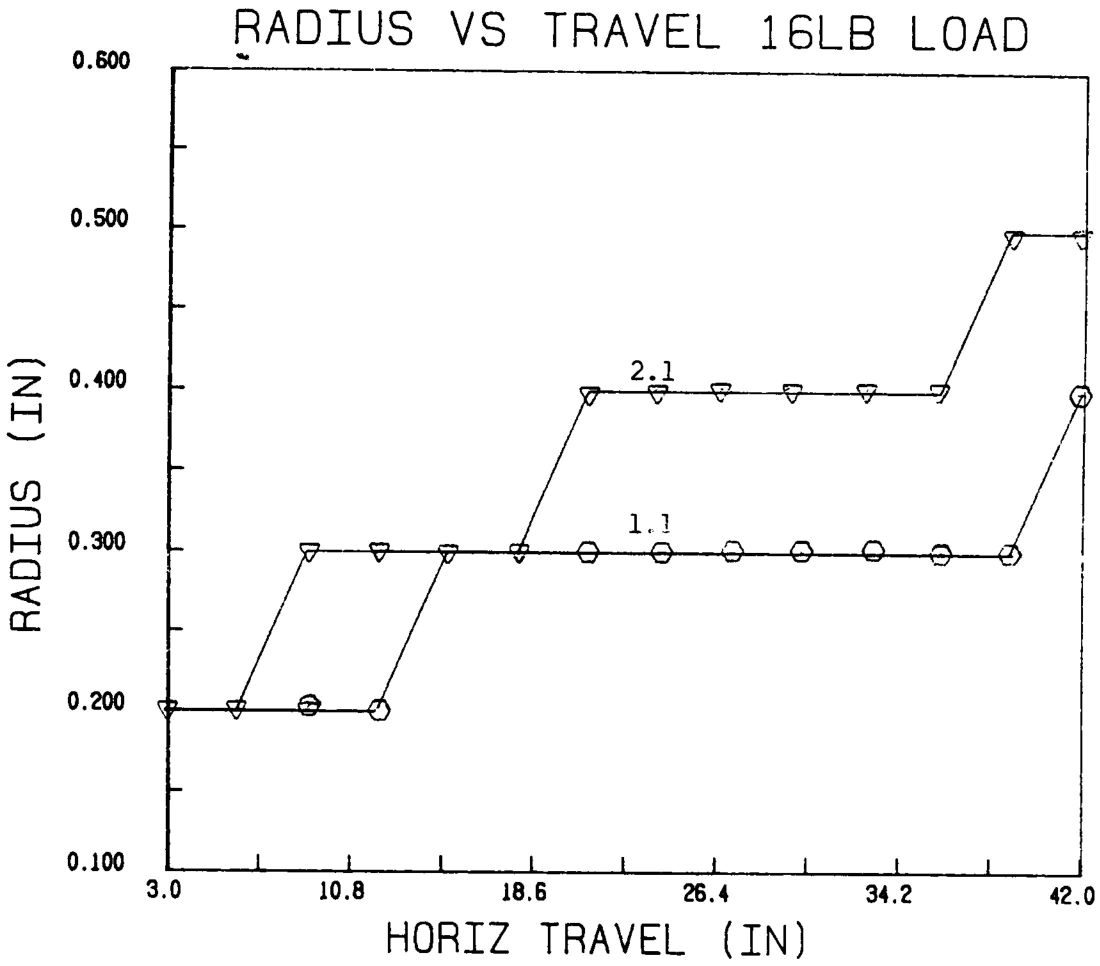
RADIUS VS TRAVEL 16LB LOAD
0.600
0.500
0.400
0.300
0.200
0.100
RADIUS (IN)
2.1
1.1
3.0
10.8
18.6
26.4
34.2
42.0
HORIZ TRAVEL (IN)

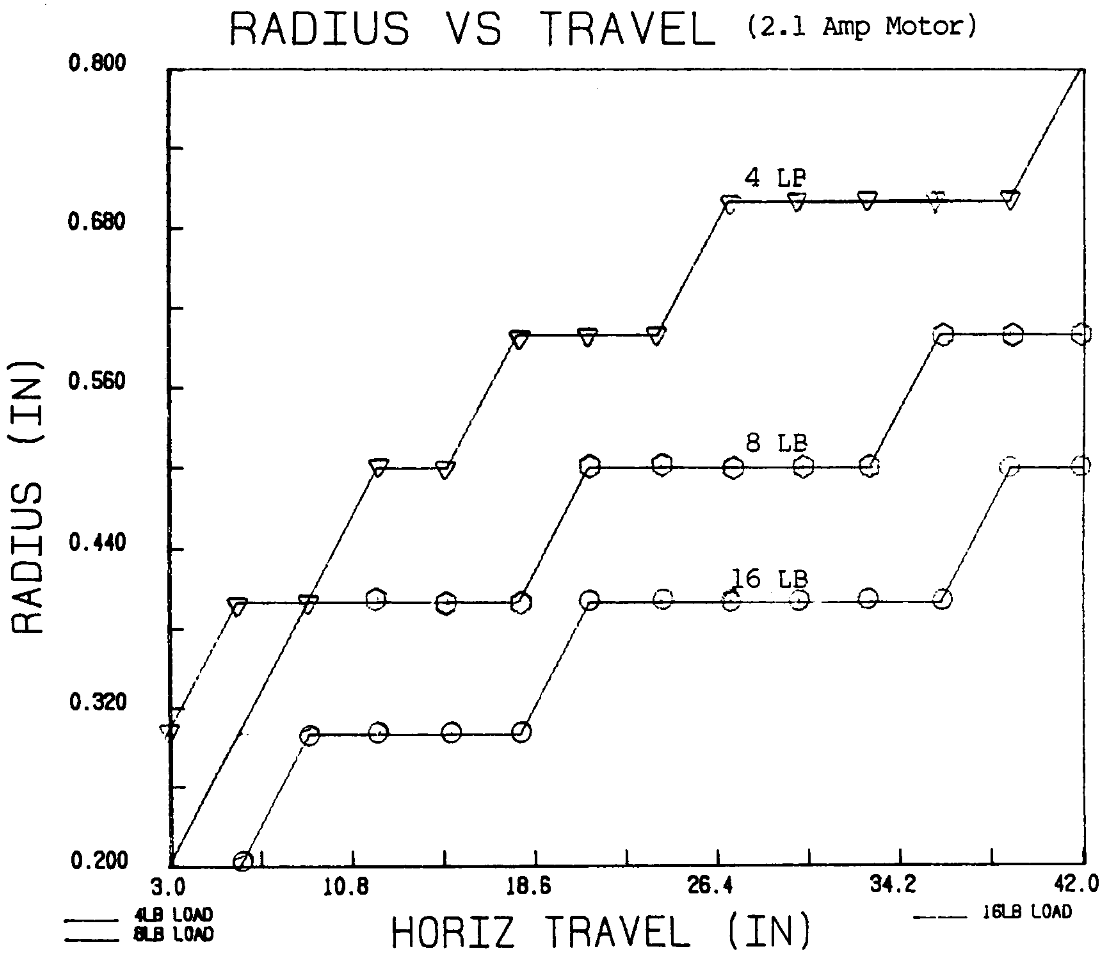
RADIUS VS TRAVEL (2.1 Amp Motor)
0.800
0.680
0.560
0.440
0.320
0.200
RADIUS (IN)
4 LB
8 LB
16 LB
3.0
10.8
18.6
26.4
34.2
42.0
4LB LOAD
8LB LOAD
HORIZ TRAVEL (IN)
16LB LOAD

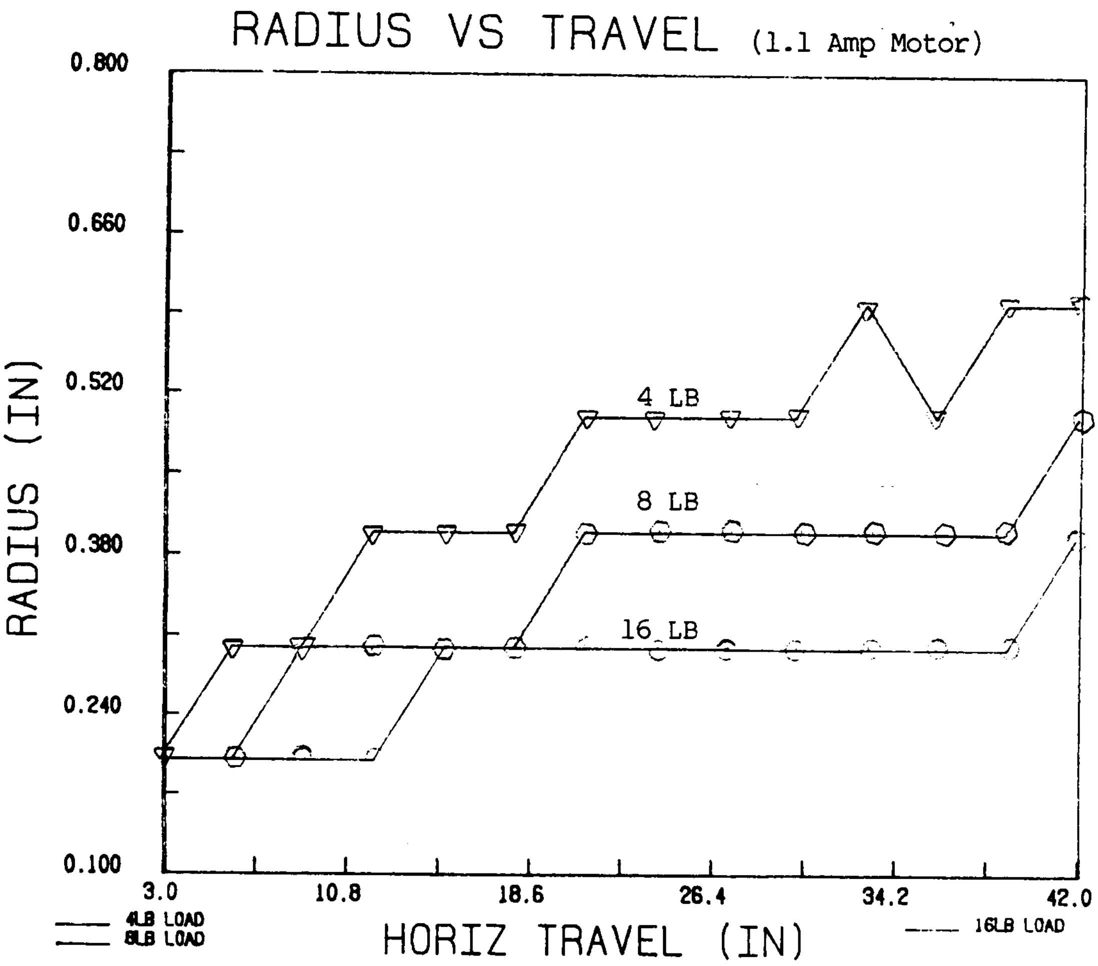

RADIUS VS TRAVEL (1.1 Amp Motor)
0.800
0.660
0.520
0.380
0.240
0.100
RADIUS (IN)
4 LB
8 LB
16 LB
3.0
10.8
18.6
26.4
34.2
42.0
HORIZ TRAVEL (IN)
4LB LOAD
8LB LOAD
16LB LOAD

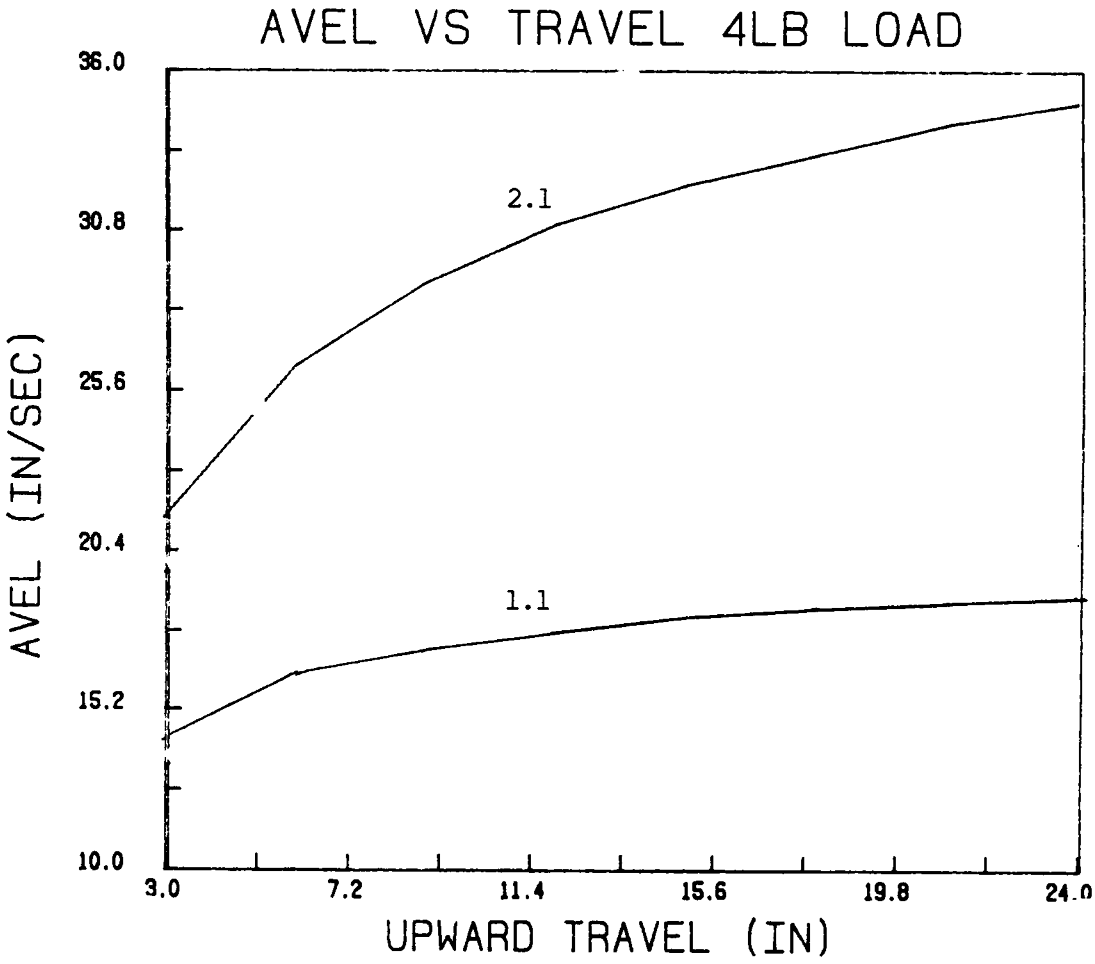
AVEL VS TRAVEL 4LB LOAD
36.0
30.8
25.6
20.4
15.2
10.0
AVEL (IN/SEC)
2.1
1.1
3.0
7.2
11.4
15.6
19.8
24.0
UPWARD TRAVEL (IN)

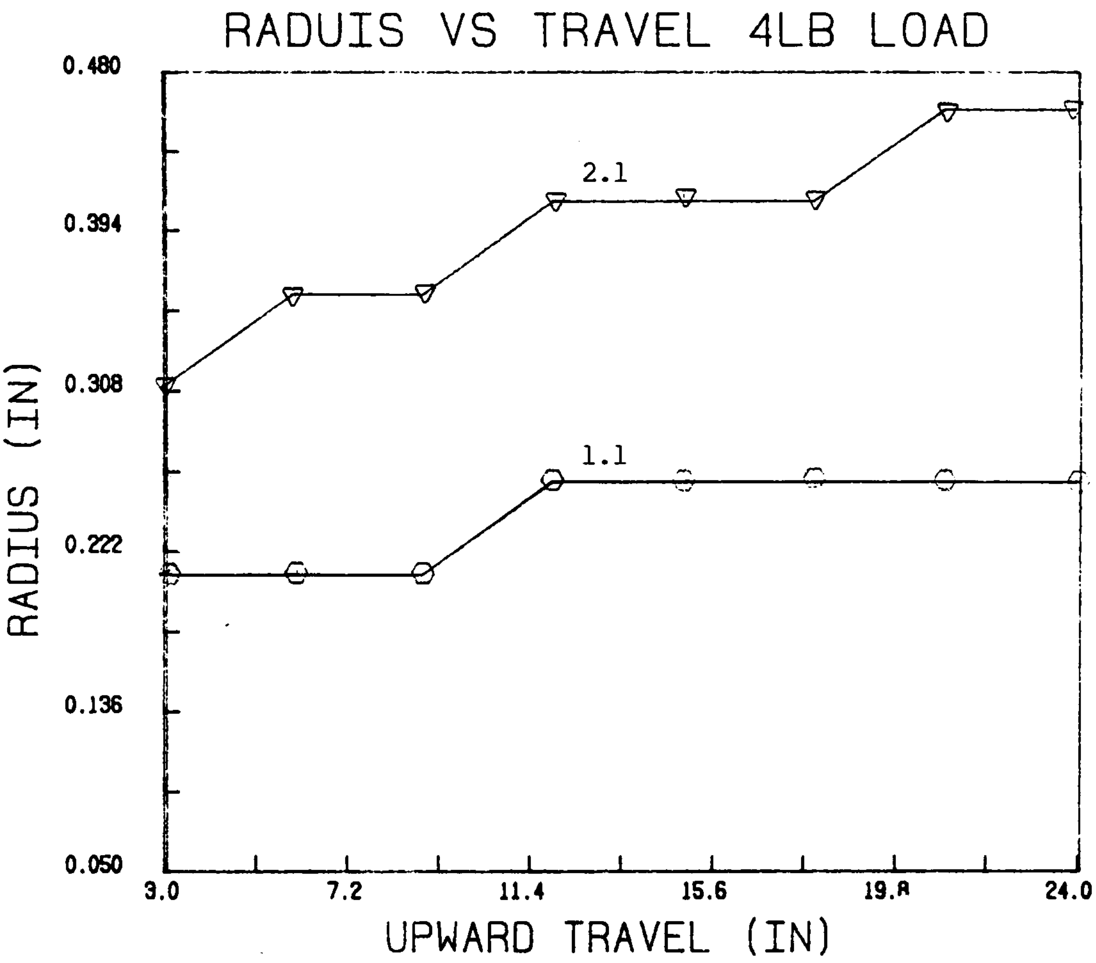
RADUIS VS TRAVEL 4LB LOAD
0.480
0.394
0.308
0.222
0.136
0.050
RADIUS (IN)
2.1
1.1
3.0
7.2
11.4
15.6
19.8
24.0
UPWARD TRAVEL (IN)

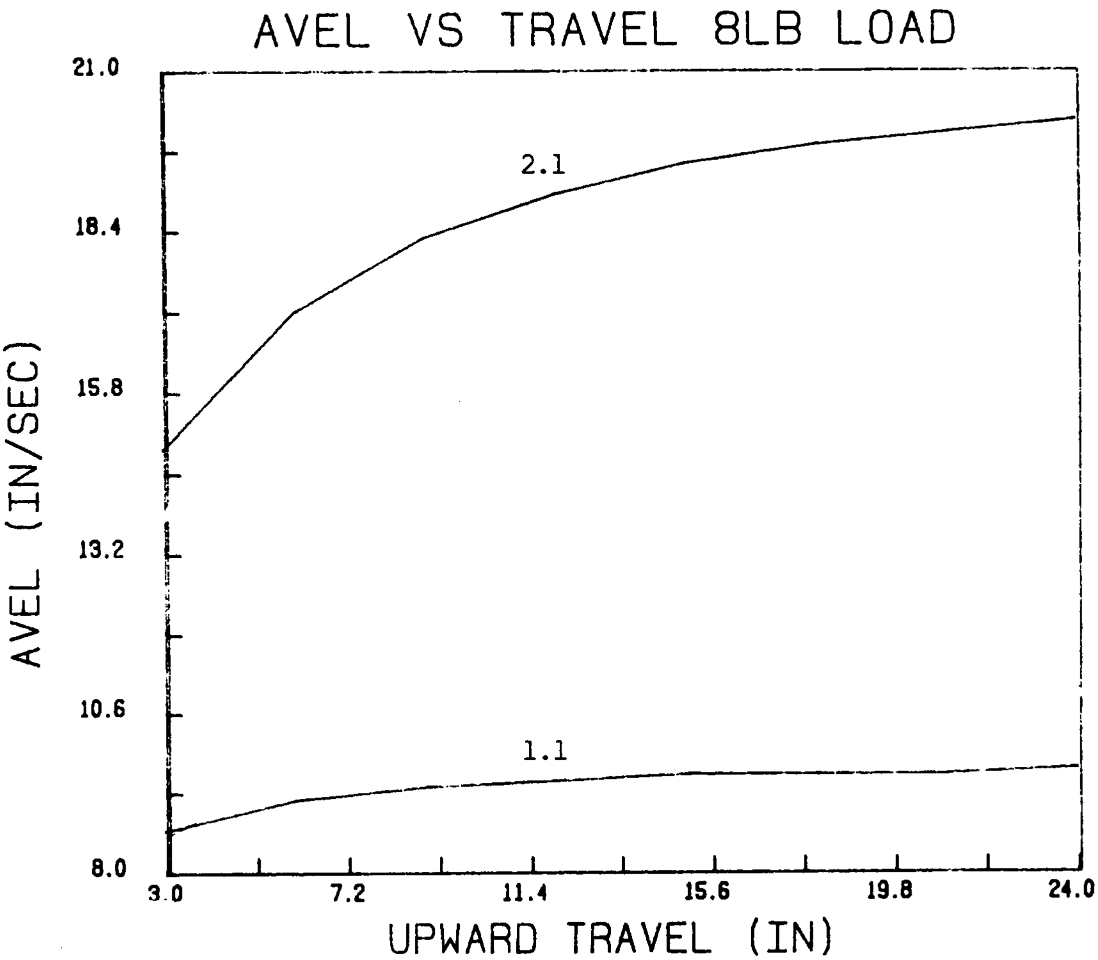
AVEL VS TRAVEL 8LB LOAD
21.0
18.4
15.8
13.2
10.6
8.0
2.1
1.1
3.0
7.2
11.4
15.6
19.8
24.0
AVEL (IN/SEC)
UPWARD TRAVEL (IN)

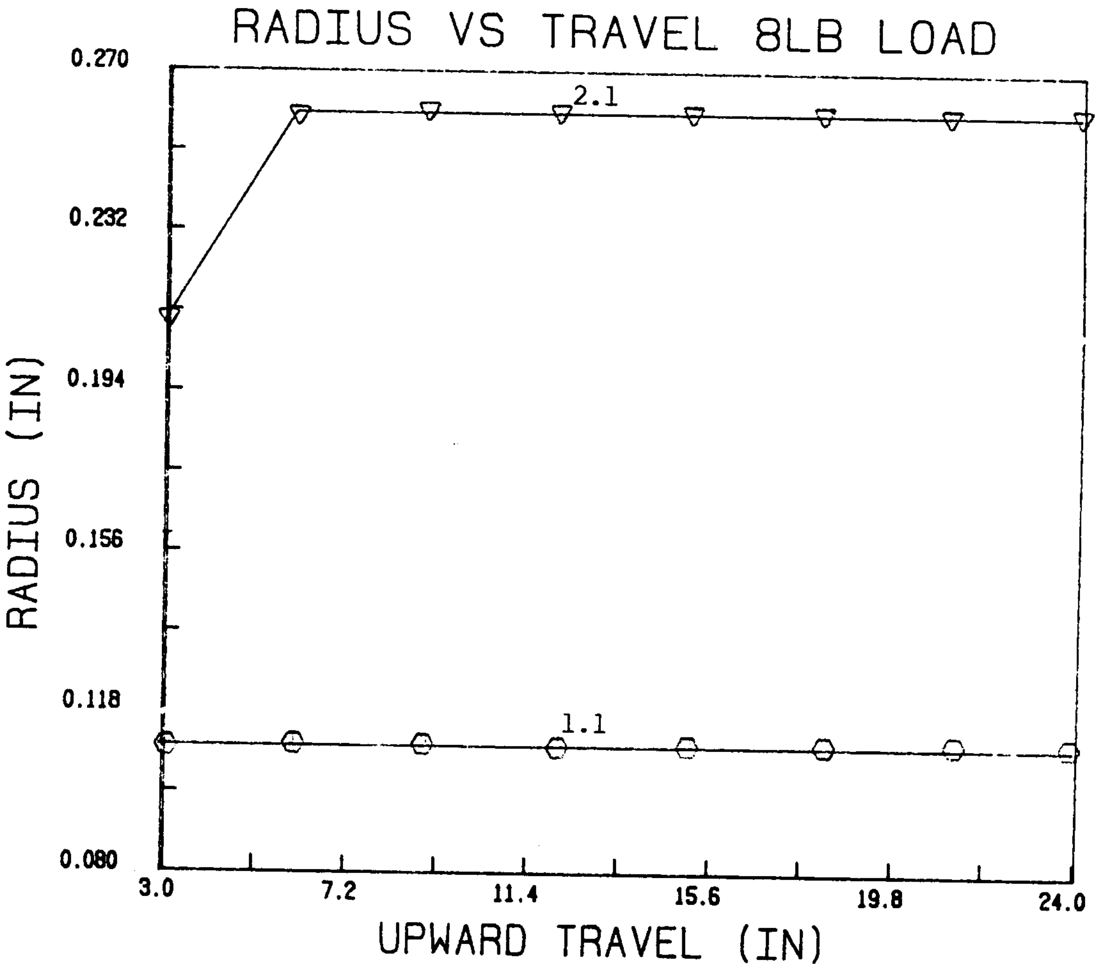
RADIUS VS TRAVEL 8LB LOAD
0.270
0.232
0.194
0.156
0.118
0.080
RADIUS (IN)
2.1
1.1
3.0
7.2
11.4
15.6
19.8
24.0
UPWARD TRAVEL (IN)

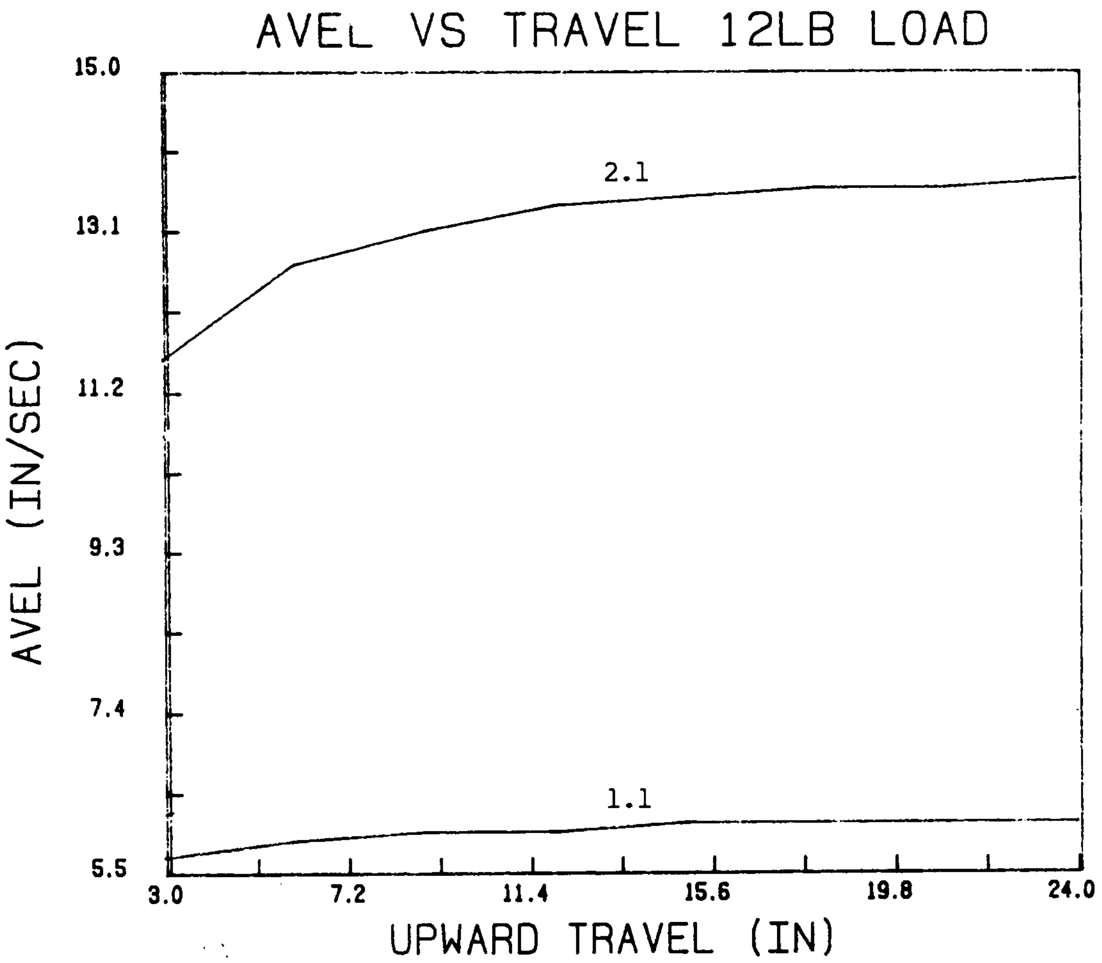
AVEL VS TRAVEL 12LB LOAD
15.0
13.1
11.2
9.3
7.4
5.5
AVEL (IN/SEC)
2.1
1.1
3.0
7.2
11.4
15.6
19.8
24.0
UPWARD TRAVEL (IN)

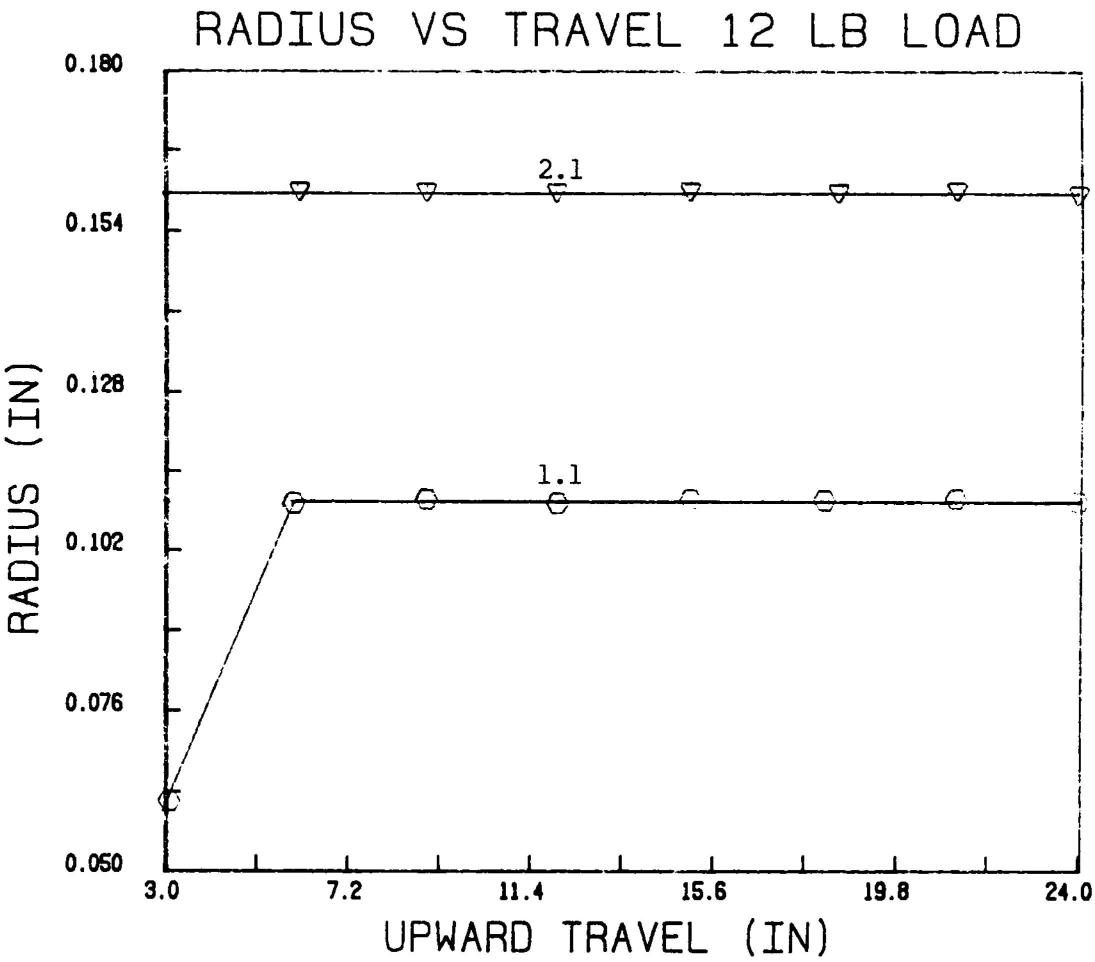

RADIUS VS TRAVEL 12 LB LOAD
0.180
0.154
0.128
0.102
0.076
0.050
RADIUS (IN)
2.1
1.1
3.0
7.2
11.4
15.6
19.8
24.0
UPWARD TRAVEL (IN)

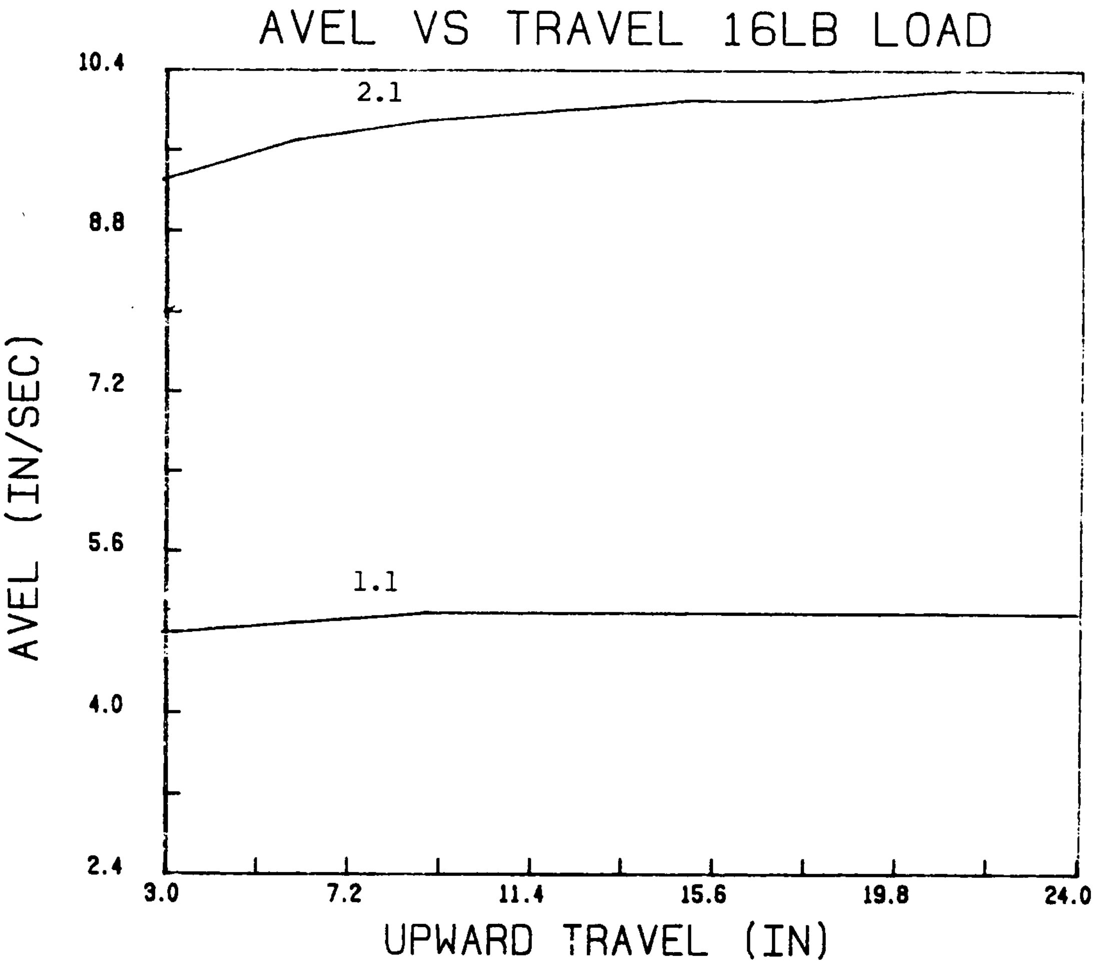
AVEL VS TRAVEL 16LB LOAD
10.4
8.8
7.2
5.6
4.0
2.4
AVEL (IN/SEC)
2.1
1.1
3.0
7.2
11.4
15.6
19.8
24.0
UPWARD TRAVEL (IN)

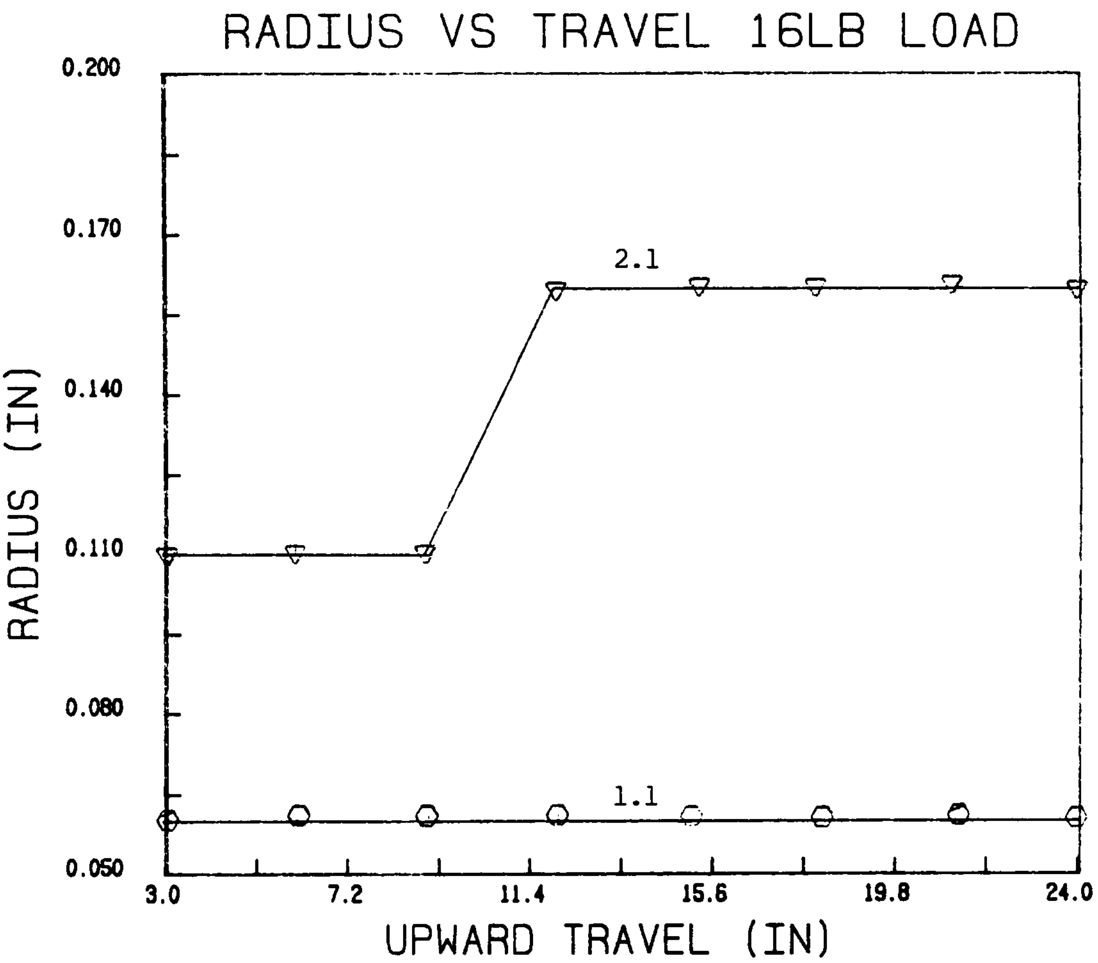
RADIUS VS TRAVEL 16LB LOAD
0.200
0.170
0.140
0.110
0.080
0.050
RADIUS (IN)
2.1
1.1
3.0
7.2
11.4
15.6
19.8
24.0
UPWARD TRAVEL (IN)

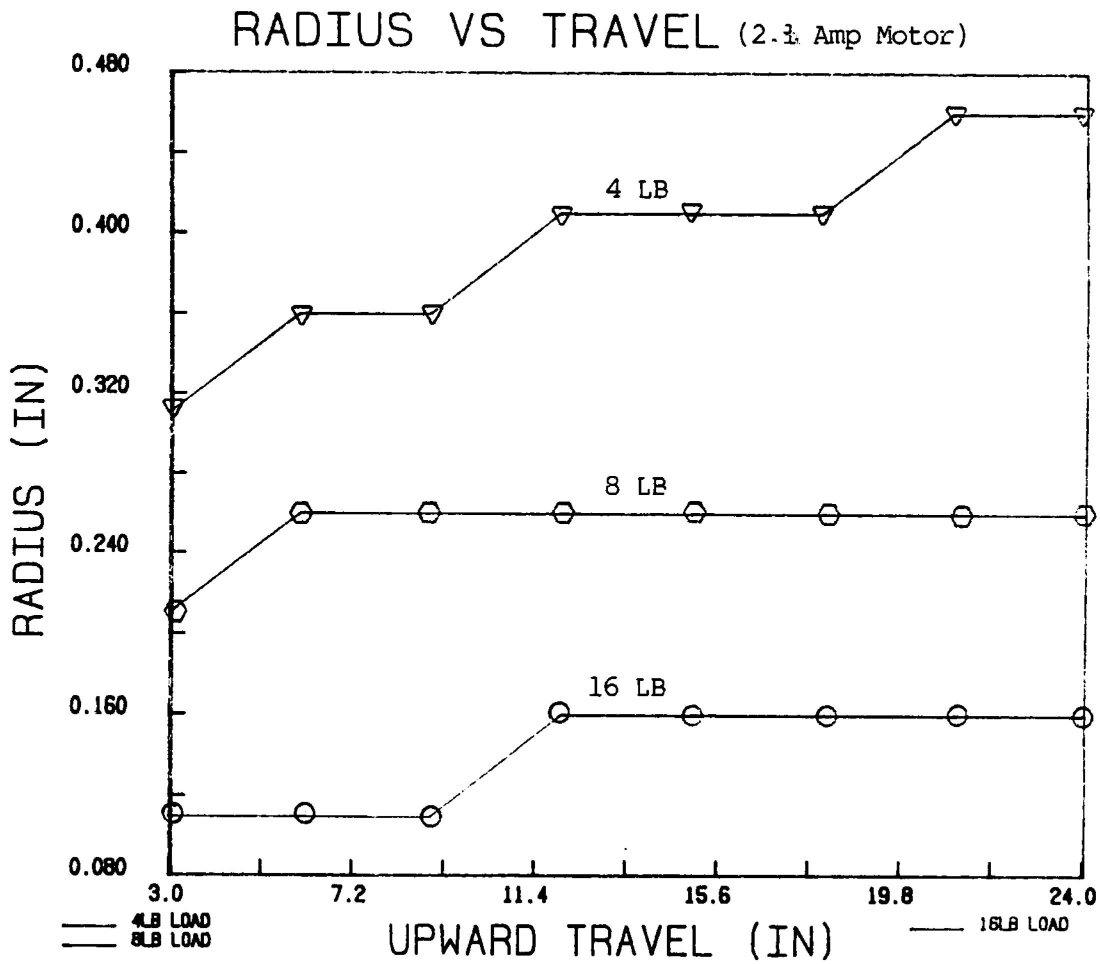

RADIUS VS TRAVEL (2.1 Amp Motor)
0.480
0.400
0.320
0.240
0.160
0.080
RADIUS (IN)
4 LB
8 LB
16 LB
3.0
7.2
11.4
15.6
19.8
24.0
4LB LOAD
8LB LOAD
UPWARD TRAVEL (IN)
16LB LOAD

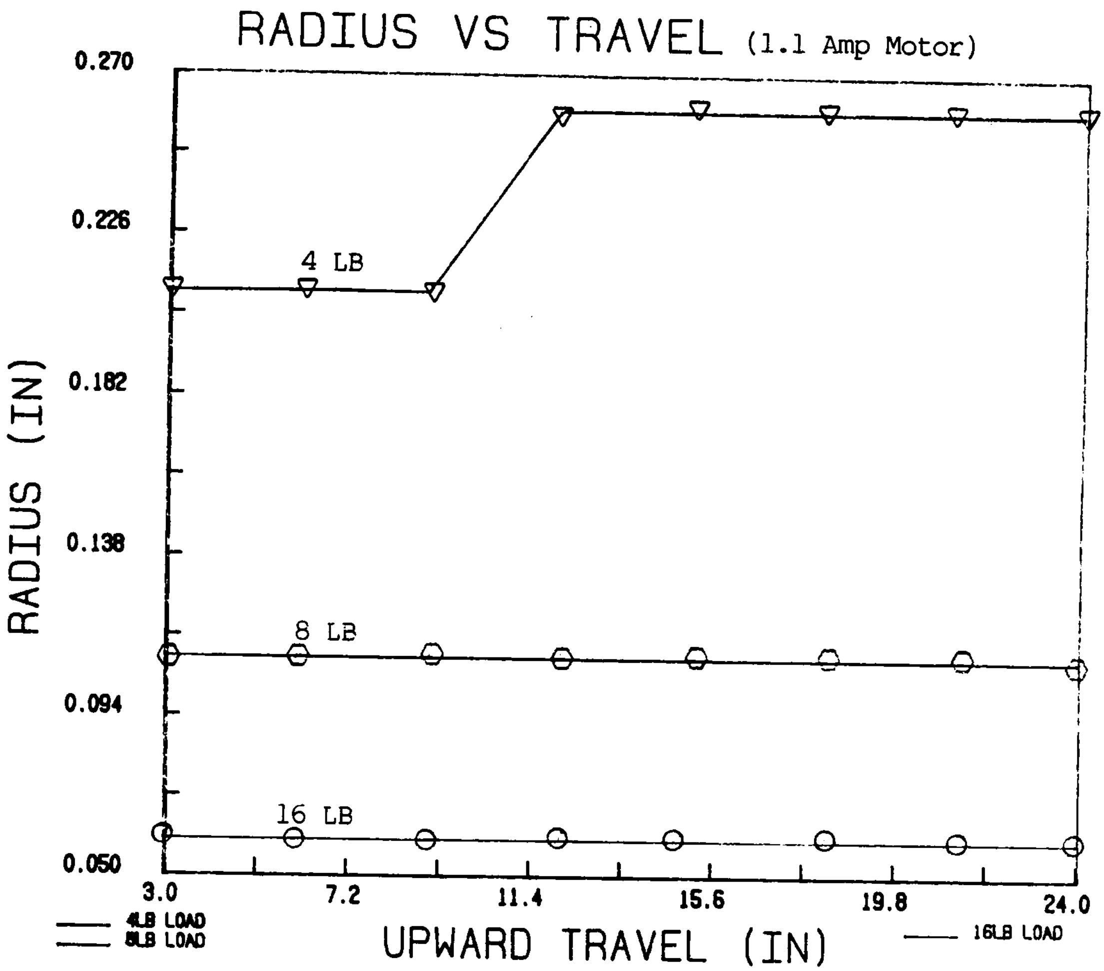
RADIUS VS TRAVEL (1.1 Amp Motor)
0.270
0.226
0.182
0.138
0.094
0.050
RADIUS (IN)
4 LB
8 LB
16 LB
3.0
7.2
11.4
15.6
19.8
24.0
UPWARD TRAVEL (IN)
4LB LOAD
8LB LOAD
16LB LOAD

PROGRAMS USED TO OBTAIN HORIZONTAL MOTION PLOTS

Three programs are required to obtain the data for the motion plots. The first program calculates the average velocity data for all combinations of moves. This program uses the motor torque and load parameters to determine the equations of motion for the model. The equations of motion are numerically integrated for a complete robot move. The combinations of moves vary by the type of motor, travel distance, pulley radius, and loading. The second program sorts the data to determine which pulley radii give maximum velocity for specific types of moves. The third program sorts maximum velocity data into many files that represent each curve show on the plots. This is required so that the graphing program can graph the data.

```
10  ' *****************************************************
20  ' ** DATA ACQUISITION PROGRAM USED TO DETERMINE MOTORS **
30  ' ** AND OPTIMUM TRANSMISSION RATIOS FOR IBM ROBOT     **
40  ' **                                                   **
50  ' ** BY: MARK GRANGER                                  **
60  ' **     UNIVERSITY OF TENNESSEE MECHANICAL ENGINEERING**
70  ' **                                                   **
80  ' ** LAST EDITED MAY 28, 1987                          **
90  ' *****************************************************
100 '
110 DIM K(4,80),Y(80),Z(80),YD(80)
120 OPEN "MOT2B.DAT" FOR OUTPUT AS #1       '--FILE OUTPUT--'
130 PI = 3.14159
140 '
150 '****** LOOP FOR THE 5 AVAILABLE MOTORS ******

160 FOR MOTO = 1 TO 4
170 '
180 '****** STEP MOTOR DATA *****
190 '----TORQUE ACC=A*OMEG^2+B*OMEG+C  TORQUE DEACC=D*OMEG^2+E*OMEG+C--
200 '----MOTOR ROTOR INERTIA = IMOT (OZ-IN-S-S) -- TORQUE = IN-OZ -----
210 ON MOTO GOTO 220,240,260,280
220 A=-1.017E-06:B=-.002043:C=28.08:IMOT=.00156
230 D=1.38E-06:E=-.00711:F=-27.25:GOTO 320
240 A=-2.144E-06 : B=-.004162: C=59.08
250 D=1.86E-06:E=-.00621:F=-69.91001:IMOT=.00165:GOTO 320
```

```
260 A=-9.452E-07 : B=-.00278 : C=31.71
270 D=8.7E-07:E=-.00475:F=-34.68:IMOT=.00751:GOTO 320
280 A=-7.327E-07: B=-.003295: C=42.69
290 D=6.17E-07:E=.0000735:F=-47.54:IMOT=.00159:GOTO 320
300 'A=-.0000002: B=-.0028: C=7.6
310 'D=-1.017E-07:E=-.002043:F=28.08:IMOT=.0028
320 '
330 ' ***** LOOP FOR 3 TYPE OF MOVES *****
340 '- 1=HORIZONTAL MOVEMENT-- 2=UPWARD MOVEMENT-- 3=DOWNWARD MOVEMENT
350 'FOR MOVES = 1 TO 3
360 MOVES =2
370 '
380 ' ****** LOOP FOR LOADS VARING FROM 2 LBS TO 16 LBS *****
390 FOR LOOD = 4*16 TO 16*16 STEP 4*16
400 '
410 '----TEX = TORQUE EXTERNAL-- SWT = TIME TO SWITCH TO SLOW DOWN --
420 IF MOVES = 1 THEN TEX = 0      : SWT = 1!: STP = .05 : GOTO 470
450 '
460 ' ***** LOOP TO VARY GEAR RADIUS FROM .125 TO .5 INCHES ****

470 FOR R = .01 TO .52 STEP .05
480 IF MOVES=2 AND R*LOOD>C THEN 810          '--CHECK FOR MAXIMUM LOAD--'
490 IF MOVES=3 AND R*LOOD>ABS(F) THEN 810    '--CHECK FOR MAXIMUM LOAD--'
494 IF MOVES = 2 THEN TEX = LOOD*R :SWT = 1.5: STP = .05: GOTO 500
495 IF MOVES = 3 THEN TEX = -LOOD*R: SWT = 1!: STP = .05
500 '
510 IGEAR = 1.6*PI*R^4/(8*386)           '----GEAR INERTIA (OZ-IN-S-S)--'
520 IEQ = IGEAR + IMOT + (LOOD*R^2)/386 '--EQUIVALENT SYSTEM INERTIA---'
530 PRINT "IEQ" IEQ
540 '
550 Y1 = 0: Y2 = 0: TT = 0           '---INITIAL CONDITIONS FOR NEW TS---'
560 '
570 ' **** LOOP TO VARY TIMES TO START SLOWING DOWN MOTOR*****
580 TS = .05: DD = 3
590 '
600 ' **** CALCULATE ACCELERATION DATA ***
610 SS=1
620 GOSUB 910
630 'PRINT "RETURNED:" Y(1),Y(2)
640 Y1 = Y(1): Y2 = Y(2): TT = T
650 '
660 ' **** CALCULATE DEACCELERATION DATA ***
670 SS = 0
680 GOSUB 920
690 '
695 ' *** LINEARLY INTERPOLATE DISTANCES TO STANDARD DISTANCES ***
700 DIS = R*Y(1): AVEL = DIS/T
710 IF DIS >= DD THEN 720 ELSE 770
720 VEL = AVEL - (DIS - DD)*(AVEL - AVOLD)/(DIS - DOLD)
730 PRINT #1, USING "###.## ##.## #.### ### #";DD,VEL,R,LOOD,MOTO
731 PRINT USING "###.## ##.## #.### ### #";DD,VEL,R,LOOD,MOTO
```

```
740 DD = DD + 3
750 IF DD>24 THEN 800
760 ' *** PRINT AND STORE DATA ***
770 PRINT USING "#.### ###.## ##.## .### ### # #.##";
    T,R*Y(1),R*Y(1)/T,R,LOOD,MOTO,TT
780 DOLD = DIS: AVOLD = AVEL
790 TS = TS + STP: GOTO 590
800 NEXT R
805 LPRINT "LOOD WAS" LOOD
810 NEXT LOOD
820 'NEXT MOVES
825 LPRINT "MOTO WAS" MOTO
830 NEXT MOTO
840 CLOSE #1
850 END
860 '
870 '*** SUBROUTINE USING 4TH ORDER RUNGE-KUTTA INT METHOD TO SOLVE**
880 '*** SYSTEMS OF FIRST-ORDER ORDINARY DIFFERENTIAL EQS WRITTEN BY **
890 '*** F.H. SPECKHART  UNIVERSITY OF TN. MECHANICAL ENGINEERING *****
900 '
910 Y(1)=Y1: Y(2)=Y2: T=TT
920 IF SS=1 THEN T9 = TS ELSE T9 = 3*TS   '--T9 = MAXIMUM RUN TIME ----'
930 T8 = 1!                           '---T8 IS EQUAL TO THE PRINT INTERVAL ----'
940 D1 = .005                          '--D1 = INCREMENT OF INTEGRATION STEP SIZE
950 T8 = T8/D1
960 N = 2                              '----N = NUMBER OF FIRST ORDER D.E.s----'
970 '
980 ' ********* START OF SUBROUTINE **********
990 FOR I = 1 TO 10
1000 Z(I)= Y(I)
1010 NEXT I
1020 T7 = 9.000001E+09
1030 GOTO 1260
1040 FOR J = 1 TO 4
1050 ON J GOTO 1190,1060,1110,1150
1060 T = T+D1*.5
1070 FOR I = 1 TO N
1080 Y(I) = K(1,I)*D1*.5 + Z(I)
1090 NEXT I
1100 GOTO 1190
1110 FOR I = 1 TO N
1120 Y(I)= K(2,I)*D1* .5 + Z(I)
1130 NEXT I
1140 GOTO 1190
1150 T = T + .5*D1
1160 FOR I = 1 TO N
1170 Y(I) = K(3,I)*D1 + Z(I)
1180 NEXT I
1190 GOSUB 1390
1200 FOR JK = 1 TO N
1210 K(J,JK) = YD(JK):    NEXT JK
```

```
1220 NEXT J
1230 FOR I = 1 TO N
1240 Z(I) = Z(I) + D1*(K(1,I) + K(4,I) + 2*(K(3,I)+K(2,I)))/6
1250 NEXT I
1260 FOR I = 1 TO N
1270 Y(I)= Z(I)
1280 NEXT I
1290 IF Y(2) < 0 THEN RETURN      '-----VELOCITY CHECK----'
1300 T7= T7+1
1310 IF T7<= T8-.0002 THEN 1370
1320 T7=0
1330 '
1340 ' **** PRINT STATEMENTS ****
1350 'PRINT USING "T= ##.###  y(1)= ###.##  y(2) = ####.####
     YD(2)= ####.##";T, Y(1), Y(2),YD(2)
1360 '
1370 IF T= < T9 THEN 1040
1380 RETURN
1390 '
1400 '***** DIFFERENTIAL EQUATIONS OF MOTION AND MOTOR TORQUE *****
1410 ' -Y(1)=ANGULAR POSITION (RADIANS) -Y(2)=ANGULAR VELOCITY (RAD/SEC)
1420 ' ---YD(2)=DERIVATIVE OF Y(2) OR ANGULAR ACCELERATION (RAD/SEC/SEC)
1430 YD(1) = Y(2)
1440 SPS = Y(2)*100/PI              '----CONVERT RAD/SEC TO STEP/SEC----'
1450 IF SS=1 THEN TMOT = A*SPS^2+B*SPS+C ELSE TMOT = D*SPS^2+E*SPS+F
1460 YD(2) = (TMOT - TEX)/IEQ
1470 RETURN
```

```
10 '****************************************************************
20 '***** PROGRAM TO DETERMINE HIGHEST AVERAGE VELOCITY AND GEAR ***
30 '***** RATIO BY SORTING "MOT2B.DAT"                           ***
40 '******                                                      ***
50 '****** BY: MARK GRANGER            LAST EDITED: JUNE 6, 1987 ***
60 '****************************************************************
70 DIM DIS(1009),AVEL(1009),R(1009),LOOD(1009),MOTO(1009)
80 '
90 OPEN "A:CMOT2B.DAT" FOR OUTPUT AS #2
100 OPEN "MOT2B.DAT" FOR INPUT AS #1
110 '
120 '----- FOR EACH MOTOR INPUT ALL DATA ASSOCIATED WITH THE MOTOR ---
130 FOR M = 1 TO 4
131 IF M = 1 THEN NUM = 152: GOTO 140
132 IF M = 2 THEN NUM = 256: GOTO 140
133 IF M = 3 THEN NUM = 176: GOTO 140
134 IF M = 4 THEN NUM = 216
140 FOR I = 1 TO NUM:INPUT #1, DIS(I),AVEL(I),R(I),LOOD(I),MOTO(I)
145 'PRINT DIS(I),AVEL(I)
150 NEXT I
160 '
170 '-DIFFERENTIAL LOAD OCCURS EVERY 126 DATA LINES: FOUR 8 LOADS EXIST --
```

```
180 L = 0
190 '
198 PRINT "load change : position is" L, " new load is " LOOD(L+1)
199 PRINT "avel(l+10)" AVEL(L+10)
200 '-8 TRAVEL DISTANCES EXIST IN THE DATA (3 INCHES TO 24 STEP 3) --
210 FOR N = 1 TO 8
220 BVEL = AVEL(N+L): BR = R(N+L)      '--INITIAL BEST VELOCITY---'
230 '
240 ' RADII EXIST: THIS LOOPS FOR SAME LOAD AND DIST BUT DIFFERENT R -
250 FOR R = 1 TO 11.100001#
260 IF LOOD(N+R*8+L)<>LOOD(N+L) THEN COLD = C: GOTO 320
270 ' ---ANGULAR VELOCITY CHECK ---
275 'PRINT "AVEL" AVEL(N+R*8+L), C
280 IF AVEL(N+R*8+L)>BVEL THEN BVEL=AVEL(N+R*8+L):BR=R(N+R*8+L)
290 '
300 C = C +1
310 NEXT R
320 PRINT USING " ## ##.# .### ### ####";
    DIS(N+(R-1)*8+L),BVEL,BR,LOOD(L+1),L
330 PRINT #2,USING " ## ##.# .### ### #";
    DIS(N+(R-1)*8+L),BVEL,BR,LOOD(L+1),M
332 '
333 C = 0
340 NEXT N
345 PRINT "------NEXT LOAD ***" L
350 L = L + (COLD+1)*8
355 IF L <> NUM THEN 198 ELSE 356
356 PRINT "****NEXT MOTOR ****" L, M
370 NEXT M
380 CLOSE #1
390 CLOSE #2
400 END
```

```
5' *** PROGRAM TO PUT DATA IN GRAPHING FILES ***
10 DIM DIS(64),AVEL(64),R(64),LOOD(64),MOTO(64)
20 OPEN "A:CMOT2B.DAT" FOR INPUT AS #1
30 FOR M = 1 TO 4
40 FOR I=1 TO 32: INPUT #1, DIS(I),AVEL(I),R(I),LOOD(I),MOTO(I):NEXT
50 '
60 FOR L = 0 TO 3
66 LL = 4*L + 4
70 B$=STR$(LL): B$=MID$(B$,2): C$=STR$(M):C$=MID$(C$,2):
   PV$="A:HPL"+B$+C$
72 PV$="A:VPB"+B$+"V"+C$
80 PR$="A:VPB"+B$+"R"+C$
90 OPEN PV$ FOR OUTPUT AS #2
100 OPEN PR$ FOR OUTPUT AS #3
110 '
120 FOR D = 1 TO 8
130 PRINT #2, USING "## ##.#"; DIS(D+L*8), AVEL(D+L*8)
```

```
140 PRINT #3, USING "## .###"; DIS(D+L*8), R(D+L*8)
145 PRINT DIS(D+L*8),AVEL(D+L*8),R(D+L*8)
150 NEXT D
155 PRINT "  "
160 CLOSE #2: CLOSE #3
170 NEXT L
180 NEXT M
185 CLOSE #1
190 END
```

APPENDIX H: VENDORS AND PRICE REFERENCES

VENDORS

PRODUCT	ADDRESS	CONTACT
GRAPHITE EPOXY	DIVERSIFIED FABRICATORS, INC 978 EAST 4TH ST. P.O. BOX 646 WINONA, MINNESOTA 55987 (507) 454-3799	STANLEY PROSEN
	COSTAL ENGINEERING 1105 MAIN ST. VARNVILLE SC 29944 (803) 943-4538	MR. DELOACH
FIBERGLASS	MORRISON MOLDED FIBERGLASS CO. P.O. BOX 508-TR BRISTOL, VA 24203 (703) 669-1181	MR. STONE
CENTERLESS GRINDING OF COMPOSITES	PRECISION FIBERGLASS INDUSTRIES INC. DEPT. T, P.O. BOX 606 NEWBERRY, SC 29108 (704) 525-6443	
	LYNCO (213) 773-2858	MR. HOLOGARTH
ALUMINUM AND STEEL	KILSBY ROBERTS CHARLOTTE, NC (800) 438-3450	

HORIZONTAL MOTION PART PRICE REFERENCES

PART	INDIVIDUAL COST	PRICE REFERENCE
CORNER BRACKET	1.00	P. HACKENWORTH-IBM
SLIDER BRACKET	1.00	P. HACKENWORTH-IBM
BELT ALIGNER	1.00	P. HACKENWORTH-IBM
2.1 AMP STEP MOTOR/DRIVER	45.00	SANYO STEP-SYN
1.1 AMP STEP MOTOR/DRIVER	16.00	SANYO STEP-SYN
GUIDE ROD	2.00/FT.	MOTION INDUSTRIES
STEEL	1.75/FT.	KILSBY ROBERTS
ALUMINUM	1.50/FT.	KILSBY ROBERTS
GRAPHITE EPOXY	4.75/FT.	DIVERSIFIED FABRICATORS.
FIBERGLASS	1.00/FT.	MORRISON MOLDED FIBER GLASS
DURALON BEARINGS	2.51	DIXIE BEARING
ROLLER	17.79	ROLLER
IGUS	.49	IGUS
TIMING GEARS	1.00	MAT GALATHA-IBM
TIMING BELT	3.00	MAT GALATHA-IBM
ROLLER BEARINGS	1.45	STOCK DRIVE PRODUCT
ELECTRICAL CONTROL	90.00	SIAK YEO-U.T.

APPENDIX I: CLOSED FORM SOLUTION FOR EQUATIONS OF MOTION FOR A LOAD DRIVEN BY STEP MOTORS

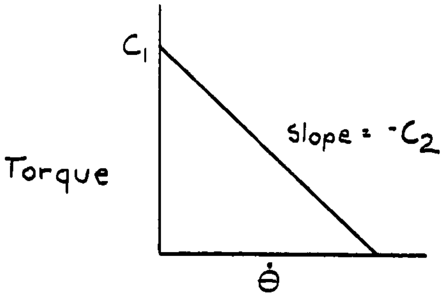

From the above schematic, the torque delivered to the system is:

$$T_d = C_1 - C_2\dot{\theta}.$$

The torque required to move the conservative robot mass is:

$$T_r = (m + I/r^2)\ddot{x}r.$$

The motor pulley radius is r. The torque required for nonconservative loading is:

$$T_{nc} = Fr.$$

F is the sum of the nonconservative forces like the friction force and force required to lift the mass. Adding the torques:

$$C_1 - C_2\dot{\theta} = (m + I/r_2)\ddot{x}r + Fr.$$

Letting $(m + I/r_2) = MM$ and simplifing:

$$\ddot{x} + C_2\dot{x}/MMr^2 + (Fr - C_1)/MMr = 0$$

Letting $A = C_2/MMr^2$, $B = D/MMr$, and $D = Fr - C_1$:

$$\ddot{x} + A\dot{x} + B = 0.$$

From the above equation:

$$x = C_3 + C_4e^{-At} - Bt/A, \quad x = -AC_4e^{-At} - B/A.$$

To solve for C_3 and C_4 for acceleration, it is known that:

$$\dot{x}_1 = 0 \text{ at } t_1 = 0.$$

x_1 is the position during acceleration. t_1 is the time during acceleration. x_2 is the postion during deceleration. t_2 is the time during deceleration. Substituting the above into the velocity equation:

$$B/A^2 = -C_4.$$

At $t_1 = 0$, $x_1 = 0$. Substituting this into the position equation:

$$C_3 = B/A_2.$$

To solve for C_3 and C_4 during deceleration, it is known that:

$$\dot{x}_{2initial} = \dot{x}_{1final} \text{ at } t_2 = 0.$$

Substituting this into the velocity equation:

$$C_4 = -(\dot{x}_{1final} + B/A)/A.$$

At $t_2 = 0$, $x_{2initial} = x_{1final}$. Substituting this in the position equation,

$$C_3 = x_{1final} - C_4.$$

VITA

Mark Granger is a 25 year old native Californian, who after several moves across the United States is has lived in Tennessee for the last 15 years.

Mark completed a bachelor of science degree in mechanical engineering at the University of Tennessee in June 1986. As an undergraduate, Mark had co-op experience in the power and automobile part manufacturing industry. As a graduate student, Mark was an IBM pre-professional in Charlotte, North Carolina. Currently, Mark is working part time at the Oak Ridge National Laboratory.

After the completion of this paper, Mark will explore the mountains of the western United States by foot and bike. Upon completion of the two month trek, a formal job search will be performed.